

THE STRESS-STRAIN CURVES OF SOILS

Steve J. Poulos

January 1971

GEOTECHNICAL ENGINEERS, INC.

1017 Main Street

Winchester, Massachusetts 01890

THE STRESS-STRAIN CURVES OF SOILS

Steve J. Poulos

January 1971

TABLE OF CONTENTS

1	INTRODUCTION	1
2	DEFINITIONS	4
	2.1 Soil	
	2.2 Soil Structure	
	2.3 State of a Soil	
	2.4 Contractive and Dilative Behavior of Specimens	
	2.5 The Steady State of Deformation	
	2.6 Method of Loading	
3	QUALITATIVE DISCUSSION OF FACTORS CONTROLLING SHAPE OF STRESS-STRAIN CURVES	14
4	IDEALIZED STRESS-STRAIN CURVES FOR SOILS IN 'DRAINED' SHEAR	17
	4.1 Uncemented Soils with Hard, Bulky Grains	
	4.2 Uncemented Soils with Substantial Proportion of Platey Grains	
5	EXAMPLES OF STRESS-STRAIN CURVES FOR SOILS IN 'DRAINED' SHEAR	25
	5.1 Uncemented Soils with Bulky Grains	
	(a) Highly Contractive Sand ('Very Loose')	
	(b) Slightly Dilative Sand ('Medium Dense')	
	(c) Highly Dilative Sand ('Dense')	
	5.2 Uncemented Soils with Substantial Proportion of Platey Grains	
	(a) Highly Contractive Clay (Normally Consolidated)	
	(b) Very Highly Contractive Clay (Quick)	
	(c) Highly Dilative Clay (Heavily Overconsolidated)	

6	IDEALIZED STRESS-STRAIN CURVES FOR SOILS SHEARED AT CONSTANT VOLUME	37
6.1	Uncemented Soils with Hard Bulky Grains	
6.2	Uncemented Soils with Substantial Proportion of Platey Grains	
7	EXAMPLES OF STRESS-STRAIN CURVES FOR SOILS SHEARED AT CONSTANT VOLUME	45
7.1	Uncemented Soils with Bulky Grains	
	(a) Highly Contractive Sand ('Very Loose')	
	(b) Sand Close to Steady State Void Ratio	
	(c) Highly Dilative Sand ('Dense')	
7.2	Uncemented Soils with Substantial Proportion of Platey Grains	
	(a) Very Highly Contractive Clay (Quick)	
	(b) Highly Contractive Clay (Normally Consolidated)	
	(c) Highly Dilative Clay (Overconsolidated)	
8	APPLICATIONS	55
8.1	Significance of the Terms "Normally Consolidated" and "Loose"	
8.2	Selection of Apparatus for Measurement of Stress-Strain Behavior	
8.3	Relation between Failures in Laboratory Specimens and Failures in the Field	
8.4	Relation between Pore Pressures Before and After Failure	
8.5	Selection of Shear Strength for Stability Analysis	
	(a) Soils Containing Chiefly Bulky Grains	
	(b) Soils Containing Chiefly Platey Grains	
	(c) Comments on Use of Tables 3 and 4	
9	CONCLUDING REMARKS	74

THE STRESS-STRAIN CURVES OF SOILS

SYNOPSIS

The steady state of deformation is defined as the state in which a specimen deforms continuously and monotonically without change in shear stress, effective normal stress, volume, or velocity of deformation. Using the steady state as a unifying concept, idealized shapes of stress-strain curves for drained and constant-volume tests are given for bulky-grained and platey-grained soils (Figs. 5,7,15,16). Typical test results are presented in detail.

To illustrate their practical utility, the generalizations made about stress-strain curves are used to evaluate the relative accuracy of typical laboratory tests (Tables 1 and 2), to aid in selecting shear strength for stability analysis (Tables 3 and 4), to understand the relationships between stress-strain curves of sands and clays, and to understand where liquefaction and residual strength fit into the general view of the stress-strain characteristics of soils.

The major factors affecting the shapes of stress-strain curves and the shear strength of soils are: (a) the soil, represented chiefly by its mineralogy and grain shape, (b) the initial structure of the specimen, (c) the initial state (void ratio, effective normal stress, and shear stress), and (d) the method of loading. The effects of each of these major factors on the stress-strain curves are discussed qualitatively.

THE STRESS-STRAIN CURVES OF SOILS

Steve J. Poulos

January 1971

1. INTRODUCTION

The main purpose of this monograph is to provide a systematic qualitative understanding of the shapes of stress-strain curves obtained in triaxial compression, direct shear, direct simple shear and rotation shear tests on fully saturated, uncemented soils. A secondary purpose is to provide insight into the use of this information in geotechnical engineering.

Problems involving the application of stresses to soils may be divided into those in which (a) deformations of the foundation soil (or rock) control design and (b) failure of foundation soil controls design. Those in which failure controls are a special case: i.e., the end point of the class of problems in which deformation controls. Failure problems themselves may be subdivided into shear failures and tension failures, but only shear failures are considered herein. This classification is merely a somewhat more general way of referring to the traditional "settlement" and "bearing capacity" problems of soil mechanics.

The distinction between deformation-controlled and failure-controlled problems may be understood by considering a building on a soil foundation. If the building is rigid or very flexible then the deformations of the foundation soil do not affect the competence of the building, and it is only necessary to assure that the foundation soil is safe against failure. Yet, if the building has intermediate flexibility, such that it fails when the deformations of the foundation soil are small (relative to those that are developed when

the foundation soil fails), or if the deformations of the building must be limited for some other reason, then the foundation soil must not deform excessively. In short, if the building fails first, excessive deformations of the foundation soils must be prevented; if the foundation soil fails first, failure of the foundation soil must be prevented.

For problems in which deformations of a mass of soils must be computed, it is well accepted that the computations can be made properly only if the shapes of the stress-strain curves involved are taken into account. But it is less widely appreciated that the shapes of the stress-strain curves must also be known in connection with most failure problems.

For failure problems the precise shape of the stress-strain curve need not be known if the shear stress reaches a maximum and then remains constant even at very large strains. In such a case, the fact that the shear stress varies along a given failure surface in-situ has no practical consequence, because when the strains are sufficient the maximum shear stress will be developed simultaneously along the entire failure surface (assuming that the test used to measure shear strength is a proper model of in-situ conditions). Thus, one would be safe in using the shear strength for computing the factor of safety.

The methods of stability analysis presented in the literature to date include, often only implicitly, the assumption that the stress-strain curve of all soils involved reach a maximum shear stress which then remains constant with further strain. However, the stress-strain curves of soils show a peak under most condition⁵, although conventional tests are usually not carried to sufficient strain to display the drop in shear stress after the maximum is reached. If the stress-strain curve of the soil along a failure surface

does ~~not~~ contain a peak, it is practically never possible to develop the peak shear stress simultaneously along the entire failure surface. The average shear stress mobilized along the failure surface at failure will be smaller than the peak shear stress. The difference between the peak shear stress and the average mobilized shear stress is due to "progressive" failure (Watson, 1940, P.150; Taylor, 1948, P. 348; Casagrande, 1950, P. 237). It is caused by the non-uniform stresses and strains that develop in the failure mass, and it occurs both in the field and in the laboratory.

The occurrence of progressive failure makes it necessary to analyze the distribution of strains within a mass of soil in order to estimate the average shear stress that can be mobilized simultaneously along a failure surface at failure. Alternatively, one can perform model tests to gain insight into the proportion of the maximum shear stress then can be simultaneously mobilized (Rowe, 1969). But the first step that is necessary to estimate the magnitude of the effect of progressive failure in any given case is to determine correctly the shape of the entire stress-strain curve. Only then is it possible to establish whether a given problem is controlled by deformation or by shear failure, and, if it is a failure problem, to make a proper estimate of average shear stress than can be mobilized along a given failure surface.

Progressive failure is but one of many examples that could be used to show why it is important to understand the shape of the entire stress-strain curve of a soil. This monograph is intended as an aid to such understanding.

2. DEFINITIONS

Definitions are given below for the terms: (1) soil, (2) soil structure, (3) steady state of deformation, (4) contractive and dilative behavior, and (5) method of loading. The purpose of these definitions is to facilitate discussion in subsequent chapters of the major variables that affect the shapes of stress-strain curves of soils. The definitions have been prepared with this purpose in mind and, as a result, they differ in some respects from previously published definitions.

2.1 Soil

A soil is a mass of discrete particles that are the products of decomposition and disintegration of rocks and organic matter by natural processes. A soil is assumed to be completely described by: (1) the composition of its solids, (2) the composition of the liquids, gases, and sometimes solids (including dissolved and suspended materials) in its pores, and (3) the distributions of size, shape, and angularity of its grains. Thus the term "soil" refers to the basic soil material and not in any way to the arrangement of the grains relative to each other.

It should not be inferred that it is possible at present to measure quantitatively each of the above-mentioned items, with the exception, in some cases, of the grain size distribution. But it is important to note that if any one of these items is changed, the soil itself and, hence, its properties are also changed.

Although in this paper the principal interest is in soils, the concepts subsequently presented can very likely be applied to any particulate mass, regardless of composition. The numerical values associated with various stress-strain characteristics change with composition, but the basic pattern of stress-strain characteristics of all particulate materials are likely to be the same.

2.2 Soil Structure

The term "soil structure" is used herein to refer to the arrangement of individual grains and groups of grains relative to each other and to the forces that bind these grains and groups of grains into a unit.

To describe the structure of a soil completely, one must observe it at every scale that is pertinent to the engineering application at hand, starting with the scale of individual grains, and moving up to the scale of the entire mass of soil that is involved. On the scale of individual grains one is concerned with the orientation of the grains (Lambe, 1953, P. 38) and with the number of contacts per grain and the magnitudes of forces between grains (Marsal, 1967, P. 40, 46). On a larger scale one might observe layering or stratification, slickensides, joints, and root holes. On a still larger scale one might find old major failure surfaces, holes made by animals, joints and slickensides of very large extent, and hard or soft inclusions of any size and shape. It is not unusual for the large-scale structural patterns to have a far greater influence on the engineering properties of a soil in-situ than does the structure at the scale of individual grains.

The forces between grains or groups can be divided into two types: (1) those that impart strength to the soil only when the effective stress is greater than zero, and (2) those that impart strength to the soil when the effective stress is zero. If the latter forces exist, the soil will exhibit strength when the effective stress is zero. In this monograph the latter forces are referred to as "cementation bonds". Uncemented soils are the main subject of this monograph.

2.3 State of a Soil

The state of a soil is defined by the void ratio and the effective stresses on a specimen at any given moment. For the purposes of this monograph, the state of a specimen will be monitored by the void ratio, e , and the effective minor principal stress*, $\bar{\sigma}_3$, at any stage during a test. A plot of these two variables yields the state diagram, Fig. 1. These coordinates are the same as those used for plotting compression curves from triaxial consolidation tests. They are also used to advantage for following the results of shear tests in which changes in the principal stress ratio, as well as void ratio, occur during shear.**

* For tests in which the effective minor principal stress is not known, an appropriate known effective stress will be used. For direct shear tests, the effective stress on the horizontal plane, $\bar{\sigma}_h$, is convenient.

** The changes that occur during shear are better represented in a plot of void ratio versus average principal effective stress, as suggested by Roscoe, Schofield and Wroth (1958 P. 27). However, for many types of tests the three principal stresses are not known. Therefore, it is expedient to compare series of tests of the same type by plotting the void ratio versus one of the known effective normal stresses.

The potential range of changes in void ratio can be visualized with the aid of the sketch at the left in Fig. 1. By viewing void ratio changes with reference to certain void ratio benchmarks, such as $e = 0$, $e = e_{\max}$, $e = e_{\min}$, or the void ratios corresponding to the liquid and plastic limits, one is able to judge whether the results of a given shear test are reasonable or not.

The temperature of the specimen should be included to define its state more completely, but this variable is not considered herein.

2.4 Contractive and Dilative Behavior of Specimens

A specimen is said to be contractive if it tends to decrease in volume when the shear stress is increased during a given test, and dilative if it tends to increase in volume when the shear stress is increased (Casagrande and Poulos, 1964, P. 3).

These terms refer to volume changes that occur due to shear stresses, not to those caused by isotropic changes in effective normal stresses. An isotropic increase in effective normal stress always causes compression and a decrease causes expansion. Such is not the case for shear stresses.

The term "contractive" is applied to a specimen whether or not it actually contracts during a test, and the same applies to the term "dilative." For example, if contraction is prevented, the specimen is nevertheless referred to as contractive. But to prevent contraction, the isotropic effective normal stress must be reduced sufficiently to counterbalance the tendency for volume decrease that is caused by the shear stress. Thus, if the specimen were fully saturated and volume decrease were prevented by maintaining constant water content, the pore pressure would increase sufficiently to cause the required decrease in isotropic effective stress.

The degree to which a specimen is contractive or dilative is dependent on the soil, its structure, its initial state, and the method of loading (Section 2.6).

2.5 The Steady State of Deformation

The "steady state of deformation" is that state in which a particulate material of any composition or particle shape deforms continuously under a constant state of effective stress at constant velocity and at constant void ratio. This constant void ratio is the "steady state" void ratio.*

Therefore, one can measure the steady state void ratio only during deformation, since the soil mass will assume a different void ratio when deformation stops, even in clays. If the velocity of deformation is changed, the steady state void ratio is also changed. If one prepares a specimen of soil at the steady state void ratio, that specimen does not reach the steady state until it has been sheared to very large deformations. The "structure" of the specimen in the steady state is created by the applied shear stresses and is very different from its structure as initially prepared.

* The term "steady state void ratio" is synonymous with the term "critical void ratio," which was introduced by Casagrande (1936, P. 18) for the case of sands. The term "steady state" is used for two reasons: (1) It conveys correctly (by analogy to steady-state flow of liquids) the concept of flow that the author has in mind. (2) The term "critical state," which, historically, may be applied to the steady state, has been applied by subsequent authors to a completely different condition of soils (Roscoe, Schofield and Wroth, 1958, P. 28; Schofield and Wroth, 1968, P. 19; Schofield, 1970).

Tests on sands (Watson, 1938, Plates BII - 8 and 9) and on steel balls (Roscoe, Schofield, and Wroth, 1958, Fig. 37) have shown that the steady state void ratio decreases with increasing effective stress* as shown schematically in Fig. 1. Although this relationship has not been adequately demonstrated for clays, by analogy the author assumes that a similar relationship will hold.

The principal characteristic that makes the steady state concept so useful is that a soil will tend to the steady state when sheared to sufficiently large strains. Thus, one can expect that specimens prepared at states lying above the steady state line in Fig. 1 will change volume or effective stress during shear such that the state point will move towards the steady state line. These specimens will be contractive. Specimens prepared at states below the steady state line will experience changes that ultimately move the state point towards the same steady state line, i.e., these specimens will be dilative at some stage during a test. The extent to which this behavior applies to real soils is discussed in subsequent chapters. It will be seen that although the steady state line provides an

* Watson measured the void ratio at which the specimen would show no net change in volume at peak deviator stress in consolidated-drained triaxial compressions tests. This void ratio was defined by Casagrande (1938, P. BII-8) as the "lower critical void ratio." Casagrande introduced this definition merely for convenience because he recognized the difficulty of measuring the void ratio in the steady state of deformation, which he referred to as the critical void ratio. Watson showed that the lower critical void ratio decreased with increasing confining pressure. From Watson's data Casagrande (1938, P. BII-7, 9) estimated that the critical void ratio varied in the same way but was higher than the lower critical void ratio by about 0.06 for one fine, uniform silty sand (Franklin Falls sand).

important reference in the state diagram, the path by which a soil may move towards the steady state may be rather complicated.

For soils composed primarily of bulky grains, the physical mechanism of steady state deformation is viewed by the author as a continuously changing arrangement of the particles throughout the deforming mass, accompanied by local increases and decreases in void ratio and effective stresses, such that a sufficiently large mass of the material displays no change in the average (or macroscopic) void ratio and effective stresses.

Given a material with bulky grains, there may be little tendency for the development of a preferred orientation of grains in response to the applied shear stresses.* However, materials composed only of platy or elongate grains (e.g., mica, kaolinite, attapulgite and halloysite) ultimately reach a condition in which the grains are orientated parallel with each other in the direction of movement (see Skempton, 1964). In this case, a single or a small number of shiny shear surfaces develop.** At this stage of the shearing process, and at no other stage, such platy-grained soils are able to deform

* If the steady state void ratio is a function of particle size, then a material composed of bulky particles with a range of sizes probably would develop a preferred distribution of its grains of various sizes when the steady state is reached. The major movements may then occur between particles in a given size range only, while the balance of the particles move much smaller distances relative to their neighbors. Obviously the steady state void ratio would then be a function of the grain size distribution as well as the size of the particles.

** Whether shiny surfaces would develop in soils with elongate (needle-shaped) grains, such as halloysite and attapulgite, has not yet been established.

continuously at constant velocity, void ratio and effective stress. Therefore, this state is, according to the definition given herein, the steady state of deformation. Clearly the zone in which the steady state develops in platey-grained soils is very thin, and it becomes almost impossible to measure the steady state void ratio. This feature does not diminish the usefulness of the concept, since its use as a working hypothesis for clays as well as sands permits one to view the stress-strain curves of all types of soil in one organized framework.

In real soils the platey particles are never absolutely flat, and the platey or elongate particles are practically always mixed with bulky particles. Therefore, the zone in which a steady state develops in real soils contains a number of particle thicknesses. For example, Fig. 2 contains two scanning electron microphotographs that were taken by viewing normal to the surface of a natural slickenside in Bearpaw Shale which was exposed when a drying crack formed during preparation of the specimen for the microscope (LaGatta, 1971). The photograph at the lower magnification shows that large-scale layering exists. At the higher magnification, layering at the scale of the individual particles in this soil can be seen. Approximately six layers, less than one micron apart vertically, are apparent. If appropriate measurements were made, the void ratio of this zone of the specimen could be determined.

The greater the percentage of bulky particles, the greater will be the volume of soil that reaches the steady state and the less shiny will be the resulting planes of shear. But even small percentages of platey particles may congregate in one zone and cause the steady state strength and void ratio to be controlled by these particles rather than by the entire grain-size distribution of the material.

When a soil is sheared, the contact stresses, if sufficiently great, cause grain breakage. Thus the soil itself changes during deformation. In such cases, the steady state cannot be defined unless the deformations are continued until grain breakage ceases. But in that case, the steady state reached applies to the new soil, not to the original soil.

2.6 Method of Loading

The method of loading is the manner in which a specimen is brought to failure. To define the method of loading, one must know the shear and total normal stresses or the deformations on each boundary of a homogeneously stressed specimen at every stage of a test, and one must describe the degree to which the void ratio is allowed to change. For example, the method of loading is defined for a conventional unconfined compression test by stating that the total minor and intermediate principal stresses are maintained at zero while the total major principal stress is increased from zero, without allowing change in water content of the specimen at any time. As a condition of this test, the top and bottom of the cylindrical specimen, which are major principal planes, are forced to remain plane by the end caps. The friction between the specimen and these end caps causes stress non-uniformities in the specimen. Therefore, the method of loading for this test is not truly known unless these boundary friction forces are known.*

* Often the effects of the boundary friction are ignored, for various reasons, but lubrication (Rowe, 1962, P. 507) minimizes the effects.

The changes in effective normal stress and shear stress that are caused by any given method of loading are conveniently followed by plotting them on a Mohr diagram in the form of a stress path, Fig. 3 (Lambe, 1964, P. 45). The stress path shows how the location of the top point of the Mohr circle (in terms of effective stress) changes during the test.*

The state path and the stress path in combination (Figs. 1 and 3) provide a record of the changes in void ratio, effective normal stress and shear stress that result from the method of loading used for any test.

The stress-strain characteristics of soils are strongly dependent upon the method of loading. Therefore, it is essential in laboratory testing that the stress-strain curves be determined for a method of loading that models, as closely as possible, the method of loading that will be applied in-situ.**

* The stress path for the plane inclined 45° to the principal planes is used herein because its coordinates are easily computed. The stress paths of the effective principal stresses are superior from the theoretical viewpoint, but all three are not usually known. When some of the stresses are not known, such as in a direct shear test, the stress path is plotted for that plane on which the shear and effective normal stresses are known.

** Alternatively, one must be able to use the results from one method of loading for predicting results for another method of loading. Stress-strain theories are currently being developed with this object in mind (e.g. Schofield and Wroth, 1968). But verification of the utility of such theories remains dependent upon large-scale field tests or on model tests (e.g. Avgherinos and Schofield, 1969).

3. QUALITATIVE DISCUSSION OF FACTORS CONTROLLING

SHAPE OF STRESS-STRAIN CURVES

The major factors* that control the shape of stress-strain curves of soils are:

- (a) Soil type (particularly mineralogy and grain shape)
- (b) Initial structure
- (c) Initial state
- (d) Method of loading

Each part of a stress-strain curve is affected to a different degree by each of these factors. The author's opinions about these effects are described in Fig. 4, which shows a stress-strain curve with sufficiently general shape for this purpose.

The initial portion (the early part of Zone A, Fig.4) of the stress-strain curve is affected by all four of the above factors. For example, one can expect that:

- (1) As one passes through the range of soils with hard, bulkly grains to soils with soft, platy grains, the stiffness, i.e., the slope $d\tau/d\epsilon$ should decrease.

* Secondary factors, which are important in certain cases, include: (1) rate of loading, (2) temperature of specimen, (3) absolute pressure in pore fluid, and (4) magnitude and frequency of stress cycles, if any. These items are not discussed in this monograph.

- (2) As the void ratio increases and the effective stress decreases, i.e., as the initial state moves towards the upper left corner of the state diagram (Fig. 1) the stiffness decreases.
- (3) The stiffness changes with structure, be it undisturbed, remolded, compacted wet, compacted dry, etc.
- (4) The method of loading affects the measured stiffness substantially. For example, Cornforth (1964, Fig. 17) reported that the strain at maximum shear stress is much lower in plane strain than in triaxial compression.

The shear stress in the steady state (beyond Point s in Fig. 4) is not likely to be influenced by the initial structure, or the initial state, or the stress path followed during loading. Only the soil type and the end point of the stress path are likely to control its value. The specimen loses its memory of how it arrived at the steady state. The strain required to reach the steady state can be expected to be dependent on the initial structure, the initial state, and on the method of loading, as well as the soil type.

The above effects are summarized in the following table:

EFFECTS OF MAJOR FACTORS CONTROLLING SHAPE OF
STRESS-STRAIN CURVES

Factor	Qualitative Estimate of Effect of Each Factor on:				
	Initial modulus of deformation	Peak point		Steady State	
		Shear Stress	'Width' of peak and strain at peak	Shear stress	Strain
Soil type	High	High	High	High	High
Initial state	High	High- Med.	High- Med.	None	Low
Initial structure	High	High- Med.	High- Med.	None	Low
Method of loading	High	High	High	Med.- Low	Low

When the grains of a soil are weak, angular, platy, or elongate, and when the soil is tested at sufficiently high effective stresses, significant grain breakage occurs during testing. (In drained tests grain breakage will result in continuous volume decrease with an accompanying change in shear stress. In constant volume tests it will result in a decrease of the effective normal stresses.) Only after grain breakage has ceased (for practical purposes) can the changes in volume and shear stress cease also. The final, steady-state shear stress probably still is dependent chiefly on the soil that was used and on the method of loading, even though the soil has been transformed into a new soil by the shearing process. But the strain required to reach the steady state is likely to be increased by grain breakage.

4. IDEALIZED STRESS-STRAIN CURVES

FOR SOILS IN 'DRAINED' SHEAR

4.1 Uncemented Soils with Hard, Bulky Grains

Curve 1 in Fig. 5 (a) shows the stress-strain curve for a triaxial compression test on a very loose (highly contractive) specimen of sand composed chiefly of hard, bulky grains. The shear stress increases gradually with strain until a maximum is reached at Point ' s_c '. The shear stress then remains constant with further strain. The volume decreases continuously as the shear stress is applied until a void ratio is reached that remains constant with further strain, Fig. 5 (b). At Point ' s_c ' the soil has reached the steady state of deformation.

The void ratio change in the state diagram (the state path) is simply a vertical straight line which starts at the initial state and moves continuously down toward the steady state line, Fig. 5 (c), since the effective minor principal stress is not allowed to change during this test. The stress path, Fig. 5 (d), is a straight line inclined at 45° . It ends at Point 's'.

A series of specimens tested in triaxial compression starting from states well above the steady state line and at various effective consolidation pressures would yield stress-strain curves similar in shape to Curve 1 in Fig. 5 (a). The initial tangent modulus would decrease as the void ratio after consolidation, e_c , increased and as the effective consolidation pressure, $\bar{\sigma}_{3c}$, decreased. The strain required to reach the steady state increases with increasing e_c and with increasing $\bar{\sigma}_{3c}$.

In no case would a peak develop. The specimen would be contractive throughout test until the steady state is reached, and the end points of the state paths would define a steady state line as illustrated in Fig. 5 (c). The corresponding steady state strength line, Fig. 5 (d), would be a straight or slightly curved line passing through the origin.

Specimen 2, consolidated isotropically to Point c_d in Fig. 5 (c), which is below the steady state line, first contracts slightly (Watson, 1940, P. 46) and then, as strains become large enough to cause grains to interfere with one another, it dilates until the same steady state void ratio is reached as for Specimen 1, as also shown in Fig. 5 (b). The stress-strain curve for Specimen 2, Fig. 5 (a), displays a peak at Point m when the void ratio is increasing at the maximum rate, due to the energy required to increase the volume against the confining pressure (Taylor, 1948, P. 346; Rowe, 1962, P. 501, 514). At larger strains the same steady state is reached as for Specimen 1.

The ratio of the peak to the steady state strengths from the drained test is defined by the author as the "drained sensitivity." This parameter is analogous to the usual sensitivity that was introduced by Terzaghi (see Skempton and Northey, 1952, P. 30) to describe the sensitivity of saturated soils to remolding at constant water content. To distinguish between the two, the latter will be called "undrained sensitivity" in this monograph. Both are useful indications of the potential magnitude of the effects of progressive failure.*

* Bishop (1967, P. 145) has suggested that brittleness be defined by $I_b = (\tau_m - \tau_s)/\tau_m$. This index "has the advantage that it expresses directly the maximum percentage error which can arise due to progressive failure in a brittle soil." The drained sensitivity (τ_m/τ_s) is used here because it is analogous to and has the same utility as the undrained sensitivity which is presently in common use.

The stress path for Specimen 2 is again a straight line inclined at 45° . It crosses the steady state strength line at a strain smaller than peak strain, rises to the peak Point m, and then doubles back on itself to stop on the same steady state strength line as found for Specimen 1. If a series of tests is performed on specimens prepared at the same void ratio as for Specimen 2, but at various values of $\bar{\sigma}_{3c}$, i.e., at states lying on a horizontal line through Point c_d in Fig. 5 (c), the stress paths would pass through a peak and then reverse direction to stop on the steady state strength line. The locus of these peak points would form the curved peak strength envelope shown in Fig. 5(d). This envelope must be curved since: (a) at zero confining pressure an uncemented soil has no strength, so that the peak strength envelope must pass through zero, (b) at sufficiently high confining pressures, the initial state of the specimens would be well above the steady state line, so that no peak would develop and the peak strength envelope would have to merge into the steady state envelope, (c) grain breakage would be more severe at high pressures, which could be expected to cause lower peak strengths than those that would obtain for no grain breakage, and (d) interparticle friction decreases with increasing interparticle force (Rowe, 1962, P. 505). The last two items would also cause a concave downward curvature of the steady state strength line, although it is shown as a straight line in Fig. 5 (d).

Test series on specimens prepared at constant void ratios e_1 , e_2 , and e_3 in Fig. 6 (a) would yield the series of strength envelopes shown in Fig. 6 (b). The utility of the concept of steady state lies in the hope that regardless of their initial state all specimens of the same soil tested with the same method of loading will show strengths corresponding to a unique steady state strength line (always plotted in terms of effective stress), as shown in Fig. 6 (b), if the tests are carried to sufficient strains.

Specimens prepared at void ratios equal to the steady state void ratio, Points 1, 2, and 3 in Fig. 6 (a), must display a peak in their stress-strain curves in triaxial compression tests. These specimens first contract and then dilate back to their original void ratio, the peak probably occurring at the point of maximum dilation rate. Although such specimens are prepared at the steady state void ratio, they are not in the steady state until they have been sheared to large strains. To form the steady state "structure" the initial structure must be altered appropriately by the shear stresses. This behavior in triaxial compression leads to the conclusion that there exists a line above the steady state line such that specimens prepared at states on or above that line will be contractive throughout a test until the steady state is reached. This boundary, shown dashed in Fig. 6 (a), will be referred to as the DC boundary. It may prove to have significant practical value since specimens prepared at states above this line would show a continuous decrease of the effective minor principal stress during a consolidated, constant-volume test. Thus it may form the boundary between specimens that liquefy and those that do not liquefy under the particular set of test conditions that is used to establish the DC boundary.

The steady state void ratio for bulky-grained soils decreases with increasing effective consolidation stress, yet tests on one sand have shown that the steady state envelope is nevertheless straight for effective normal stresses less than about 4 kg/cm^2 (Castro, 1969, Fig. 19). It appears that in this stress range any decrease in resistance due to the increasing stress level (which would result from decreased interparticle friction and increased grain breakage) is counterbalanced by the lower void ratio of the steady state. Similarly, the void ratios at peak decrease with increasing stress. Thus,

none of the envelopes shown in Fig. 6 (b) are envelopes for constant void ratio at failure. It would be possible to define peak strength envelopes for which the void ratio at peak is a constant. But one cannot do the same for the steady state, if the steady state void ratio and the effective normal stress are uniquely related as postulated.

4.2 Uncemented Soils with Substantial Proportion of Platey Grains

The ideal behavior illustrated in Fig. 5 for hard, bulky-grained soils must be modified for the case of soils that contain large amounts of platey or elongate grains, because as strain occurs the grains become increasingly orientated in the direction of movement (Skempton, 1964, P. 83) and the mobilizable shear stress decreases as a result. At extremely large strains a steady state degree of orientation, and, hence, a steady state strength, is reached.

Specimen 1 in Fig. 7 (c) is prepared at a state well above the steady state line, such that it is contractive throughout shear, as seen in Fig. 7 (b). The stress-strain curve in Fig. 7 (a) has a peak even though the volume is decreasing at a rapid rate at peak (Point m_c). In this case the peak is not the result of dilation, but instead it is due to the loss in strength that follows when the particles in the failure zone become distinctly orientated. The axial strain required to develop the peak is very large because substantial movement between grains is needed to cause the necessary orientation. (Even at 20% axial strain, the relative movement between grains in any soil is still rather small.) Although the void ratio decreases after peak, due to

which a gain in resistance might be expected, the efficiency of the orientated structure is such that a net loss of resistance is observed. If the soil contained a larger percentage of bulky particles, the net effect would be no loss of resistance when the steady state is approached, as in Fig. 5 (a), Specimen 1. The relation between the distribution of particle shapes and the drained sensitivity of such a contractive specimen remains to be investigated.

The maximum shear stress for Specimen 1 occurs at a void ratio that lies above the steady state line (Fig. 7c) by an amount that depends on the initial state, the initial structure, and on the magnitude of the effect of orientation on the grains. The stress path in Fig. 7 (d) also shows the peak at Point m_c . It then reverses on itself to stop at Point s.

Consider a series of specimens prepared at states lying along a virgin compression curve, which will be assumed to pass through Point c_c in Fig. 7 (c). Consolidated-drained tests on these specimens will yield a line of peaks on the state diagram that lies above the steady state line and passes through Point m_c as shown. The location of this line of peaks is dependent on the initial state and structure of the specimen, because at peak the structure of the specimen has not yet been completely altered by the strains. As the effective consolidation pressure is increased, the line of peaks probably merges toward the steady state line, as shown in Fig. 8 (Lines b and c). This change with pressure is anticipated because the difference between the structure of the soil at peak and steady state can be expected to diminish gradually as $\bar{\sigma}_3$ increases. Thus, even for soils with very thin, platey grains one may observe no peak in the stress-strain curve of normally consolidated specimens tested at very high pressures in drained shear.

Corresponding to the line of peaks in Fig. 7 (c) for contractive specimens, the beginning of a peak strength envelope is shown passing through Point m_c in Fig. 7 (d). This peak strength envelope is the one that is usually referred to as the "effective stress envelope" for a given soil. One can see from the discussion in this monograph that this envelope is far from unique. It is a function not only of the soil, but also of the structure, states, and method of loading for the particular test series used to define the envelope. One can obtain very wide ranges in measured "friction angle" for any given soil. But the steady state strength line is likely to be more unique, being dependent only on the soil and the particular set of boundary conditions that exist during steady state deformation.

Specimen 2 in Fig. 7 (c) is prepared at a state below the steady state line and at the same effective stress as Specimen. 1. In this case the specimen contracts slightly and then dilates with strain until the steady state is reached. Again, the strain required to reach steady state is very large because of the shape of the grains. The peak point on the stress-strain curve probably corresponds closely to the maximum rate of dilation because the strains required to reach peak in a highly dilative specimen are not sufficient to cause a marked orientation of the grains. (If a specimen were prepared at Point s in Fig. 7 (c), the grain orientation when the shear stress is near its maximum may cause a noticeable difference between the strain at peak and the strain at the point of maximum rate of dilation.)

The peak point for Specimen 2 is shown in Fig. 7 (c) to lie below the steady state line. If a series of specimens were prepared at states lying on a swelling curve, such as that shown dashed, a line of peaks for these dilative specimens could be defined, corresponding to the peak strength envelope passing

through Point m_d in Fig. 7 (d). Again it is seen that this "effective stress envelope" for "overconsolidated" (dilative) clays, is far from unique. Furthermore, the effective stress envelopes for contractive and dilative specimens cannot be expected to be the same (even after the resistance due to dilation rate is taken out), except by rare coincidence. Only when the steady state has been reached can one expect the effect of the initial state and structure of the specimens to be deleted, thus yielding a unique steady state envelope. The postulated relationship between the steady state line, the compression and swelling curves, and the lines of peaks, over the full range up to maximum past pressure, is shown in Fig. 8. The stress level AA' corresponds to the situation shown in Fig. 7 (c).

From Figs. 7 and 8 one can see that normally consolidated specimens have void ratios substantially greater than the steady state void ratio. Their behavior is analogous to that of loose sands. The differences between the shapes of stress-strain curves of normally consolidated clays and loose sands is accounted for chiefly by the distribution of grain shapes, which leads in clays to greater strain at failure and to the possibility of significant grain orientation due to the shear stresses. Quick clays and silts may be compared with extremely loose sands that might be slightly cemented--the cementation bonds being one mechanism through which extremely high void ratios may be maintained in a natural environment.

5. EXAMPLES OF STRESS-STRAIN CURVES FOR
SOILS IN 'DRAINED' SHEAR

The stress-strain curves, volume change curves, stress paths and state paths for drained tests are discussed below for the following examples:

(a) Uncemented Soils with Bulky Grains

Highly contractive sand ('very loose') - Fig. 9

Slightly dilative sand ('loose') - Fig. 10

Highly dilative sand ('dense') - Fig. 11

(b) Uncemented Soils with substantial proportion of Platey Grains

Highly contractive clay (normally consolidated) - Fig. 12

Very highly contractive clay (quick) - Fig. 13

Highly dilative clay (heavily overconsolidated) - Fig. 14

5.1 Uncemented Soils with Bulky Grains

(a) Highly Contractive Sand ('Very Loose')

Fig. 9 shows the stress-strain curve, volume change curve, stress path and state path for a consolidated-drained triaxial compression test on a fine quartz sand. The notations at the bottom of the figure have the following meanings:

- | | | |
|-----------|---|--|
| D_{10} | - | 10% of grains (by weight) are finer than D_{10} |
| C_u | - | Coefficient of uniformity |
| s_s | - | Specific gravity of soil solids |
| e_{max} | - | Maximum void ratio. Obtained by carefully pouring oven-dried sand into mold. |

- e_{\min} - Minimum void ratio. Obtained by vibrating oven-dry sample.
 $\bar{\sigma}_{3c}$ - Effective isotropic consolidation pressure
 e_c - Void ratio after consolidation under $\bar{\sigma}_{3c}$
 R_{dc} - Relative density after consolidation under $\bar{\sigma}_{3c}$

$$R_{dc} = \frac{e_{\max} - e_c}{e_{\max} - e_{\min}}$$

- u_c - Back pressure (applied to saturate specimen)
 w - Water content

The stress coordinates in the graphs have been normalized by dividing each by $\bar{\sigma}_{3c}$.

The relative density at start of shear was only 17%, which is below the range of relative density usually encountered in practice. The results of this test are representative of the idealized case shown for Specimen 1 in Fig. 5.

The stress-strain curve shows a gradual rise to the maximum measured resistance at Point m. Even with lubricated ends and the comparatively large axial strain of 24%, the maximum shear stress was not reached. The resistance was still rising and the volume still decreasing when the test was stopped.* At Point m, the shear stress was $1.1\bar{\sigma}_{3c}$ and the volume had decreased 3.0%. If the test had been carried to completion, a steady state would have been reached at a somewhat greater shear stress and slightly lower void ratio. Thus Point m on the state diagram, at a relative density of 32.5%, is probably

* Arithmetic plots of stress-strain curves are often misleading because they make it appear that a maximum or a steady state condition has been reached when it has not. A plot of strains on a logarithmic scale quickly demonstrates whether these states truly have been achieved (LaGatta, 1970, P. 2-5).

slightly above the true steady state line, and the friction angle in terms of effective stress, ϕ_m , of 31.6° is somewhat smaller than the steady state friction angle.* The steady state relative density for this effective consolidation pressure (1.0 kg/cm^2) is about 35%, which in practice would be considered a "medium-loose" state (Gibbs and Holtz, 1957, Fig. 5).

The state diagram also contains a plot of the effective normal stress on the 45° plane versus the void ratio. This plot is a 'compression' curve for a test in which the principal stress ratio is continuously increasing, as compared with the more familiar compression curve for one-dimensional consolidation in which the principal stress ratio remains approximately constant (shown dashed in the state diagram). At shear stresses greater than about $0.3\tau_m$, the specimen becomes more compressible in the triaxial test than in one-dimensional compression. This result is reasonable because it is at this point that the shear stresses on the specimen in the two tests begin to deviate from each other. Whether or not the reversal of curvature at the end of the curve is real or an artifact of the test is unknown.

(b) Slightly Dilative Sand ('Medium Dense')

Fig. 10 shows the results of a consolidated-drained triaxial compression test on a slightly coarser (than that used for the test of Fig. 9) but still fine, uniform sand from the Sacramento River. It is composed primarily of

* Note that the slope angle, θ , of the line from the origin to Point m in the stress path in Fig. 9 is 27.6° . The angle ϕ is the slope of a line through the origin tangent to the Mohr circle_m through Point m. Thus $\sin \phi_m = \tan \theta_m$. In this case, $\sin 31.6^\circ = \tan 27.6^\circ$.

quartz but has some feldspar grains, which are less bulky and more angular than quartz grains. In this case, the relative density after isotropic consolidation is 39%, which would make the specimen 'medium' dense according to Gibbs and Holtz (1957, Fig. 5). Comparison with Fig. 9 shows that the more contractive specimen was less stiff and required larger strain to reach the maximum shear stress. These differences exemplify the effects of decreasing contractiveness.

The test of Fig. 10 was again not carried to sufficient strain to define the steady state. At point s, the end of test, the shear stress was dropping slowly and the void ratio was increasing slowly. By extrapolating these curves, one can estimate that the steady state void ratio lies between Points c and s on the state path, perhaps at a relative density of 43%. Therefore, this specimen was prepared at a state slightly below the DC boundary (refer to Fig. 6) but probably slightly above the steady state line. The DC boundary would appear to lie about 5% in relative density, or 0.025 in void ratio, above the steady state line. The two lines are rather close together; for practical purposes it seldom would be necessary to distinguish between them for this soil.

Comparison of Figs. 9 and 10 gives:

	$\frac{e_s}{}$	$\frac{\bar{\sigma}_{3c}}{}$	$\frac{C_u}{}$	<u>Description of Grains</u>
Fig. 9	0.72	1.0	1.8	Bulky, subrounded to subangular
Fig. 10	0.85	4.5	1.3	Bulky to somewhat elongate, angular to subrounded

The steady state void ratio was considerably higher for the case in Fig. 10 because the soil contained elongate and angular grains and was slightly more

uniform. If the $\bar{\sigma}_{3c}$ values had been equal, the difference would have been even larger. (At $\bar{\sigma}_{3c} = 4.5 \text{ kg/cm}^2$ for the soil of Fig. 9, $e_s = 0.70$.) Differences in grain shape and uniformity of grain size that appear small at first glance have substantial effect on the value of the steady state void ratio.

The peak point friction angle in Fig. 10 is 34.6° . If the test were carried to sufficient strain to define the steady state, a slightly lower friction angle would be obtained at that state.

The upward curl at the end of the state path for $\bar{\sigma}_{45}$ in Fig. 10 reflects the observed dilation at large strains and seems to be a logical change from the corresponding curve in Fig. 9. Therefore, the upward concavity at the end of the curve in Fig. 9 may not be a test error. Of course, a similar error could have occurred in both tests (although the tests were performed in different laboratories) at axial strains greater than about 12%.

(c) Highly Dilative Sand ('Dense')

Fig. 11 contains the results of a consolidated-drained triaxial compression test on the same soil used for the test on the highly contractive specimen in Fig. 9. In the present case, the relative density was 95%, as compared with only 17% before.

A definite peak (drained sensitivity of 1.4) was observed and the specimen dilated substantially. The maximum dilation rate corresponds well with the peak. It is this type of result that permits the idealization shown in Fig. 5.

Comparison of Figs. 9, 10, and 11 shows the transition in shape of stress-strain curves for bulky-grained soils as the density is increased. One

finds increasing stiffness, increasing shear strength, lower strain to reach the maximum shear stress, increasing drained sensitivity, and increasing dilation.

Comparison of Figs. 9 and 11 shows that the steady state void ratio lies for this soil between 0.68 and 0.73 (for $\bar{\sigma}_{3c} = 1.0 \text{ kg/cm}^2$), which are values measured at the end of these two tests. In neither case was the strain sufficient to reach the steady state. Because failure planes developed in the highly dilative specimen, the measured volume changes are more suspect. Therefore, it is likely that the steady state void ratio is closer to 0.73, and the previously estimated value of 0.72 (relative density of 35%) may be reasonable.

The shear strength of the dilative specimen is $1.8\bar{\sigma}_{3c}$ as compared with $1.1\bar{\sigma}_{3c}$ for the very loose specimen. These values correspond to $\phi_m = 39.6^\circ$ and 31.6° , respectively. Increasing the density of this soil is very effective in providing increased shear strength.

The state path for $\bar{\sigma}_{45}$ in Fig. 11 shows in another form that the shear stress caused volume increase, whereas one-dimensional compression from the Point c would yield the dashed curve. The stresses applied during the triaxial test cause compression similar to one-dimensional compression up to the point when the shear stresses reach about one-half of the peak shear stress.

5.2 Uncemented Soils with Substantial Proportion of Platey Grains

(a) Highly Contractive Clay (Normally Consolidated)

Fig. 12 shows the results of a consolidated-drained rotation shear test on a very thin, annular specimen of remolded Pepper shale. This test is representative for the idealized case shown in Fig. 7, Specimen 1.

It was consolidated from a water content of 61% (liquidity index = 0.80) to an effective normal stress on the horizontal plane of 4.0 kg/cm^2 . The new notations in Fig. 12 are:

$\bar{\sigma}_h$	Effective normal stress on horizontal plane
a	Denotes stage of test after consolidation under the effective normal stress in complete (just before start of loading). The consolidation stresses are anisotropic, hence the use of 'a'.
i	Subscript to denote initial or as-molded state
τ_h	Shear stress on horizontal plane
H	Thickness of specimen
δ	Peripheral displacement
γ	Shear strain (= δ/H_a)
v	Volumetric strain
G_w	Degree of saturation
L_w	Liquid limit
P_w	Plastic limit

The stress-strain curve shows a peak at the extremely large shear strain of 63% and then a very gradual decrease in shear stress, as the grains become better orientated, until a constant shear stress is reached at a "shear strain" of 5260%. Many published stress-strain curves for remolded, normally consolidated specimens in drained shear show a gradual rise to a maximum without subsequent reduction in shear stress. Such results are

obtained if the tests are stopped at conventional low strains. The shear strain at peak of 63% is approximately equivalent to an axial strain of 40% in triaxial compression (assuming the method of loading has no effect on strain at peak). Neither triaxial tests nor direct simple shear tests can be carried to sufficient strain to define the entire stress-strain curve shown in Fig. 12. Two features of this test accentuate formation of a peak: (1) the specimen was anisotropically consolidated at $\sigma_1/\sigma_3 \approx 2$ and (2) it was prepared at $w_l = 61\%$ (liquidity index = 80). It is unlikely that their combined effect would reduce the drained sensitivity appreciably below the observed value of $S_d = 1.7$. If behavior at large strains is to be represented, the assumption that a normally consolidated clay will fail plastically in drained shear must be discarded.

The 'shear strains' that are plotted beyond peak in Fig. 12 are much smaller than the actual strains in the failure zone because a very thin shear zone must begin to form approximately when the peak is reached. (The shear surface observed after test was a very shiny slickenside.) The true shear strains in the failure zone are probably many times greater than those plotted, so it may be more appropriate to speak of the displacements that are required to reach a given point beyond peak. The peripheral displacement at Point m is 0.084 cm, compared with 7.0 cm when the steady state is reached at Point s.

The measured peak shear stress is only $0.22 \bar{\sigma}_{ha}$ and the steady state shear strength is only $0.13 \bar{\sigma}_{ha}$, corresponding to a peak friction angle of 12.5° and a steady state friction angle of 7.5° . The very low peak friction angle may be partially the result of grain orientation, which may already have become significant at the large strain at which this peak occurred.

The volume of the specimen decreased throughout the test. In this case, the peak was not formed because of dilation* against $\bar{\sigma}_h$, but instead was the result of grain orientation at large strains. Even at Point s, where it is estimated that the steady state had been reached, the volume was decreasing at a very slow rate. Thus, Point s does not fully satisfy the definition of steady state. When the peripheral displacement was increased from 7 to 23.5 cm the shear stress remained constant and the volume continued to decrease. It seems probable that these volume decreases were due to loss of soil, (although extreme care was taken to contain this fine-grained clay) because one would expect a gain in strength if the void ratio actually decreased from 0.70 at Point s to 0.62 at Point u. Also, a steady state void ratio close to the void ratio at the plastic limit ($e = 0.61$) seems, intuitively, too low for $\bar{\sigma}_{ha} = 4.0$ kg/sq cm. Further investigation is needed into the void ratio changes that accompany large deformations in rotation shear. It is likely that none of the void ratios in Fig. 12 represent the void ratio in the very thin failure zone in this specimen, except perhaps at the very early stages of the test.

(b) Very Highly Contractive Clay (Quick)

On the basis of Fig. 7, one would expect that a drained test on a 'quick' clay, which is a very highly contractive soil, would give a stress-strain curve with a substantial peak, since even a remolded, normally consolidated specimen showed a drained sensitivity as high as 1.7 (Fig. 12). Although no drained tests on quick clays have yet been carried to large

* In fact, a small amount of energy was being released by this specimen due to volume decrease at peak. This energy causes the magnitude of the peak shear stress to be smaller than it would be if the volume were not changing at peak.

enough strains to prove whether or not a peak does occur, some information on this point may be gained from a study of Fig. 13. It contains the results of a consolidated-drained direct shear test on a Norwegian clay with an undrained sensitivity of 40 to 150. The specimen was consolidated to $\bar{\sigma}_{ha} = 0.58$ kg/sq cm, which is equal to the in-situ effective overburden pressure. The void ratio after consolidation was about 1.19, as compared with void ratios of 0.70 and 0.56 at the liquid and plastic limits, respectively.

The stress-strain curve showed a break* at $\tau = 0.22 \bar{\sigma}_{ha}$, rose to $\tau_m = 0.4 \bar{\sigma}_{ha}$ at a shear strain of 42%, and it displayed no peak. The volume decreased continuously throughout the test. If this test could have been continued to large strains, the shear stress would have increased still further - - to a friction angle greater than 21.9° . It is not clear whether a reduction in shear stress would have occurred at very large strains, but according to Skempton (1964) a soil such as this, with 48% of its grains finer than two microns, would have a steady state friction angle between 10° and 21° . Thus, it is plausible to expect a peak in the stress-strain curve for this quick clay. The drained sensitivity probably would lie between 1.1 and 2.

The state diagram in Fig. 13 shows that the void ratio at Point m was 0.98, which is substantially greater than the void ratio at the liquid limit. One could expect a large volume decrease before reaching steady state in this specimen. The shear stress may therefore increase before decreasing again to the steady state friction angle estimated above.

* Bjerrum and Landva (1966, P. 15) explained the presence of the break as due to breakdown of the sensitive, undisturbed structure of the specimen.

(c) Highly Dilative Clay (Heavily Overconsolidated)

Fig. 14 shows the results of a consolidated-drained rotation shear test on a specimen of remolded Pepper shale that was consolidated to 100 kg/cm² and swelled back to 1.0 kg/cm² before start of rotation. This test is representative for the idealized test shown in Fig. 7, Specimen 2. The stress-strain curve shows the expected sharp peak at a shear stress of $0.5 \bar{\sigma}_{ha}$ and a shear strain of 20%. This shear strain is equivalent to an axial strain of about 12% in the triaxial cell (assuming no effect of method of loading), which is a reasonable peak strain for a heavily overconsolidated, remolded clay. The peak friction angle is 26.6°. At the steady state the shear stress is $0.14 \bar{\sigma}_{ha}$, and the friction angle is 8.2°. The drained sensitivity of 3.4 is not unusually high for such a heavily overconsolidated clay.*

The steady state friction angle of 8.2° in Fig. 14 compares well with the value of 7.5° shown in Fig. 12. (Both of these tests were performed on specimens from the same batch of soil.) The small difference between the two results is practically eliminated when the friction against the confining ring is subtracted. The small horizontal tick marks on the stress paths in Figs. 12 and 14 just below Points s show the steady state strength after removal of this friction. This equality of residual (steady state) friction angles for normally and heavily overconsolidated specimens was anticipated by Skempton (1964, Fig. 6).

* The degree of progressive failure that takes place in a specimen of these dimensions is probably not sufficient to reduce the measured peak shear stress, and hence the drained sensitivity, by more than 20%.

The volume of the specimen of Fig. 14 increased at the maximum rate near the peak point of the stress-strain curve and continued to increase at larger strains, but the point of maximum dilation rate cannot be determined very precisely from these data. When the steady state was reached at Point s, the volume had increased 8%, and beyond that point there was no change in volume or shear stress. In this case, no effect of squeezing out of soil was apparent. But because a shiny slickenside was formed, the observed volume increase very likely represents changes in only a thin zone of the specimen. It is likely that the actual percent volume increase within the failure zone was substantially greater than the recorded value, and that squeezing out was occurring simultaneously. In any event, the shear stress did reach a constant value.

The best estimates of the steady state void ratios from Fig. 12 and 14, assuming uniform specimens in each case, are:

	$\bar{\sigma}_{ha}$ kg/cm ²	Overconsolidation ratio	e_a	e_s (est.)
Fig. 14	1.0	100	0.68	0.81
Fig. 12	4.0	1	0.84	0.70

Although these values may be grossly in error, they do decrease with increasing effective stress as expected.

6. IDEALIZED STRESS-STRAIN CURVES FOR SOILS
SHEARED AT CONSTANT VOLUME

6.1 Uncemented Soils with Hard, Bulky Grains

Fig. 15 shows the idealized relationships among stress-strain curves, changes in effective stress, stress paths, and the state paths followed during constant-volume shear of specimens composed of hard, bulky grains.

For Specimen 1, prepared in a highly contractive state, the stress-strain curve rises to a rather sharp peak and then drops to a steady state shear stress at large strains. The undrained sensitivity shown for this example is about 2. The corresponding stress path shows that the maximum shear stress (Point m) is reached when the effective principal stress ratio is smaller than its value at the steady state (Point s). When Point s is reached, the stress path simply stops--no further change in shear stress or effective normal stress occurs. The state path starts at Point c (Specimen 1) and moves horizontally to the left, since the void ratio is held constant, passing the peak shear stress at Point m and continuing to the left until the steady state line is reached. The line of peaks through Point m lies well above the steady state line. In Fig. 15 (d) the effective minor principal stress is seen to decrease continuously with strain until the steady state is reached. There is no obvious change in curvature as the peak shear stress, Point m, is passed.

Assuming that Specimen 1 was fully saturated and that volume was maintained constant by allowing no change in water content, the stress-strain behavior may be explained qualitatively as the combination of two effects:

(1) the continuous increase in the mobilized effective principal stress ratio with strain, and (2) the simultaneous build-up of pore pressure and consequent reduction of the effective minor principal stress due to the tendency for volume decrease under shear stress.

During the early stages of the test, the shear stress rises because the effect of the increasing principal stress ratio is greater than the effect of the reduction of $\bar{\sigma}_3$. At some point during the test, the effect of the increased principal stress ratio is exactly offset by the effect of the decreasing $\bar{\sigma}_3$. At this point, the peak occurs in the stress-strain curve. At larger strains, the rate of pore pressure build-up is so rapid that, even though the effective principal stress ratio continues to rise slowly, the net effect is a decrease in shear stress, as shown at points beyond Point m in Figs. 15(a) and 15(b). In this case, the drop in shear stress beyond peak is not due to increasing void ratio, as it was in the case of drained tests, nor is it due to orientation of grains. It is merely the effect of a continuous rise in pore pressure as the structure collapses. For this bulky-grained soil, one would expect no decrease of $\bar{\sigma}_1/\bar{\sigma}_3$ even at very large strains, because grain orientation effects should be small.

Specimen 2 is prepared at an initial state that is below the steady state line, Point c, in Fig. 15(c). Again the observed behavior is due to the combined effects of the changes in the effective principal stress ratio and the effective minor principal stress. During the early stages of shear, the pore pressure increases slightly, the effective principal stress ratio rises, and a net increase in shear stress results. The slope of the stress-strain curve decreases up to Point q in Fig. 15(a). But with greater strains,

the soil grains start interfering with each other and the specimen tries to increase in volume. Since the volume increase is prevented by maintaining constant water content, the pore pressure drops so that the effective minor principal stress increases, Fig. 15(d). At this stage, both the changes in $\bar{\sigma}_3$ and in $\bar{\sigma}_1/\bar{\sigma}_3$ tend to increase the shear stress. The combination causes the stress-strain curve to "stiffen," i.e., its slope increases, at Point q in Fig. 15 (a). Subsequently, the pore pressure drops continuously and, therefore, the mobilizable shear stress increases continuously until the steady state is finally reached at very large strains.

The stress path, Fig. 15 (b), shows that the maximum principal stress ratio (Point p) occurs at some stage prior to the stage when the maximum shear stress is reached (Point m). For some time the author felt that such data were the result of test errors. However, Wroth and Bassett (1965, Fig. 7) have shown that the peak principal stress ratio should occur before Point m, at the point when the rate of change of effective minor principal stress is a maximum, i.e., at Point p in Fig. 15 (d). This relationship is analogous to the development of the peak principal stress ratio (or peak shear stress) in drained tests at the point when volume is increasing most rapidly.* Although the principal stress ratio decreases at strains beyond Point p, it does not decrease enough (from this cause) to result in a net decrease in shear stress.

* In the present case, an increased principal stress ratio is needed to increase the effective minor principal stress at constant volume rather than to increase volume at constant stress. For contractive specimens in undrained tests, a smaller principal stress ratio is needed because of the continued decrease in effective minor principal stress. Thus the stress path for Specimen 1 should not be expected to cross the steady state envelope in Fig. 15 (b).

By comparing Fig. 15 for constant volume tests with Fig. 5 for drained tests, one can see the value of the concept of steady state as displayed on the state diagram. Given the steady state line, one can predict the end point for a test on a specimen prepared at any initial state, and one can estimate the shape of a stress-strain curve and the changes in volume or effective stress that will occur as the steady state is approached. More information is needed to judge the conditions that develop at peak, but the location of the steady state line relative to the starting point for the test does set certain broad limits on the resistance and effective stresses that develop at peak.

6.2 Uncemented Soils with Substantial Proportion of Platey Grains

Fig. 16 shows the idealized stress-strain curves, stress paths, state paths and effective minor principal stress curves for contractive and dilative specimens of a platey-grained soil in constant-volume shear.

The major difference between Figs. 15 and 16 results from the substantial grain orientation that can occur in a soil containing chiefly platey (or perhaps elongate) grains. The principal stress ratio that can be mobilized first increases and then decreases appreciably at larger strains, as the grains in the failure zone become orientated. Superimposed on these changes are the changes of effective minor principal stress that are caused by the constraint on volume change.

For the contractive case, Specimen 1, the stress-strain curve can be expected to show a substantial post-peak loss of resistance due to the

combined effect of pore pressure build-up and grain orientation at large strains. The effect of grain orientation at very large strains can be expected to be small, if the specimen remains homogeneous, because the void ratio is so high that the particles are not too close together in any case. The undrained sensitivity shown for this example is about 3.7. The stress path shows that in the steady state the principal stress ratio for this type of soil has a value smaller than its maximum at p_c , which is quite different from the result for bulky-grained soils wherein the maximum principal stress ratio occurs at the steady state. The principal stress ratio drops at large strains as a result of grain orientation. Usually, only at very large strains is there sufficient orientation to observe this drop in principal stress ratio in actual tests.

The state path for Specimen 1 shows Point m to the right of the steady state line. The location of the line of peaks through Point m is a function of the initial state and structure of the specimens, as before. The steady state line is reached when the grains have finally reached a steady-state orientation, just as was the case for drained tests.

The shape of the curve of effective minor principal stress vs. axial strain for Specimen 1, Fig. 16 (d), is similar to that for the bulky-grained soil of Fig. 15. In the present case, the effective minor principal stress at peak is 0.4 times its value at the end of consolidation, which corresponds to a value of Skempton's pore pressure coefficient, A_m , of 0.9. When the steady state is reached, the effective minor principal stress is only one-quarter of its original value, and $A_s = 4.2$.

For the dilative case, Specimen 2 in Fig. 15 (a), the stress-strain curve shows the same initial shape as was given for the bulky-grained specimen in Fig. 15. But in this case, a peak does form at Point m because of grain orientation at larger strains. The stress path passes the maximum principal stress ratio and then rises to the peak when the effect of increasing effective minor principal stress is just balanced by the effect of decreasing principal stress ratio, the latter being caused by grain reorientation. The peak point can be expected to lie on an envelope that is steeper than that for the contractive case, because (1) for the dilative specimen $\bar{\sigma}_3$ is increasing and for the contractive specimen $\bar{\sigma}_3$ is decreasing, and (2) the smaller effective minor principal stress for the dilative specimen may mean that a higher principal stress ratio can be mobilized due to higher interparticle friction. At the steady state, the same point is reached as for the contractive specimen, assuming a unique steady state line and ideal tests.

The line of peaks for dilative specimens, Fig. 16 (c), lies to the left of the steady state line and bears no relation to the line of peaks for highly contractive specimens.

Fig. 16 (d) shows for the dilative specimen the usual small decrease of effective minor principal stress, followed by an increase as the grains interfere and try to cause dilation. The effective stress then rises continuously until the steady state is reached. This change increases the shear resistance, but the stress-strain curve nevertheless shows a drop due to the overpowering effect of grain orientation.

Test errors make it practically impossible to observe all of the characteristics illustrated in Fig. 16. The dashed stress paths and state paths show the expected effect of void ratio changes within an individual specimen due to small initial non-uniformities in void ratio and stress distribution. Specimen 1 tries to contract during shear. On one plane in the specimen the shear stress will be more critical than on adjacent parallel planes and that plane will begin to deform more than its neighbors. In the region close to that plane, the grains will become more orientated than in the adjacent zones and the resistance will, therefore, decrease more rapidly with strain than would be expected for a uniform specimen. For a real test, the stress-strain curve beyond the peak strain would lie to the left of the idealized curve shown for Specimen 1, but at very large strains, the measured stress-strain curve would cross the ideal curve because there would be internal drainage away from the failure zone. The stress path would change from that shown as a solid line in Fig. 16 (b) to that shown dashed. A similar argument leads to the stress path shown dashed for the dilative specimen. Therefore, although for ideal constant-volume tests one might expect to reach the same steady state strength for both dilative and contractive specimens; test errors prohibit that observation. (Specimen non-uniformities also develop in drained tests and they cause errors in measurement of the steady state void ratio. But the steady state strength in drained tests for both contractive and dilative specimens are in closer agreement, as shown in Fig. 6)

In Fig. 16 (d) the Point p (maximum principal stress ratio) is shown at the point where $\bar{\sigma}_3$ is increasing most rapidly, in accordance with the prediction by Wroth and Bassett (1965, Fig. 7). However, observations have not yet confirmed this prediction, as will be seen in Section 7.2.

7. EXAMPLES OF STRESS-STRAIN CURVES FOR SOILS

SHEARED AT CONSTANT VOLUME

7.1 Uncemented Soils with Bulky Grains

(a) Highly Contractive Sand ('Very Loose')

Fig. 17 shows the results of a consolidated-constant-volume triaxial compression test on a fine, uniform sand consolidated to an effective stress of 4.0 kg/cm^2 at a relative density of only 27%. This test illustrates the idealized behavior shown for Specimen 1 in Fig. 15.

The stress-strain curve has a sharp peak, at the low axial strain of 1%, followed by a large drop in shear stress and simultaneous decrease of the effective minor principal stress. At peak the A-value was 1.28, which is in the same range as A-values measured in sensitive, normally-consolidated clays. When Point s was reached, the A-value had increased to about 16! These changes correspond to a loss of all but 3% of the effective consolidation pressure, and an undrained sensitivity of about 8, all of which were caused by the collapse of the very loose structure of this specimen. From the stress path, it is seen that the peak point is reached at $\phi = 30^\circ$. The maximum principal stress ratio developed only at the larger strains corresponding to Point s. Since grain orientation in this soil probably has small effects, no drop of the principal stress ratio occurred even at 20% strain. The point on the state path corresponding to the peak, Point m, occurred at a substantial distance from Point s.

This test result demonstrates the shape of stress-strain curve that occurs when specimens liquefy in the laboratory under static loading. After

test, such specimens segregate into soil at the bottom with a layer of water at the top. A similar shape of curve may be expected to occur in-situ during liquefaction. But a specimen at the same void ratio in-situ would be more unstable than might be deduced from Fig. 17, because of anisotropic consolidation. For example, assume that in-situ $\bar{\sigma}_1/\bar{\sigma}_3 = 1.5$ and $\bar{\sigma}_3 = 3 \text{ kg/cm}^2$, corresponding to Point a in Fig. 17. Then the shear stress need be changed by only $0.05 \bar{\sigma}_{3c}$ to cause liquefaction (Castro, 1969, Fig. 63). Because the strength after liquefaction ($.03 \bar{\sigma}_{3c}$) would be lower than the shear stress at Point a ($.19 \bar{\sigma}_{3c}$), one can expect very large deformations before cessation of movement after liquefaction. Cyclic shear stresses of even smaller magnitude than $.05 \bar{\sigma}_{3c}$ would be sufficient to cause liquefaction in such a specimen.

A. Casagrande has postulated that the liquefied state (Point s in Fig. 17) is a special state in which the particles have adjusted themselves, after collapse of the structure that existed at Point c, so as to offer a minimum resistance to deformation. He referred to this new structure as the "flow structure."* This hypothesis by Casagrande requires investigation, as its implications are important for complete understanding of liquefaction and the interparticle processes that govern the shapes of the stress-strain curves of soils.

* Casagrande made this suggestion in his lectures on soil mechanics that the author attended in 1959 and had made it in previous years also, probably for the first time in the early 1950's or perhaps even earlier.

It seems reasonable that such a state might exist over a limited (but very important in practice) range of strain just after the initial structure collapses. At that stage one might visualize that all particles are momentarily practically floating ($\bar{\sigma}_3 \sim 0$) until sufficient strain occurs to cause them to contact each other again and to tend towards the steady state. The movement between particles that is required to achieve an overall axial strain of 20% is very small. Therefore, Point s in Fig. 17 may not be the steady state as defined in this paper, but it may be a temporary neutral state which will be lost at large strains. If so, the stress path would reverse and move up to the right along a strength envelope inclined at about 30° , and the steady state would be reached at some very large strain not achievable in the triaxial cell. In the state diagram, the steady state would then lie to the right of Point s, and could lie even to the right of Point m.

(b) Sand Close to Steady State Void Ratio

Fig. 18 shows the results of a consolidated-constant-volume triaxial compression test on a fine, uniform, river sand. The specimen was consolidated to the high effective minor principal stress of 35.1 kg/cm^2 at a relative density of 48.5%. This curve deserves considerable attention because it represents behavior of soils prepared at a state close to the steady state.

The early portions of the plots in Fig. 18, up to Point q, look much like the early portion of the corresponding plots in Fig. 17. The following points in the two figures are probably analogous:

	<u>Fig. 18</u>	<u>Fig. 17</u>
Maximum shear stress prior to		
collapse of soil structure	b	m
Maximum pore pressure build-up		
due to collapse of structure	q	s

It is interesting that at Point b (Fig. 18) $\bar{\sigma}_3 = 0.39 \bar{\sigma}_{3c}$, which compares well with the value of $0.40 \bar{\sigma}_{3c}$ at the analogous point in Fig. 17. But the subsequent pore pressure build-up was much less in Fig. 18, reaching a maximum at Point q, where $A = 1.12$, as compared with $A = 16$ at Point s in Fig. 17. Consequently, the drop in shear stress from Point b to Point q in Fig. 18 was slight.

The shape of the curve beyond Point q in Fig. 18 may represent the true behavior of this specimen or it may be due to test error. If it is true behavior, one may explain it with the aid of Casagrande's postulate that just after collapse of the soil structure the particles orientate themselves in such a manner as to offer least resistance to deformation. At this stage, the pore pressure would build up to a maximum value. Subsequent strains would cause the particles to interfere with each other somewhat, resulting in a slight decrease in pore pressure until the steady state is finally reached at large strains. Similar behavior would not be observed in looser specimens (Fig. 17) because extremely large strains would be needed to reach the steady state.

Alternatively, the shape of the stress-strain curve beyond Point q may be due to non-uniform void ratio in the specimen. It may well be that the deformations between Points b and q were concentrated within a small zone that was approaching the steady state of deformation. During this process, the

zone would be contractive and water would flow to adjacent zones. The shear stress would then have to be increased until a fairly large zone of the specimen was in a steady state of deformation. A void ratio variation of only about 0.004 (!) would be sufficient to cause the behavior displayed in Fig. 18. If this interpretation is correct, and if the specimen had a truly uniform void ratio, then the stress-strain curve and the pore pressure curve in Fig. 18 would be as shown dashed. In such a case, one could conclude that this specimen had been prepared at a void ratio almost precisely on the DC-boundary (Fig. 6).

The drop in shear stress at strains beyond Point m is consistent with the probability that grain breakage was occurring during this rather high-pressure test. But if such were the case, the pore pressure probably should have risen simultaneously, which is opposite to what was observed. Therefore, the behavior beyond Point m might be attributed to a test error (due to a slight specimen non-uniformity or slightly incorrect "area correction") or to a combination of grain breakage and test error.

(c) Highly Dilative Sand ('Dense')

Fig. 19 shows results of a consolidated-constant-volume triaxial compression test on a fully saturated specimen of a uniform, medium sand. It was consolidated to $\bar{\sigma}_{3c} = 6.6 \text{ kg/cm}^2$ at a relative density of 84%. A very high back pressure of 63.5 kg/cm^2 was used to ensure that full saturation was maintained throughout shear.

The doubly-curved stress-strain curve that results as the specimen passes from the contractive to the dilative state is very well demonstrated.

The explanation for this shape was given qualitatively by Hirschfeld (1958, P. 144). Later this behavior was explained quantitatively by Wroth and Basset (1965, Fig. 7). The maximum principal stress ratio occurs at the second inflection point of the stress-strain curve, which is also close to the point at which the rate of increase of $\bar{\sigma}_3$ is a maximum, as anticipated by Wroth and Bassett. The A-value for this specimen varies from +0.13 at start of loading to -0.42 at peak and, because of the strong negative pore pressures, the peak shear stress is about $9\bar{\sigma}_{3c}$, or 25 times greater than the maximum shear stress measured for the loose specimen of Fig. 18.

The steady state for this specimen is probably near Point m. But grain breakage was occurring at that stage (Wissa, 1970), which means that the steady state could not truly be reached until grain breakage ceased. The reversal of the stress path beyond peak may be due to cavitation of the pore water, grain breakage, and perhaps to small test errors.

7.2 Uncemented Soils with Substantial Proportion of Platey Grains

(a) Very Highly Contractive Clay (Quick)

Fig. 20 shows the results of a consolidated-constant-volume simple shear test on a normally consolidated specimen of a quick silty clay. The undisturbed specimen was consolidated to an effective stress on the horizontal plane, $\bar{\sigma}_{hc}$, of 2.0 kg/cm^2 at a void ratio of 0.76. The void ratio at the liquid limit is 0.67 and at the plastic limit 0.53 for this soil. Therefore, the undisturbed soil must be very sensitive to disturbance of its structure. The measured undrained sensitivity, obtained by vane tests on several specimens ranged from 40 to 150.

The stress-strain curve displays a slight drop after peak. Because of the presence of platy grains, the shear strain at peak is relatively high, 15% (equivalent to $\epsilon_1 \approx 10\%$), as compared with only 1% axial strain at peak for the very loose, bulky-grained sand of Fig. 17. At the end of test the shear stress and the effective stress on the horizontal plane are still dropping, and the stress path indicates that the effective principal stress ratio is still increasing. If there is to be any drop in the principal stress ratio due to orientation of grains, as anticipated by the stress path for Specimen 1 in Fig. 16, the strains were not sufficient in this test to display that effect. Judging from the undrained sensitivity of 40-150, one might expect that if strain were continued the stress path would continue its movement downward and to the left. For this soil the strains required to reach the steady state would be very large. The steady state probably has not been even closely approached during this test, although it probably was closely approached when the vane tests were performed to measure undrained sensitivity. The A-value at peak is about 1.2, as for the very loose sand of Fig. 17. The steady state A-value probably would be about 100 for this specimen of quick clay.

(b) Highly Contractive Clay (Normally Consolidated)

Fig. 21 shows the results of a consolidated-constant-volume triaxial compression test for a typical normally consolidated clay. The specimen was fully saturated and consolidated to $\bar{\sigma}_{3c} = \text{kg/cm}^2$ at a void ratio of 1.55.

The void ratio at the liquid limit is about 2.2 and at the plastic limit about 1.1.

The stress-strain curve shows the gradual rise to peak, as usually reported for such soils, and the peak strain of 5% is typical. The effective minor principal stress is still dropping at Point m. Therefore, the steady state has not yet been reached for this specimen. The reported undrained sensitivity of 10 means that the stress-strain curve and stress path would stop approximately on a line where $\tau_{45}/\bar{\sigma}_{3c} = 0.04$, as shown on the stress-strain curve.

The peak point A-value was 0.9 and the A-value at the steady state would probably be about 20. Thus the stress-strain curve shown in Fig. 21 is only part of the entire curve and it does not demonstrate whether the principal stress ratio would drop at large strains due to grain orientation. The balance of the curve cannot be obtained in the triaxial test although its shape can be estimated with the aid of vane tests. The corresponding stress path that might have been followed if the test were carried to large strains is shown dashed.

A slightly more complete stress-strain curve for a normally consolidated clay is shown in Figure 22. A specimen of London clay was consolidated from a slurry at a water content of 163% to an effective consolidation pressure of 60.2 kg/cm^2 . It was loaded at constant volume in triaxial compression. In this case the stress-strain curve shows a slight peak--the maximum shear stress occurring at an axial strain of 8.5%, which is not too great when one considers the very high effective consolidation pressure. At peak, $\bar{\sigma}_3$ was still decreasing

and $\bar{\sigma}_1/\bar{\sigma}_3$ was increasing, as for the previous example. But with further strain $\bar{\sigma}_1/\bar{\sigma}_3$ reached a peak and showed a slight drop at the largest strains, as shown by the stress path.

When the test was stopped at 20% strain, ϕ had dropped from a maximum of 16.5° to 15.3° . The latter figure is only 0.3° greater than the steady state (residual) value of 15° reported by Bishop, Webb, and Skinner (1965, Fig. 11) for this soil. This final drop of the principal stress ratio occurred chiefly towards the end of the test where the stress-strain curve turns down slightly. Therefore the change could be due to test error rather than to orientation of grains. Nevertheless, the small difference between the final ϕ -value and the steady state value indicates that the steady state was closely approached in this test. The small difference between ϕ_m and the steady state ϕ is due to the high pressure used. In Fig. 8 it is indicated that the line-of-peaks and the steady state line can be expected to converge at high pressure. It would be expected that the corresponding ϕ -values should converge also.

(c) Highly Dilative Clay (Overconsolidated)

Fig. 23 shows the results of a consolidated-undrained triaxial compression test on a fully saturated, compacted specimen tested at $\bar{\sigma}_{3c} = 2.1 \text{ kg/cm}^2$ and $e_c = 0.5$. The void ratio at the liquid limit is 0.94 and at the plastic limit it is 0.41. Therefore the specimen could be expected to be dilative at the low consolidation pressure used for this test.

The stress-strain curve shows the expected double curvature and gradual rise to maximum shear stress. At the end of test the shear stress and effective minor principal stress are still rising, indicating that the true maximum, i.e., the steady state, could be developed only after substantial additional strains. The first point of inflection corresponds closely to the minimum value of effective minor principal stress, and the second inflection point approximately to the point at which the maximum principal stress ratio is reached. A small reduction of the principal stress ratio occurs at large strains. This change probably is due to the change in rate of increase of $\bar{\sigma}_3$ rather than to orientation of grains.

The steady state was more closely approached in the example illustrated in Fig. 24. An undisturbed, heavily-overconsolidated specimen of London clay was tested at constant volume in triaxial compression at $\bar{\sigma}_{3c} = 1.05 \text{ kg/cm}^2$. In this case the reversal of curvature of the early portion of the stress-strain curve was not observed and the effective minor principal stress dropped extraordinarily rapidly - almost to zero - before starting to rise again. The A-value for this portion of the curve was close to one-third, as shown in the stress path, which is the value exhibited by perfectly elastic materials. It may be inferred that this specimen was cemented.* The cementation accounts for the fact that no reversal of curvature is observed in the stress-strain curve for this specimen.

* Bishop (1969) has shown that London clay does have tensile strength, i.e., it is cemented.

At the peak Point m, a thin failure zone developed along which subsequent displacements were concentrated. (The horizontal axis was given in percent axial displacement rather than strain, since the strains in the failure zone were unknown beyond peak.) Therefore, the clay grains in the failure zone probably became orientated. Also the failure zone probably increased in water content at the expense of adjacent zones (thus the state path for the failure zone is not truly horizontal for this test). These effects would be expected to cause reduction in shear stress and principal stress ratio from Point m to Point s, as was observed. At 11% axial displacement the strains in the failure zone were already large enough to cause the stress path to approach the steady state strength line very closely. This stress path is related to the dashed stress path for the highly dilative specimen in Fig. 16.

8. APPLICATIONS

Several specific examples of how the information presented in Figs. 5, 7, 15 and 16 can be used to help understand soil behavior are given in the subsequent paragraphs of this chapter.

8.1 Significance of the Terms "Normally Consolidated" and Loose"

The distinguishing quality of normally consolidated specimens of water-deposited clays is that they are contractive if tested at effective stresses equal to or higher than the in-situ stresses. (The degree to which they are contractive, as measured by the height of the virgin compression curve above the steady state line, is dependent upon every detail of their geologic history because their composition and structure are dependent upon this history.) Overconsolidation, on the other hand, causes the state of a clay to move toward or even below the steady state line, and a heavily overconsolidated clay is generally dilative if tested at effective stresses equal to or less than the in-situ stresses.

Residual clays are an exception because they may be normally consolidated, never having been subjected to higher effective normal stress than currently exists, and yet have low enough void ratio to be dilative at low effective stresses.

For sands, the term overconsolidation has little meaning because normal stress alters the state of a sand much less than it does the state of a clay. As one passes from clean sands (or rockfills) to clays, there is an increasing influence of pre-existing effective normal stresses on the void ratio after removal of those stresses.

For sands, the term "loose," as defined by Gibbs and Holtz (1957), refers to specimens that have relative densities in the range 15% to 35%. Such specimens generally lie near the steady state line, or perhaps slightly above, and "very loose" refers to specimens lying well above the steady state line. Therefore, relative to stress-strain behavior, the term "very loose", as applied to sands, and "normally consolidated," as applied to clays, are analogous. Similarly, a "dense" sand specimen, for low effective stresses, lies below the steady state line, as do heavily overconsolidated specimens of clay. But a loose sand or a normally consolidated clay tested at high effective stress will be highly contractive, and a dense sand or a heavily overconsolidated clay tested at high pressure may well be contractive also. Thus, one must not attempt to predict the behavior of a specimen unless the stress level is given together with the terms loose, dense, or normally or overconsolidated.

From the above discussion it becomes clear that, with respect to stress-strain characteristics, the state of any soil specimen may be better measured by its position relative to the steady state line.* For example, one could define a "degree of dilativeness" or a "dilativeness index" as:

$$D_i = \frac{e_s - e_{ss}}{e_s}$$

If $D_i = 0$, the specimen is at the steady state void ratio. Negative values of D_i would refer to specimens at void ratios above the steady state line, regardless

* Wroth (1965) apparently was first to use the distance from his critical state line as a measure of the state of a specimen.

of stress level. It would be of interest to investigate the usefulness of such an index in practice. One problem in use, as with other such indices, is that the location of the reference line, in this case the steady state line, must first be determined.

8.2 Selection of Apparatus for Measurement of Stress-Strain Behavior

The stress-strain curve of a soil depends mainly on (a) the soil, (b) its structure, (c) the initial state of the specimen, and (d) the method of loading. If one assumes that a specimen has been carefully selected to be representative of the soil as it exists in the field, then items (a), (b), and (c) are given. To obtain the desired stress-strain curve, it remains only to select a method of loading for the laboratory test that will model the loading that will be followed at any given point in-situ. None of the available apparatus for laboratory shear testing can model every aspect of the stress and strain that occurs during most field loadings (such as earthquakes, lowering or raising of external water level, cutting of a slope, embanking or other loading at top of slope, erosion at toe of slope, wave forces, lowering of groundwater or seepage within slope from reservoir or rainwater). The only condition that leads to failure and that can be modeled reasonably well in the usual laboratory tests is the loss of strength of the soil with time due to pore pressure increases at practically constant shear stress.

One must then, at this stage of development, consider all laboratory stress-strain curves only as indicators of the stress-strain curves that will develop in-situ.

Given the assumption that the laboratory stress-strain curve is at least a rational indicator of the in-situ stress-strain curve, the specimen non-uniformities that develop in most laboratory tests preclude correct determination of the entire stress-strain curve, even for the boundary conditions that are assumed to exist during the laboratory tests. Any time that a stress-strain curve contains a peak, the zone of the specimen that first reaches peak will account for the majority of post-peak deformations. Thus the strain and the void ratio that correspond to the measured shear stress are those in the failure zone, not the averages for the entire specimen. For cases in which the stress-strain curve contains no peak, a large zone failure will develop because the zone that first fails becomes slightly stronger with strain. The major deformations then are shifted to adjacent zones (Casagrande, 1938, P. 6). But, in the case of tests on dilative specimens, in which the overall volume is held constant, if the specimens are sheared slowly enough to permit internal flow of water, the failure zone may increase in void ratio, get weaker, and account for the remaining deformations. In summary, the effects of non-uniformities depend on the shape of the stress-strain curve, the state of the specimen, the constraint imposed on volume change and, if a constant-volume test, on the rate of strain or loading. In drained tests the measured shear strength is only slightly affected, whereas the corresponding average strains and void ratios are incorrect, and in constant-volume tests the average values of all three parameters - the strength, strain, and void ratio - are affected.

Tables 1 and 2 show the author's estimates of reliability of the measured strengths for several apparatus for the extreme cases of highly contractive and highly dilative specimens of bulky and plate-grained soils.

Several interesting points arise from these tables:

- (1) The steady state strength of clays in the constant-volume state probably cannot be measured in currently available apparatus (Table 2). Vane tests may be used to reach the steady state, but the stress conditions at that stage remain unknown.
- (2) The simple shear test is rated highly for a wide variety of conditions.
- (3) The steady state strength of clays in the drained case (the residual strength) is best measured in rotation shear (Table 1). The rotation shear test may be best for measuring steady state resistance of sands, but this possibility remains to be investigated.
- (4) The true triaxial test appears to offer no advantage over the ordinary triaxial test (constant $\bar{\sigma}_3$). However, it provides the opportunity of using a wide variety of stress paths and can therefore be used to model more realistically in-situ stress paths for small strains.

- (5) The triaxial or plane strain tests are reasonable tests to use (neglecting the fact that the corresponding stress paths seldom model in-situ stress paths) for determination of peak strength, except that for highly contractive clays it often is not possible to attain the large strains required to reach the peak.

The large variety of test errors not considered when formulating Tables 1 and 2 include: (1) errors in measurements of loads, volumes and deformations, and (2) leakage of soil, water and air from the specimen during tests. It is assumed that the effects of such errors are reduced to tolerable values in each case, although the difficulty of doing so varies considerably from one test to the other.

8.3 Relation Between Failures in Laboratory Specimens and Failures in the Field

The type of failure occurring in a laboratory specimen can be used to infer the type of failure that will occur in the field, so long as the laboratory stress path models the in-situ stress path reasonably well and the specimen is representative.

When the laboratory specimen exhibits a "plastic" failure and no failure plane forms for the range of strain applied in the laboratory, then the stress-strain curve will show no peak for that range of strain.. In the field, a very wide failure zone would develop in a mass of such soil. Large deformations would occur in the mass and no distinct failure plane would be observed. Such failures are not catastrophic because the deformations warn

of impending failure. Also, field observations are useful for controlling construction, and one is able to use relatively low factors of safety (high working stress) in design because of the character of the failure. In such cases the deformations usually control the design working stress rather than the strength. Obviously the selection of factor of safety (or working stress) is also a function of the consequences of failure and the reliability of the test data.

When a laboratory specimen fails along a narrow zone, the stress-strain curve usually shows a peak. Prototype failures in soils with this shape of stress-strain curve are usually catastrophic. Examples include: (a) failure of highly dilative clays in the drained condition, (b) failure of highly contractive clays (normally consolidated, sensitive or quick clays) sheared at constant volume and (c) liquefaction of sands.* Such failures are seldom preceded by adequate warning of failure, and even careful observations do not normally provide the necessary warning.

Two approaches are currently being investigated to provide predictions of deformations. One is the use of finite element analysis together with laboratory-measured stress-strain data, and the other is the use of model testing e.g. in large centrifuges. Their simultaneous application should lead in the future to substantially improved predictions of movements in-situ.

8.4 Relation between Pore Pressures before and after Failure In-Situ

For any case of constant-volume shear in which an abrupt failure surface develops it is not correct to use pore pressures measured after failure to

* In this last case failure planes are not observed even though the stress-strain curve is sharply peaked. The high pore pressures consequent to liquefaction probably spread rapidly throughout the mass and cause a substantial zone of failure. Perhaps high speed photographs of liquefaction failures in the laboratory would show a failure plane for a brief period.

compute strength parameters in terms of effective stress. After failure the pore pressures in the failure zone are quite different from the pore pressures that existed in the failure zone when the maximum shear stress was acting. Consider the case of Specimen 1 in Fig. 16. At failure (maximum deviator stress) the A-value is 0.9. At the steady state (well beyond failure) the A-value is 4.0 and the shear stress has been reduced to one third of the maximum shear stress. Therefore, the shear stress in unfailed zones adjacent to the failure zone is close to the pre-peak pore pressure, corresponding to $A = 0.3$ in this example. Piezometers in the failure zone after failure would give higher pore pressures than those that caused failure, and piezometers adjacent to the failure zone would give lower pore pressures than those that caused failure. Only by chance would the correct pore pressures be measured after failure.

To obtain reasonable estimates of the applicable strength parameters in terms of effective stress, pore pressure measurements must be made in the failure zone at, or just before, failure.

8.5 Selection of Shear Strength for Stability Analysis

The conventional method for computing the factor of safety against failure in shear involves two distinct steps: (1) computation of the average shear stress along an assumed failure surface and (2) determination of the average shear strength that can be mobilized simultaneously along the entire failure surface.* The ratio of this average shear strength to average shear stress is the factor of safety.

* These two steps are artificially uncoupled, for convenience in analysis of problems in which failure controls, by assuming: (1) a distribution of internal forces in the failure mass and (2) that the stress-strain curve contains no peak.

Stability analysis provides values of shear and normal stress at a number of points along an assumed failure surface. Hence the average shear stress is relatively easily obtained. But to obtain the shear strength that can be mobilized at any point along that surface, one must prepare the soil at the same state (void ratio, effective minor principal stress, and shear stress) and at the same structure as in-situ, and must use the same method of loading (including degree of drainage - which is affected by the degree of saturation, changes in total stresses, strain boundary conditions, and rotation of principal stresses - if any) as will cause failure in-situ.

From the measured stress-strain curves and stress paths one obtains in general, four points that might be chosen to define the shear strength.

These are:

- m Point at which maximum shear stress is reached.
- e Point at which stress path is tangent to envelope of stress paths.
- p Point at which maximum principal stress ratio is reached. Points e and p are always identical for straight-line strength envelopes. For curved envelopes they differ slightly. For the purposes of this discussion, this difference -if any - is neglected.
- s Point at which steady state is reached.

If the test conditions were a true model of those in-situ along the entire failure surface, then Point m would always be used to define strength. But it is not possible to model the degree of progressive failure that occurs along the failure surface in-situ, and it is not even possible to model the

stress path very accurately for a given point on the failure surface.*

Due to these limitations Point m must not be used in all cases to define strength. Recommendations are given below and in Tables 3 and 4 for the point that should be used to define strength and for the factor of safety that should be applied to this strength to account for the effects of progressive failure in-situ. The actual factor of safety to be applied in any given case must be larger than those given in Tables 3 and 4 to account for errors, unknowns, and the seriousness of the failure, if it were to occur. The factors of safety that have been used in the past were developed on the basis of experience with behavior of full-scale embankments and foundations and include, implicitly, the effects of progressive failure. The discussion in this section is aimed at differentiating between the effect of progressive failure and other factors that reduce the working stress.

Hard, bulky-grained soils are considered in Table 3 and platy-grained soils are considered in Table 4. To cover the full range of possibilities, each of these soil types is further divided into the highly contractive and highly dilative cases for both drained and constant-volume shear. To obtain recommendations for intermediate soils, intermediate states, and intermediate constraints on volume change, one may interpolate between the appropriate cases in this table.

* Avgherinos and Schofield (1969) advocate the use of models tested in a large centrifuge. In such a device one can model quite closely to the in-situ conditions. Its use will eventually lead to a more rational application of the results of conventional tests.

(a) Soils Containing Chiefly Bulky Grains

For Case A in Table 3 there is no ambiguity since Points m, e, and s coincide. Complete collapse cannot occur until the full shear strength is mobilized at every point along the failure surface. The absence of a peak (drained sensitivity, $S_d = 1$) means that a broad zone of failure will develop in the prototype rather than an abrupt failure plane. Thus large deformations may occur prior to failure, depending on the geometry of the problem and the strain at Point m, and may control the allowable average stress.* These deformations will warn of impending failure.

For Case B in Table 3 the shear stress at Point a, representing the in-situ condition, is greater than the steady state strength. Therefore, the in-situ condition is one of unstable equilibrium. If progressive failure were no worse in-situ than in the laboratory specimen, one could raise the average shear stress to τ_m before causing a sudden collapse (which in this case would be called liquefaction). But the shear stress at some point will reach τ_s . Therefore, the collapse will occur when the average shear stress lies between τ_m and τ_a . Its value will decrease toward τ_a as the undrained sensitivity ($S_u = \tau_m/\tau_s$) increases, as the strain ϵ_s at Point s decreases relative to ϵ_m , and as the degree of progressive failure increases (due to stress concentrations caused by hard or soft spots, cracks, holes, sharp corners in the geometry, etc.).

* The recommendations in this section apply only if shear failure controls, not if tensile failure or deformations control.

Computations by Bishop (1952) and by Janbu (1971) show that the average shear stress along the most critical surface in a slope composed of an elastic medium is about one-half of the maximum shear stress on that surface. If the stress-strain curve for Case B were linear to Point m and dropped to zero shear strength at all larger strains, and if no progressive failure occurred in the laboratory test, then one would have complete collapse as soon as the average shear stress on the critical failure surface reached about one-half of the peak value measured in the laboratory. At that stage failure would occur locally and the local resistance would drop to zero. Complete failure would ensue shortly. But if the post-peak strength were some positive value, such as τ_s for Case B, then the average stress required to cause failure would be somewhat greater. This reasoning leads the author to suggest that for Case B, the working stress that should be used in stability analysis of a homogeneous slope in such a material is about $1/2 (\tau_m + \tau_s)$. But if τ_a already has been applied (in the drained condition) and it is higher than τ_s , then the higher working stress given by $1/2 (\tau_m + \tau_a)$ should be used in the analysis. Thus, to account for progressive failure in Case B, the factor of safety should be at least:

$$F = \frac{\tau_m}{1/2 (\tau_m + \tau_a)} \quad \text{for} \quad \tau_s \leq \tau_a \quad (1)$$

$$F = \frac{\tau_m}{1/2 (\tau_m + \tau_s)} = \frac{S_u}{1/2 (S_u + 1)} \quad \text{for} \quad \tau_s \geq \tau_a \quad (2)$$

This factor of safety must be increased further if the soil is not rather homogeneous but contains discontinuities that accentuate progressive failure. Furthermore, this factor of safety does not account for other uncertainties that may necessitate a still lower working stress.

The failure for Case B will be sudden and only small deformations are likely to precede failure. Therefore one will have little, if any, warning of failure even if field observations are made. To judge when a failure is about to occur in this case it would be necessary to predict the movements that will precede failure and to compare them with measured movements.

For Case C in Table 3 the stress-strain curve has a peak, and the drained sensitivity seldom exceeds 2. Progressive failure would cause the average shear strength along a failure surface to lie between Point m and Point s. The strength may then be defined by Point m, as in the previous case, and modified by the factor of safety given by Eqs. (1) and (2) to account for progressive failure.

Rowe (1969) has made model tests which may be used to check the above recommendation. His soil was a sand with a drained sensitivity, S_d , of about 1.7, as measured in plane strain tests. Using Eq. (2), but substituting S_d for S_u , one obtains a recommended factor of safety of 1.26 to account for progressive failure. Rowe's measurements showed that the peak strength from the plane strain tests was 1.2 to 1.4 times greater than the average shear strength developed in the model tests. Thus Eq. (2) gives a reasonable estimate of the effects of progressive failure in Rowe's tests. But the degree of progressive failure varies somewhat with the geometry of the

problem and the stress level (Rowe, 1969). Additional tests of this type are urgently needed.

For Case D, a highly dilative sand sheared at constant volume, the Points m and s coincide and fall on a line that lies below the strength envelope. To be conservative one would have to choose this lower line to define the strength. But in a dilative specimen one cannot reach Point m without passing Point e. Having reached Point e, large strains will occur unless negative induced pore pressures develop. Casagrande (1959) recommended that one should not rely on development of negative induced pore pressures because gases may exist in the pore water in-situ and because internal migration of pore water toward the most critical zone may occur to greater extent in-situ than in the laboratory. Both of these effects prevent the strength shown at Point m from developing in a test or in-situ. The measured strength is likely to be slightly greater than that given by Point e. Therefore, for practical purposes it is best to use the strength envelope passing through Point e and to assume no net change in pore pressure during the constant volume shear (which is slightly more conservative than using the drained strength) unless evidence is provided to prove that negative induced pore pressures will develop in-situ. (During earthquakes, negative induced pore pressures do develop.)

The stress paths for constant-volume tests on compacted specimens from shallow depths in the upstream slope of earth dams usually have the shape shown for Case D. Therefore, it is this case that is often involved when analyzing stability against sudden drawdown. To obtain strengths for this case one must

perform undrained tests using stress paths that model reasonably well the stress paths that will occur in the dam. If negative induced pore pressures develop, it should be assumed that the pore pressure induced in-situ will be zero.

One of the test errors that occurs when measuring the stress-strain curve for Case D is migration of water toward the failure zone from adjacent zones in the specimen, just as occurs in-situ. This effect may cause development of a peak in the stress-strain curve, or at least a reduction of the shear strength below that for an ideal test. If one chooses to rely on negative induced pore pressures in-situ, then the effect of the difference in the degree of pore water migration between the laboratory and field must be evaluated.

(b) Soils Containing Chiefly Platey Grains

The conclusions listed above for bulky-grained soils apply equally to the case of platey-grained soils. The only significant differences between the stress-strain curves for the two soil types arise from the larger strains usually needed in platey-grained soils to reach a given position on the stress-strain curve, and from the reduction of principal stress ratio that occurs when grains orientate at very large strains. The latter effect causes an increased sensitivity in all cases.

For Case E, Table 4, strains in the range of 10 to 60% are needed to develop the peak. Very large movements will occur in-situ before any localized failure zone develops. The allowable shear stress will be controlled by

the allowable deformation, unless the geometry of the problem is such as to force failure within a narrow zone. Point m should be used to define the strength, but the working stress should be modified somewhat, depending on the geometry, to account for progressive failure. In this case a factor of safety given by Eq. (2) would be quite conservative to account for progressive failure, but should be applied if progressive failure is severe.

For Case F, the constant-volume failure of a contractive, platey-grained soil (e.g., a normally consolidated clay) one must use Point m to define strength, just as for the corresponding case in bulky-grained soils. It makes no sense to use Point e (= s) in this case because collapse occurs before this point is reached. The extreme sensitivity of 100 or more measured in some quick clays (Hoeg, Andersland and Rolfsen, 1969, Table 1) necessitates a substantial factor of safety to account for progressive failure. Under the best of conditions one should use a factor of safety of 2 (as given by Eq. (2)). But because the extreme values of sensitivity are obtained for soils that also have very low strain at peak, the factor of safety must be increased above 2. Tests and field studies are needed to provide information on the appropriate factor of safety for this case.

Case G, a drained test on a dilative specimen containing chiefly platey grains, is the case considered by Skempton (1964). The peak may occur at relatively small strains (15%), but extremely large strains are needed to develop the much lower steady state strength. Here the strength as defined by Point e (=m) must be modified to account for progressive failure. Skempton (1964, P. 81) pointed out that the average shear strength that is mobilized on

the failure plane in highly dilative clay drops continuously with time toward the residual (steady) state strength due to progressive failure, at least in clays or clay-shales that contain slickensides. For short times these soils can sustain shear stresses considerably greater than the steady state strength. The important variables that have to be considered when attempting to account for progressive failure in such soils are:

(1) the detailed fabric of the soil. In particular, one must scrutinize the material to determine whether it contains joints, fissures, or other discontinuities. If so, are these surfaces slickensided? What is their inclination relative to the shear stresses in the mass and what is their size and number? (2) The time available for progressive failure. (3) The amount of movement that is needed to reach the steady state.

The nature and extent of discontinuities can be expected to affect severely the rate of drop in strength toward the steady state value. If there are none, then an average shear stress near the peak strength may be mobilized for short times, even when the drained sensitivity is high ($S_d = 5$ to 10). This suggestion is different from that given for bulky-grained soils (ie., Eq. (2)), because the movements required to reach the steady state are much larger for platey-grained soils than for bulky-grained soils. Although local failure may occur when the average shear stress is as given by Eq. (2), the post-peak rate of drop in shear stress with strain is so small that a substantial proportion of the peak strength can be mobilized. If no macroscopically visible points exist at which shear stresses are highly concentrated, then it seems reasonable to expect that considerable time will be required before creep will lead to substantial orientation of grains at the sites of highest shear stress, and hence to a continuation of

the progressive failure. But the presence of visible discontinuities will speed the process. Even when visible discontinuities do not exist, discontinuities at the scale of the grains do exist and can be expected to lead to progressive failure in time.

The author refrains from making any quantitative recommendations on the effect of these variables. Instead, the reader is referred to Skempton (1964) for information on London clay and for insight into the type of data needed to make a proper judgment. At this time only guesses can be made unless full-scale behavior has been analyzed. In the future, centrifugal model testing may provide a less expensive but satisfactory means for obtaining more data, although the time (creep) effects still will remain unknown.

Case H, constant-volume shear of a highly dilative, platy-grained soil, will be less critical under similar loading conditions than the corresponding drained case, Case G. The discussion given for Case D in Table 3 applies also for Case H. For Case H the stress-strain curve would show a peak and drop-off due to grain orientation at large strains and this peak would be accentuated by the development of a thin failure zone and migration of water toward this zone, both in the laboratory and in-situ. Internal migration of water toward the failure zone in-situ would make this case revert to Case G, and the corresponding discussion would apply. The constant-volume condition cannot be maintained over very long periods of time in-situ, so that the problem of progressive failure with time is unlikely to arise for this case.

(c) Comments on the Use of Tables 3 and 4

To obtain recommended strength to be used in stability analysis, one must first compute the stresses in-situ, then perform a test that models the in-situ stress path on a specimen that is representative (in type of soil, structure, and state). From this stress-strain curve, a strength is selected based on Tables 3 and 4 and plotted as a function of the stresses at Point a. In this manner a "working" strength line is developed. The equation for this line may then be inserted in the stability analysis.

Although the effects of the following factors are not discussed herein, the reader should not neglect to consider their effects on the relation between laboratory and field stress-strain curves:

- (1) Disturbance of specimens
- (2) Presence of gravel, shells, or other hard inclusions in the specimens
- (3) Rate of loading
- (4) Effects of repeated loading
- (5) Degree of saturation (it should be the same in the laboratory as in-situ, or a conservative value should be used)
- (6) Orientation of specimen relative to applied stresses (if the specimen is anisotropic)
- (7) Temperature

Finally, it should be remembered that the recommendations given in this section apply only when shear failure controls design, and do not apply when the allowable deformations limit the allowable stress or when tensile failure may occur.

9. CONCLUDING REMARKS

The systematic view presented in this monograph on the stress-strain curves of soils, and the discussion of major factors affecting their shape, permit one to fit any individual stress-strain curve into a pattern that is very useful for: (1) isolating gaps in knowledge about the stress-strain characteristics of a given soil, (2) for minimizing the number of tests required to gain fairly complete insight into its behavior (by performing only those tests needed to define the pattern of change on the state diagram and by separating the important variables in a rational manner), (3) for discovering test errors, and (4) for understanding the application of stress-strain data to practical problems.

A review of stress-strain data that have been reported for drained and constant-volume compression and direct (or simple) shear tests on sands and clays has led the author to idealized relationships among stress-strain curves, stress paths, state paths, and volume change or change in effective minor principal stress. These relationships are illustrated in Fig. 5, 7, 15, and 16. Typical examples of test data that lend support to the idealizations, and from which the idealizations were extracted, are given in Figs. 9-14 for the drained case and in Figs. 17-24 for the constant-volume case.

The main concepts and test results that led to the generalizations in this monograph are listed below so that areas of departure from previously published work and potential areas of disagreement will be easily isolated.

- (1) The steady state of deformation is that state in which a specimen is deforming continuously and monotonically without change in shear

stress, effective normal stress, volume, and velocity of deformation.

- (2) The most important factors that control the shape of stress-strain curves of soils are:
- (a) The Soil (particularly its mineralogy and grain shape)
 - (b) Structure (large and small scale, including cementation bonds, if any, and orientation of structure relative to principal stress)
 - (c) Initial State (void ratio, effective normal stress and shear stress)
 - (d) Method of Loading (stress path in principal stress space)

Other variables that have important effects in some cases, but are not discussed herein, are: rate of loading, magnitude and frequency of cyclic stressing, temperature, absolute value of pore pressure, and test errors.

- (3) It is hypothesized that for any given soil there exists a unique steady state line:

$$e = f(\bar{\sigma})$$

where $f(\bar{\sigma})$ is affected by the velocity of deformation in the steady state but is not affected by the initial structure of the soil, its initial state, and the particular stress path used to reach a given steady state. The steady state cannot be reached unless particle breakage and particle orientation, if any, have been carried to completion. If particle breakage occurs, the steady state line applies only for the resulting soil. This steady state is identical to the critical void ratio introduced by Casagrande (1936), but is quite different, in most cases, from the concept of critical state as used by Schofield and Wroth (1968).

- (4) The stress-strain curves of normally consolidated (highly contractive) clays contain a peak in both drained and constant-volume shear tests.

- (5) The stress-strain curves of very loose sands in constant-volume shear also contain a peak, which contrasts with the "plastic" stress-strain curve that is often reported. This case is directly analogous to constant-volume shear of a sensitive clay. In sand the failure is called liquefaction, and in clay it is called a flow slide or a shear failure.
- (6) The major difference between the shapes of stress-strain curves of clays and sands is the much larger strain required to reach peak stress and the steady state shear stress in clays, due to their content of platey-shaped grains. (Time effects are also greater in clays than in sands, but these are not discussed herein.)

The understanding gained from this empirical study of stress-strain curves leads to many ideas that are useful in practice, some of which are described in Section 8. To help make this information useful to the reader, it is recommended that one perform both drained and constant-volume triaxial tests on specimens of at least one clay and one sand prepared in states on both sides of the steady state line of Fig. 1, and compare the results with the idealizations presented in this monograph.

The important factors that control the shape of the entire stress-strain curve, from small to very large strains, have been clearly stated in qualitative terms. It is hoped that the quantitative effects of each of these factors will be measured in future research programs, so that ultimately one will be able to understand the advantage and limitations of mathematical models of particulate materials.

A warning is given here concerning certain limitations in the contents of this monograph:

- (1) The idealized shapes of stress-strain curves apply only for uncemented soils. The effects of cementation are important in practice, but are not covered.
- (2) Attention was concentrated on highly dilative and highly contractive specimens and those prepared at states near the steady state line. The shapes of stress-strain curves vary between those shown for these limits. But the case of extremely dilative specimens (e.g., randomly jointed rocks) is not covered.
- (3) Practically no mention has been made of degree of saturation. It is assumed to act through its effect on the stress path that develops when the total stress changes, boundary displacements, and permissible volume changes during shear have been selected. This assumption means that if effective stress is properly defined in a partially saturated soil, the soil's behavior in terms of effective stress will be independent of degree of saturation. The assumption is reasonable for high degrees of saturation (perhaps >80%), but the behavior can be expected to change when one moves to lower degrees of saturation.

- (4) No information is given on the detailed effects of the alternative methods of loading that are available, such as axial compression, lateral extension, axial extension, rotation shear, and torsion shear. Rather, it is expected that the type of test will be selected in any given case to model the in-situ stresses and strains reasonably well.

AUTHOR'S NOTE

The information presented in this monograph is the direct outgrowth of the doctoral research carried out at Harvard University by Castro (1969) and by LaGatta (1970) on liquefaction and residual strength, respectively. These topics, both suggested by Professor A. Casagrande, at the time seemed quite unrelated. However, the research showed that both phenomena could be viewed as steady state deformations that are achieved in different ways. The information in this monograph was drafted and presented in essentially its present form during lectures on shear strength at Harvard University in the spring of 1968 and 1969. The paper was finalized while the author was on sabbatical leave at the University of Manchester from January through June, 1970.

The research of Drs. Castro and LaGatta, as well as part of the salary of the author during that time, was funded through grants to Professor Arthur Casagrande from the Waterways Experiment Station of the U. S. Army Corps of Engineers.

LIST OF NOTATIONS

A Skempton's pore pressure coefficient defined by the equation:

$$\Delta u = B \{ \Delta \sigma_3 + A (\Delta \sigma_1 - \Delta \sigma_3) \}$$

a Subscript to denote stage of a test when a specimen is anisotropically consolidated, just before start of shear at constant water content

c Subscript to denote stage of a shear test when a specimen is isotropically consolidated

cm Centimeter

C_u Coefficient of uniformity

D_{10} Size for which 10% by weight of grains in a specimen are smaller

e Void Ratio

e_{min} Minimum void ratio of a specimen

e_{max} Maximum void ratio of a specimen

G_w Degree of saturation

H Height or thickness of specimen

i Subscript to denote stage of a test when the specimen is in its initial, as-molded, or as-compacted condition

I.D. Inside Diameter

in. Inch

L_w Liquid limit

m Subscript to denote stage of a shear test when the shear stress on the specimen is maximum

m Meter

n Porosity

o Subscript used interchangeably with "i"

O.D.	Outside Diameter
P	Subscript to denote stage of a shear test when the effective principal stress ratio is a maximum
P_i	Plasticity Index
P_w	Plastic Limit
R_d	Relative density
s	Subscript used to denote stage of a shear test when the steady state has been reached. Sometimes used for the last point on the stress-strain curve if steady state has not been reached.
S_d	Drained sensitivity (= τ_m / τ_s for drained shear)
S_u	Undrained sensitivity (= τ_m / τ_s for shear at constant water content)
s_s	Specific gravity of solids
u	Pore pressure
V	Volume
v	Volumetric Strain (= $\frac{\Delta V}{V}$)
w	Water Content
w_{nat}	Natural Water Content
w_{opt}	Optimum water content from compaction test
δ	Shear strain (= δ/H)
γ_d	Dry unit weight
ϵ	Axial strain (= $\Delta H/H = \delta/H$)
θ	Slope of a line through the origin and any given point on the stress path plotted in terms of τ_{45} vs. $\bar{\sigma}_{45}$.
μ	Micron (10^{-6} meter) \equiv micrometer
σ	Total normal stress
$\bar{\sigma}$	Effective normal stress
$\bar{\sigma}_1$	Effective major principal stress
$\bar{\sigma}_3$	Effective minor principal stress
$\bar{\sigma}_{45}$	(= $(\bar{\sigma}_1 + \bar{\sigma}_3)/2$) Effective normal stress on plane inclined at 45° to the principal planes.
$\bar{\sigma}_h$	Effective normal stress on horizontal plane
$\bar{\sigma}_1 / \bar{\sigma}_3$	Effective principal stress ratio

τ Shear Stress

$\tau_{45} = (\sigma_1 - \sigma_3)/2 = (\bar{\sigma}_1 - \bar{\sigma}_3)/2 = \tau_{\max}$ Shear stress on plane inclined at 45° to the principal planes. This plane sustains the maximum shear stress in the specimen.

τ_h Shear stress on horizontal plane

ϕ Slope of line passing through origin and tangent to the Mohr circle (plotted in terms of effective stress) for a selected stage of a shear test. For example, ϕ_m = slope for Mohr circle at stage when the shear stress has reached its maximum value during a particular test.

LIST OF REFERENCES

- AVGHERINOS, P. J. and SCHOFIELD, A. N. (1969). "Drawdown Failures of Centrifuged Models," Proceedings Seventh International Conference on Soil Mechanics and Foundation Engineering, Vol.2, PP. 497-505.
- BISHOP, A. W. (1952). The Stability of Earth Dams, Ph. D. Thesis, University of London, Imperial College.
- BISHOP, A. W. (1967). "Progressive Failure - with Special Reference to the Mechanism Causing It," Proceedings of the Geotechnical Conference, Oslo, Vol. II, PP. 142-150.
- BISHOP, A. W. WEBB, D. L., and LEWIN, P. I. (1965). "Undisturbed Samples of London Clay from the Ashford Common Shaft: Strength-Effective Stress Relationships," Geotechnique, Vol. 15, No. 1, PP. 1-31.
- BISHOP, A. W., WEBB, D. L., and SKINNER, A. E. (1965). "Triaxial Tests on Soil at Elevated Cell Pressures," Proceedings Sixth International Conf. on Soil Mechanics and Foundation Engineering, Vol. 1, PP. 170-174.
- BJERRUM, L. and LANDVA, A. (1966). "Direct Simple-Shear Tests on a Norwegian Quick Clay," Geotechnique, Vol. 16, No. 1, PP. 1-20
- CASAGRANDE, A. (1936). "Characteristics of Cohesionless Soils Affecting the Stability of Slopes and Earth Fills," Journal BSCE, January PP. 257-276.
- CASAGRANDE, A. (1938). "Investigation of Critical Density of Sand from Franklin Falls, N.H." Pages BII-1 through 16 of Appendix BII from a report by the U. S. Army Engineer Office, Boston, entitled Compaction Tests and Critical Density Investigations of Cohesionless Materials for Franklin Falls Dam and dated June 1938.
- CASAGRANDE, A. (1941). Triaxial Compression Tests on Cohesive Soils, "Third Progress Report to U. S. Waterways Experiment Station on Cooperative Research on Stress-Deformation and Strength Characteristics of Soils," Harvard University, Cambridge, May.
- CASAGRANDE, A. (1950). "Notes on the Design of Earth Dams," Contributions to Soil Mechanics, 1941-1953, Boston Society of Civil Engineers, PP. 231-255. (Reprinted from Journal BSCE, Vol. 37, No. 4)

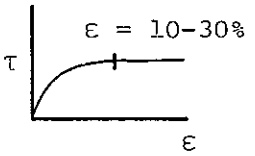
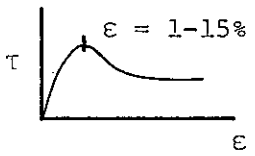
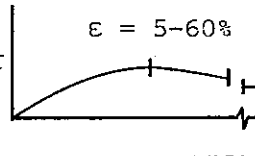
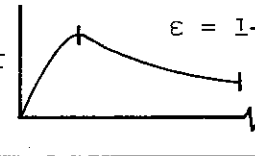
- CASAGRANDE, A. (1959). Lectures at Harvard Univeristy in the courses Soil Mechanics I and II, Engineering 261 (a) and Engineering 261(b).
- CASAGRANDE, A. and HIRSCHFELD, R. C. (1962). Second Progress Report on Investigation of Stress-Deformation and Strength Characteristics of Compacted Clays, Harvard Soil Mechanics Series No. 74, Cambridge PP. 1-82
- CASAGRANDE, A. and POULOS, S. J. (1964). Fourth Report on Investigation of Stress-Deformation and Strength Characteris of Compacted Clays, Harvard Soil Mechanics Series No. 74, Cambridge, PP. 1-82.
- CASTRO, G. (1969). Liquefaction of Sands, Harvard Soil Mechanics Series No. 81, Harvard University, Cambridge, PP. 1-112. (Ph. D. Thesis)
- CORNFORTH, D. H. (1964). "Some Experiments on the Influence of Strain Conditions on the Strength of Sand," Geotechnique, Vol. 14, No. 2, PP. 143-167.
- GIBBS, H. J. and HOLTZ, W. G. (1957). "Research on Determining the Density of Sands by Spoon Penetration Testing," Proceedings Fourth International Conference on Soil Mechanics and Foundation Engineering, Vol. I, PP. 35-39. (Also Earth Laboratory Report No. EM-460, Bureau of Reclamation, Denver, 1956).
- HIRSCHFELD, R. C. (1958). Factors Influencing the Constant-Volume Strength of Clays, Ph. D. Thesis, Harvard University, Cambridge, PP. 1-390.
- HOEG, K., ANDERSLAND, O. B. and ROLFSEN, E. N. (1969). "Undrained Behavior of Quick Clay under Load Tests at Asrum," Geotechnique, Vol. 19, No. 1, PP 101-115.
- JANBU, N. (1971). "Slope Stability Computations," Contributions to Embankment-Dam Engineering, Wiley, in preparation Sept. 1971.
- LADD, C. C. (1965). "Stress-Strain Behavior of Anisotropically Consolidated Clays During Undrained Shear," Proceedings Sixth International Conf. on Soil Mechanics and Foundation Engineering, Vol. I, PP. 282-286.
- LADD, C. C. (1970). Original data for Fig. 21, supplied by letter dated October 15, 1970, to S. J. Poulos.
- LAGATTA, D. P. (1970). Residual Strength of Clays and Clay-Shales by Rotation Shear Tests, Ph. D. Thesis, Harvard University, Cambridge.

- LAGATTA, D. P. (1971). The Effect of Rate of Displacement on Measuring the Residual Strength of Clays, U. S. Army Corps of Engineers, Waterways Experiment Station, in print Marv 1971.
- LAMBE, T. W. (1953). "The Structure of Inorganic Soil," Proc. ASCE, Vol. 79, Separate No. 315, PP. 1-49
- LAMBE, T.W. (1964). "Methods of Estimating Settlement," Journal of Soil Mechanics Division, ASCE, Vol. 90, No. SM5, Part 1, PP. 43-67.
- LANDVA, A. (1962). En eksperimentell undersøkelse av Skaerfastheten i normalkonsoliderte leirer:avhandling. Norwegian Geotechnical Institute Internal Report, F. 175-6.
- LEE, K. L. (1970). Letter dated March 11, 1970.
- LEE, K. L. and SEED, H. B. (1967). "Drained Strength Characteristics of Sands" Journal Soil Mechanics and Foundations Division, ASCE Vol. 93, SM6, PP. 117-141.
- MARSAL, R. J. (1967). Behavior of Granular Soils, Pan-American Soils Course, Universidad Catolica Andres Bello, Caracas, PP. 1-229
- ROSCOE, K. H., SCHOFIELD, A. N. and WROTH, C.P. (1958). "On the Yielding of Soils," Geotechnique, Vol. 8, PP. 22-53.
- ROWE, P. W. (1962). "The Stress-Dilatancy Relation for Static Equilibrium of an Assembly of Particles in Contact," Proceedings of the Royal Society Series A, Vol. 269, No. 1339, PP. 500-527.
- SCHOFIELD, A. N. (1970). Private Communication.
- SCHOFIELD, A. N. and WROTH, C. P. (1968). Critical State Soil Mechanics, McGraw-Hill, PP. 1-310.
- SKEMPTON, A. W. (1964). "Long-Term Stability of Clay Slopes," Geotechnique, Vol. 14, No. 2, PP. 77-102.
- SKEMPTON, A. W. and NORTHEY, R. D. (1952). "The Sensitivity of Clays," Geotechnique, Vol. III, No. 1, PP. 30-53.
- SKINNER, A. E. (1970). Letter dated June 9, 1970, containing original data used to prepare Fig. 18.
- TAYLOR, D. W. (1948). Fundamentals of Soil Mechanics, Wiley, New York.

- WATSON, J. D. (1938). "Investigation of Critical Density of Sand from Franklin Falls, N. H." Pages BII-17 through 38 of Appendix BII from a report by the U. S. Army Engineer Office, Boston, entitled Compaction Tests and Critical Density Investigations of Cohesionless Materials for Franklin Falls Dam and dated June 1938. See also Watson (1940, Chapter V).
- WATSON, JOHN D. (1940). Stress-Deformation Characteristics of Cohesionless Soils from Triaxial Compression Tests, Ph. D. Thesis, Harvard University, Cambridge.
- WEBB, D. L. (1966). The Mechanical Properties of Undisturbed Samples of London Clay and Pierre Shale, Ph. D. Thesis, University of London. (In two volumes).
- WISSA, A. E. Z. (1970). Letter dated March 30, 1970, to S. J. Poulos.
- WISSA, A. E. Z. and LADD, C. C. (1965). Shear Strength Generation in Stabilized Soils. MIT Research Report R65-17 (Soils Publication No. 173) to U. S. Waterways Experiment Station, Cambridge, Mass., June, PP 1-290.
- WROTH, C. P. and BASSETT, R. H. (1965). "A Stress-Strain Relationship for the Shearing Behavior of a Sand," Geotechnique, Vol. 15, No. 1, PP. 32-56.

TABLE 1 RELATIVE ACCURACY OF PEAK AND STEADY STATE STRENGTHS MEASURED
WITH VARIOUS APPARATUS - DRAINED TESTS

Limitations of Table (1) Relative accuracy given for uncemented, highly dilative or highly contractive specimens tested with increasing σ_1 . For intermediate states, relative accuracy is intermediate. No attempt made to consider tests with decreasing σ_1 . (2) Strengths measured in each apparatus differ due to differences among boundary conditions during loading. Correct apparatus is the one that gives best accuracy and models reasonably the in-situ method of loading. These two needs are often incompatible. (3) Use of lubrication on boundaries or special care to reduce effects of boundary friction has been assumed for triaxial and plane strain tests.

TYPE OF APPARATUS	MAXIMUM ACHIEVABLE STRAIN, %	RELATIVE SPECIMEN UNI- FORMITY AT PEAK a)	CHIEFLY BULKY GRAINS				CHIEFLY PLATEY GRAINS			
			HIGHLY CONTRACTIVE		HIGHLY DILATIVE		HIGHLY CONTRACTIVE		HIGHLY DILATIVE	
										
			PEAK	STEADY STATE	PEAK	STEADY (b) STATE	PEAK	STEADY (b) STATE	PEAK	STEADY (b) STATE
Triaxial	~30	1	No Peak	2	1	2	4-5	5	1	3 ^{c)} -5
Direct Shear	100+	4		2	2	3	4	2-5	2	2 ^{d)} -5
Simple Shear	~100	2		1	1	1	1	2-5	1	2-5
Plane Strain	~20	2		2	1	2	4-5	5	1	3 ^{c)} -5
Rotation Shear	8	3		1?	2?	1?	2	1	2	1
True Triaxial ^{e)}	~15	2?		2?	2?	2?	4-5	5	1?	3-5
Hollow Cylinder (Torsion)	?	?		?	?	?	?	5	?	5

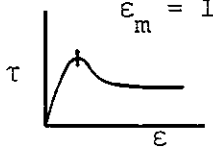
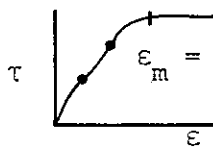
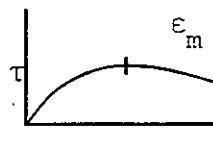
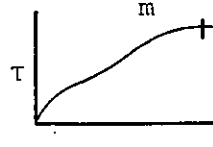
Scale of Relative
Accuracy

- 1 Best
- 2 Good
- 3 Fair
- 4 Poor
- 5 Impractical or Impossible

- a) Relative accuracy controlled by achievable strain and uniformity of specimen at each stage, in addition to parameters in table headings. Specimens are less uniform at steady state than at peak, except when both are same.
- b) Failure develops in narrow zone, or zones, in which void ratio is quite different from average value. Strains and void ratio in failure zone therefore generally unknown.
- c) Shear on pre-formed failure surface will yield a good value.
- d) Repeated reversal of shear direction will provide a reasonable value of steady state strength.
- e) Independent control of σ_1 , σ_2 and σ_3 .

TABLE 2 RELATIVE ACCURACY OF PEAK AND STEADY STATE STRENGTHS MEASURED
WITH VARIOUS APPARATUS IN CONSTANT-VOLUME TESTS

Limitations: (1) Relative accuracies are given for uncemented, highly dilative or highly contractive specimens tested by increasing σ_1 . For intermediate states, relative accuracy is intermediate. No attempt made to consider tests with decreasing σ_1 . (2) Strengths measured in each apparatus differ due to differences among boundary conditions during loading. Correct apparatus to use is the one that gives best accuracy and models reasonably the in-situ method of loading. These needs often incompatible. (3) Use of lubrication on boundaries (or special care to reduce effects of boundary friction) assumed for triaxial and for plane strain tests.

TYPE OF APPARATUS	MAXIMUM STRAIN, %	RELATIVE SPECIMEN UNIFORMITY AT PEAK a)	CHIEFLY BULKY GRAINS				CHIEFLY PLATEY GRAINS			
			HIGHLY CONTRACTIVE		HIGHLY DILATIVE		HIGHLY CONTRACTIVE		HIGHLY DILATIVE	
			$\epsilon_m = 1-10\%$ 		$\epsilon_m = 10-20\%$ 		$\epsilon_m = 5-60\%$ 		$\epsilon_m > 10\%$ 	
			PEAK	STEADY STATE	PEAK	STEADY STATE	PEAK	STEADY b) STATE	PEAK	STEADY b) STATE
Triaxial	~30	1	1	2?		2	2-4	5	1	5
Direct Shear	100+	4	3	?		2	4	5	2	5
Simple Shear	~100	2	1	2		1	1	5	1	5
Plane Strain	~20	2	1	3		2	2	5	1	5
Rotation Shear	8	3	(2)	(1)	NO PEAK	(2)	(2)	(5)	(2)	(5)
True Triaxial c)	~15	2?	1?	2?		3	2	5	2	5
Hollow Cylinder (Torsion)	?	?	?	?		?	?	5	?	5

Scale of Relative Accuracy

- 1 Best
- 2 Good
- 3 Fair
- 4 Poor
- 5 Impractical or Impossible

() Apparatus not available. Estimate included to indicate possible usefulness.

a) Relative accuracy controlled by achievable strain and uniformity of specimen at each stage of test, in addition to parameters in table headings. Specimens are less uniform at steady state than at peak except when both are same.

b) Failure develops along a single plane. Volume of failure zone changes even though overall volume is held constant. Hence measured strength lies between that for drained and constant-volume tests. Peak is slightly affected; steady state strength is strongly affected.

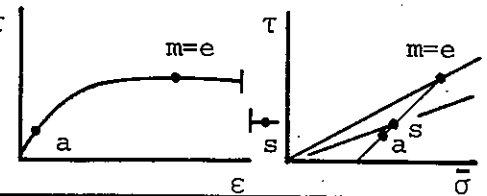
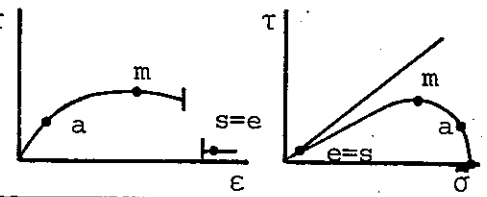
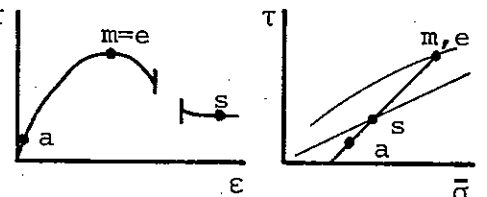
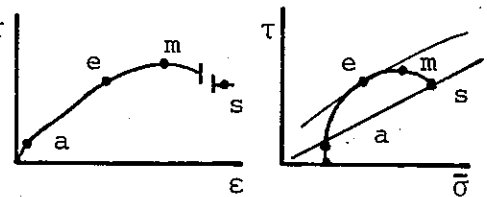
c) Independent control of σ_1 , σ_2 , σ_3 .

TABLE 3 SELECTION OF STRENGTH FOR STABILITY ANALYSIS
HARD, BULKY-GRAINED SOILS

CASE	STATE	TEST TYPE	REPRESENTATIVE STRESS-STRAIN CURVE AND STRESS PATH (Specimens anisotropically consolidated to Point a)	STRENGTH DEFINED @	FACTOR OF SAFETY FOR PROGRESSIVE FAILURE	TYPE OF FAILURE	NOTES
A	CONTRACTIVE	DRAINED		m e s	1	Gradual	Large deformations may precede failure and may control factor of safety. Undrained case is more critical (for same method of loading). If loading is transformed to undrained, liquefaction occurs.
B		CONS. VOLUME		m	$\frac{\tau_a > \tau_s}{\frac{1}{2}(\tau_m + \tau_a)}$ $\frac{\tau_a < \tau_s}{\frac{1}{2}(\tau_m + \tau_s)}$	Abrupt	Small strains precede abrupt failure (liquefaction). Extreme care necessary if in-situ shear stresses exceed steady state strength. For $\tau_a > \tau_s$, the soil is in unstable equilibrium. Larger values of factor of safety needed if conditions in situ are non-homogeneous.
C	DILATIVE	DRAINED		m e	$\frac{\tau_m}{\frac{1}{2}(\tau_m + \tau_s)}$	Abrupt	Failure is abrupt but seldom is a dilative sand loaded sufficiently to cause failure. Rowe (1967) has made model tests that show effects of progressive failure.
D		CONS. VOLUME		e	1	Gradual	Pore water migration toward zones nearest failure and presence of gas in pore water prevent negative pore pressures from developing in-situ and should not be relied upon. Drained case is lower limit.

- MAJOR ASSUMPTIONS
1. Soil tested and its structure are representative of soil at modelled point in-situ.
 2. Initial state and method of loading are both satisfactory representations of in-situ conditions.
 3. Failure in shear controls, rather than deformations or tensile cracking.
 4. Stress-strain curves of all soils along assumed failure surface have similar strains at peak and sensitivity, i.e. similar shape.

TABLE 4 SELECTION OF STRENGTH FOR STABILITY ANALYSIS
PLATEY-GRAINED SOILS

CASE	STATE	TEST TYPE	REPRESENTATIVE STRESS-STRAIN CURVE AND STRESS PATH (Specimens anisotropically consolidated to Point a)	STRENGTH DEFINED @	FACTOR OF SAFETY FOR PROGRESSIVE FAILURE	TYPE OF FAILURE	NOTES
E	CONTRACTIVE	DRAINED		m e	1 (higher if clay lies in a thin seam)	Gradual ↓ Abrupt	Very large deformations precede failure. They are very likely to control factor of safety. The undrained case is more critical (assuming all other aspects of method of loading are identical). Abrupt failure plane forms only after very large strains.
		CONS. VOLUME		m	1.1 if ϵ_m is $> 20\%$ Same as Case B if $\epsilon_m < 10\%$	Abrupt	Large deformations precede failure unless cementation, as exists in some undisturbed clays, results in quite low failure strain. Typical of normally consolidated clays. (Quick clay behavior is more closely related to that of loose sands, so Case B is applicable.) If $\tau_a > \tau_s$, the soil is in unstable equilibrium. The larger that ϵ_m is, the more likely that deformations control working stress.
G	DILATIVE	DRAINED		m e	1 to τ_m / τ_s	Abrupt	Usually large strains precede abrupt failure. Factor of safety on peak strength varies with time and with nature of existing discontinuities and with drained sensitivity. See Skempton (1964) and Skempton & Hutchinson (1969). Continuous creep toward failure if $\tau_a > \tau_s$.
		CONS. VOLUME		e	For long term, assume drained. For short term, use F=1 with τ_e	Gradual ↓ Abrupt	Pore water migration toward zone of highest shear stress causes strength to be close to drained Case G even though entire mass remains at constant volume. Large strains needed to define steady state strengths. For very rapid loading, Point m strength could be realizable for short period.

- MAJOR ASSUMPTIONS
1. Soil tested and its structure are representative of soil at modelled point in-situ.
 2. Initial state and method of loading are both satisfactory representations of in-situ conditions.
 3. Failure in shear controls, rather than deformations or tensile cracking.
 4. Stress-strain curves of soils along assumed failure surface have similar strains at peak and similar sensitivity, i.e., similar shape.

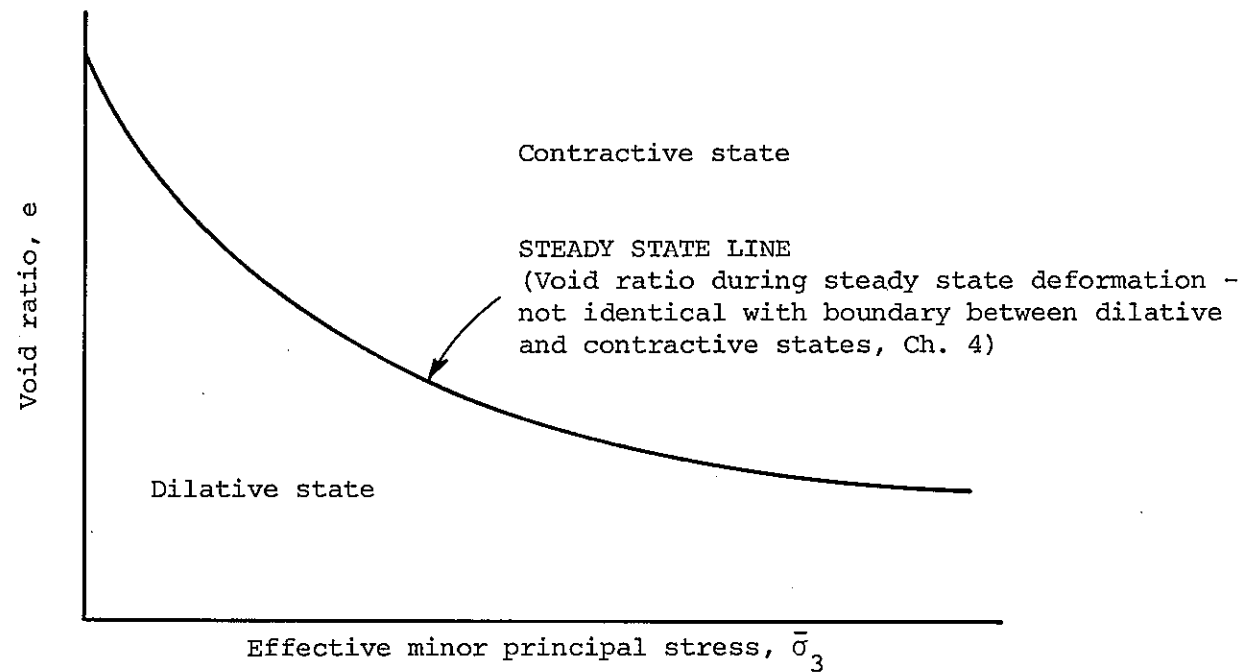
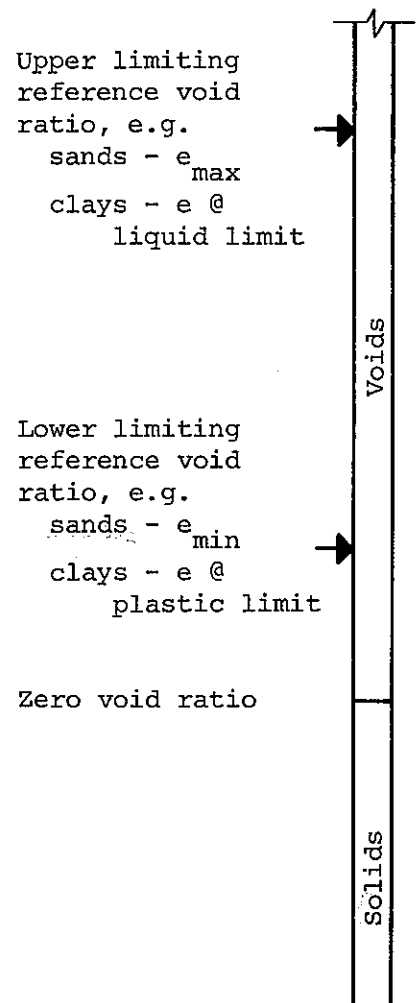
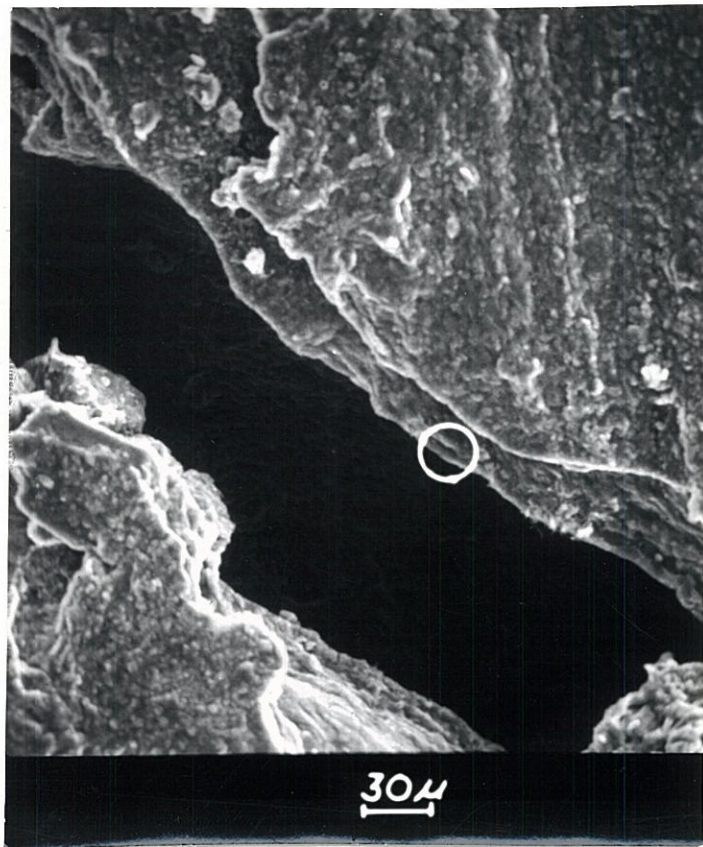
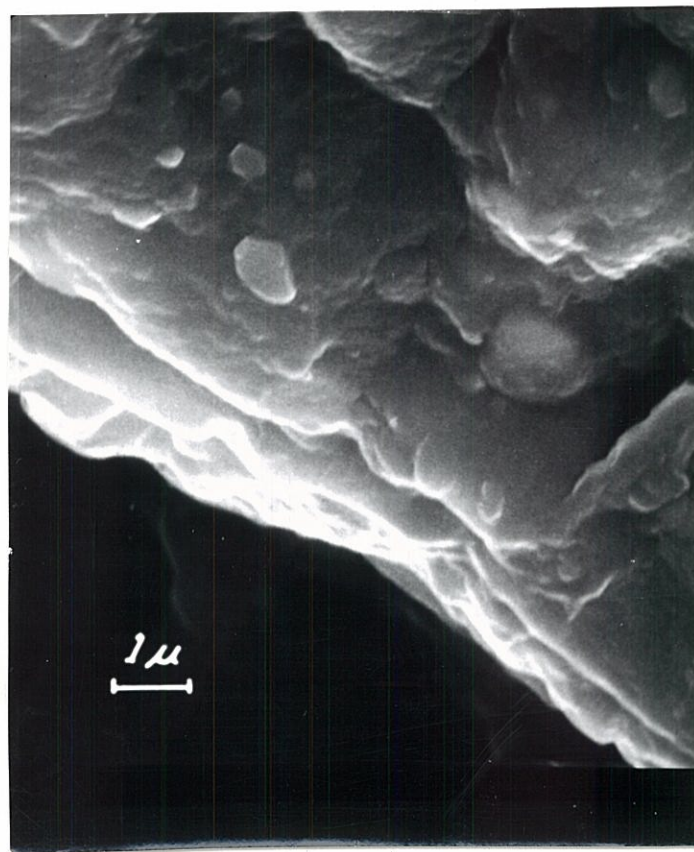


Fig. 1 The State Diagram for Soils



X333



X10000

Fig. 2

Fig. 2 Scanning - Electron Microphotographs Viewed Normal to Surface of Natural Slickenside in Bearpaw Clay-Shale

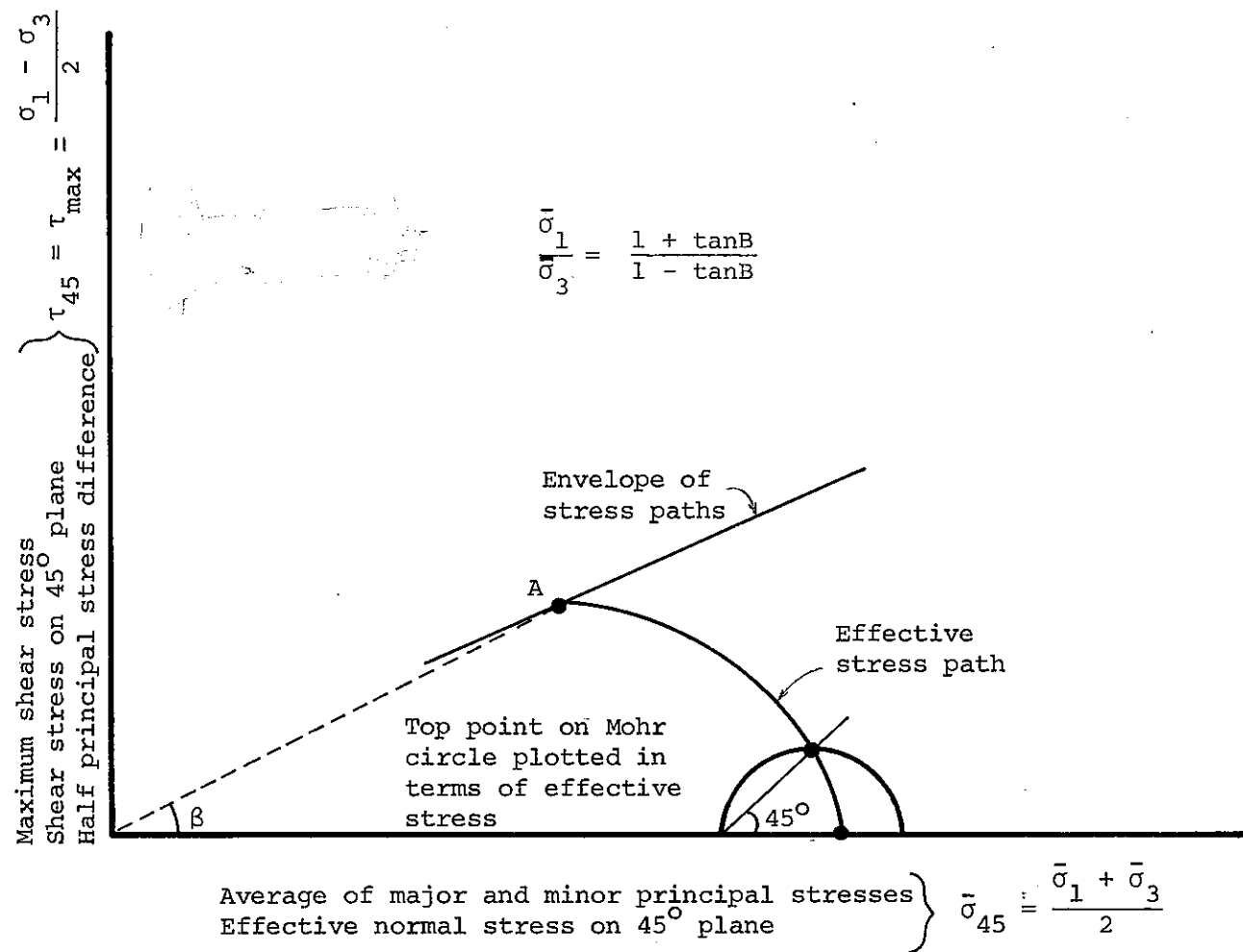
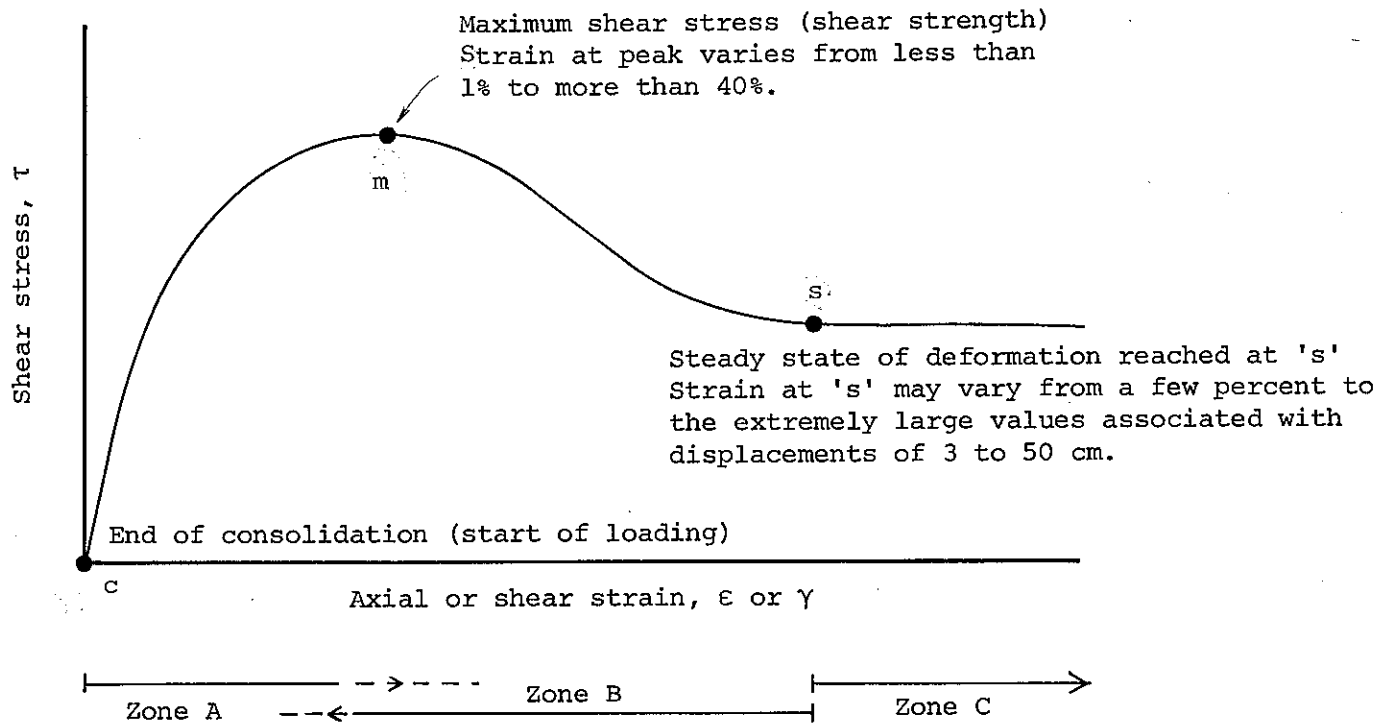


Fig. 3 The Stress Path



Zone A Shape strongly affected by soil type, initial structure, initial state, and method of loading. Initial structure (including bonds, if any) and state have more influence here than in any other zone.

Zone B Initial structure and state increasingly altered by strains until steady state of deformation is reached. Magnitude of drop from τ_m to τ_s is controlled chiefly by initial state, degree of void ratio change that is allowed, and grain shape. Initial structure and method of loading also influence magnitude of τ_m/τ_s .

Zone C At strains beyond Point 's' crushing has stopped and the grains have reached a steady state "structure." The initial structure and state have been completely altered by the loading process and have no influence on τ_s . Nevertheless the initial conditions do influence ϵ_s

Fig. 4 Development of a Stress-Strain Curve

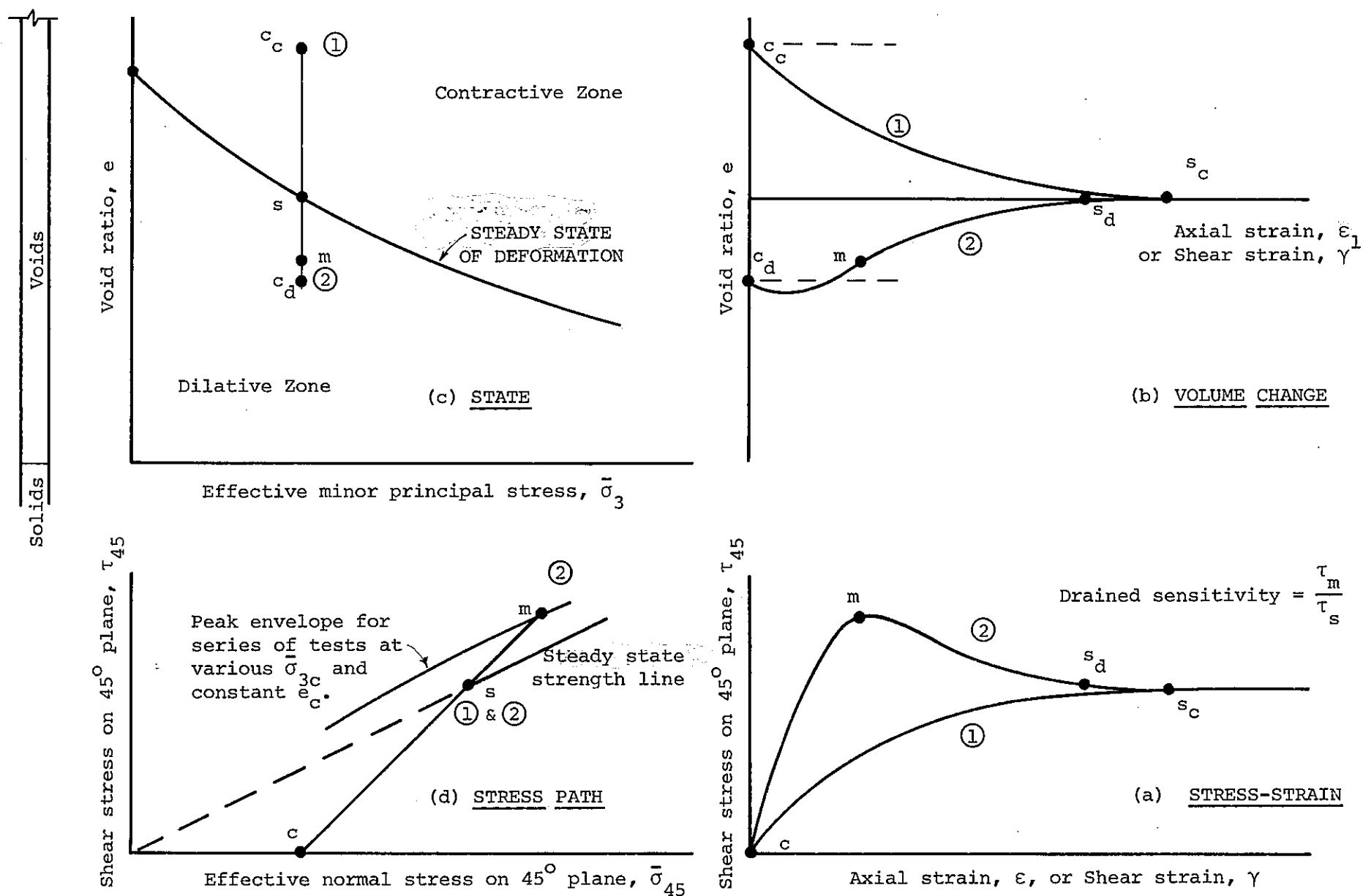


Fig. 5 Consolidated-Drained Triaxial Compression Tests
Idealized For Uncemented Soils With Bulky Grains

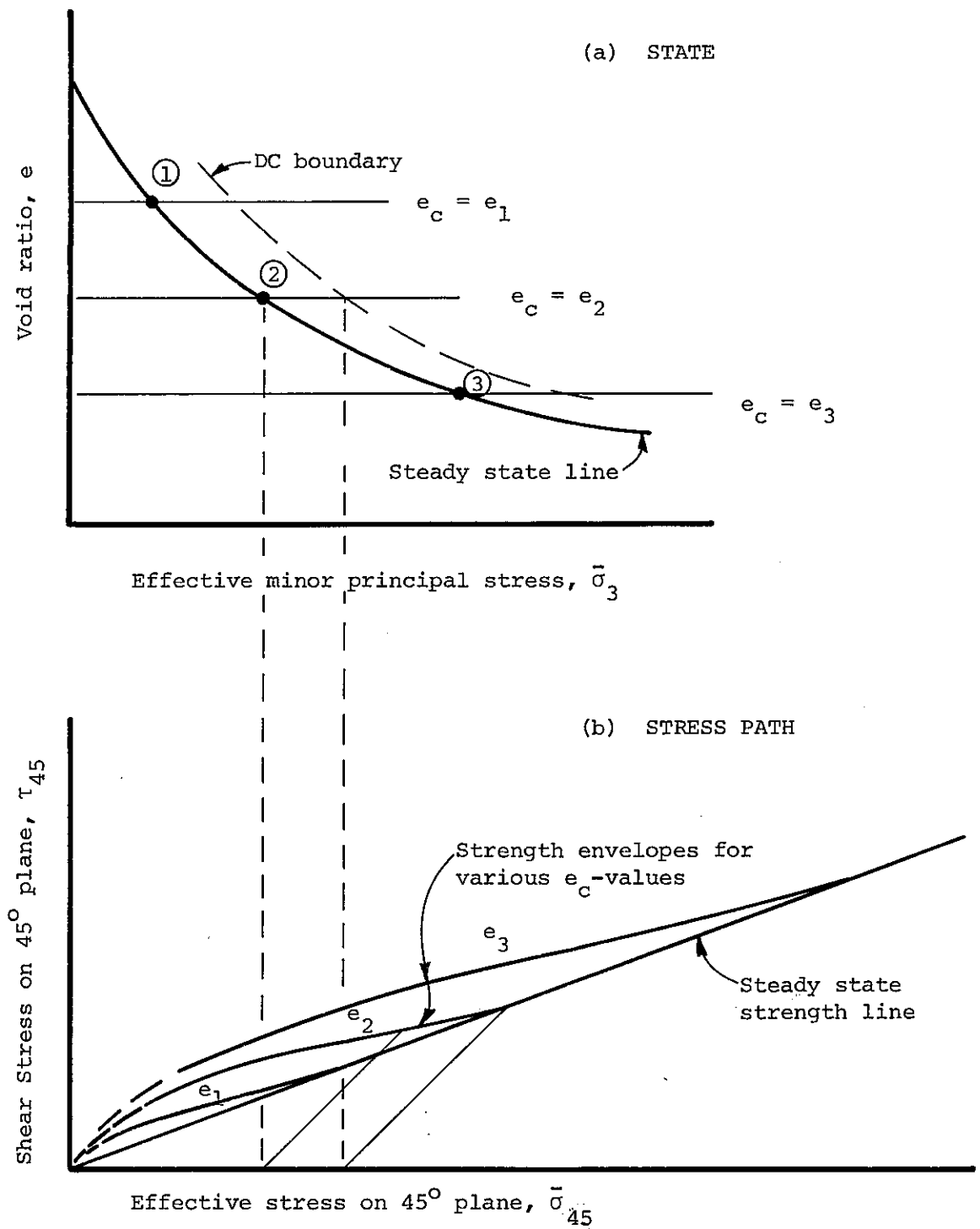


Fig. 6 Strength Envelopes for Specimens Prepared at Constant Void Ratio, e_c . Consolidated-Drained Triaxial Compression Tests.

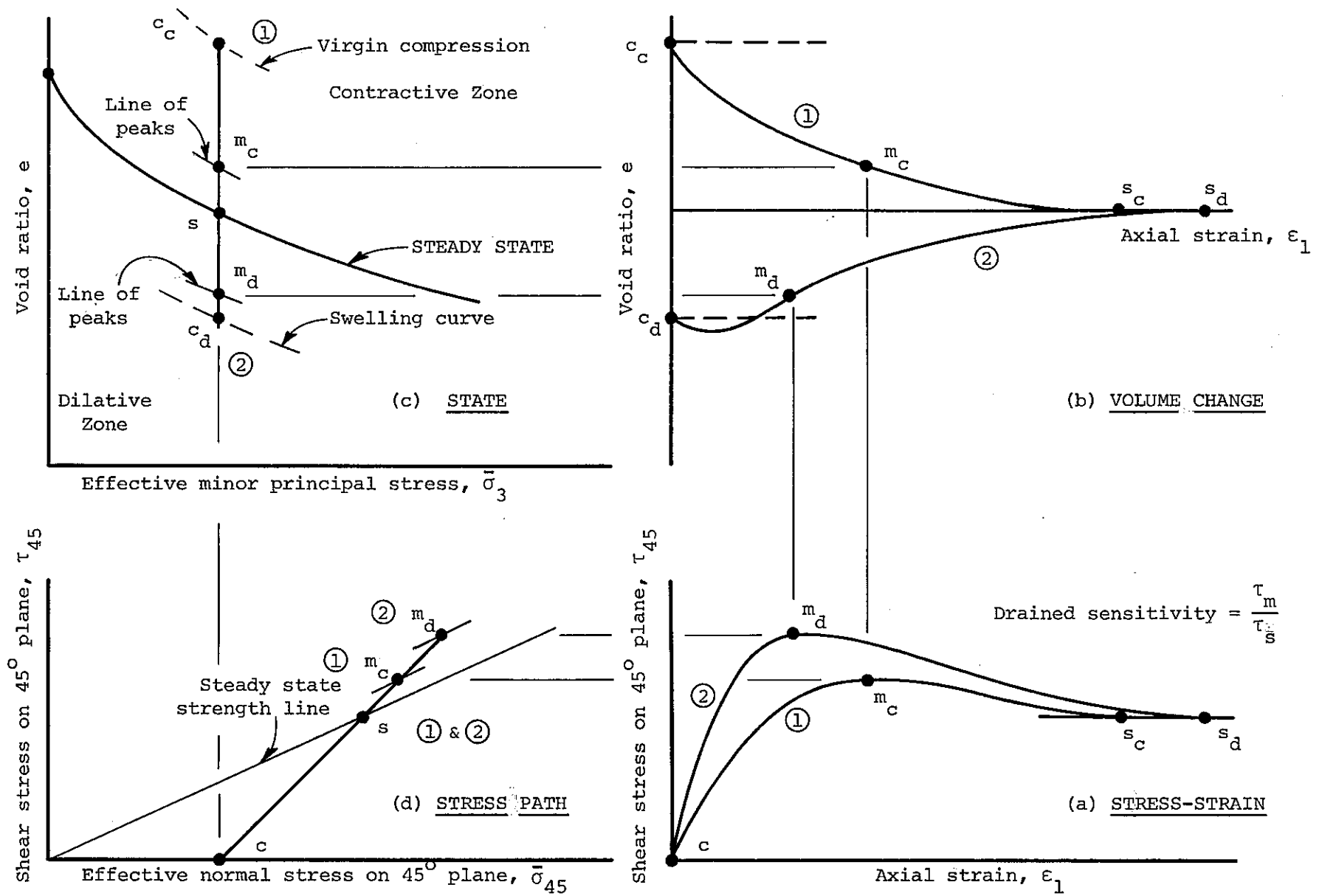


Fig. 7 Consolidated-Drained Triaxial Compression Tests On Soil Containing Substantial Proportion of Flat Grains. Low Stress Levels. Idealized.

Notes:

1. Lines (a), (b), (d) and (e) were first presented by Casagrande (1941).
2. For bulky-grained soils Lines (b) and (c) coincide. The difference between them for clays is due to orientation of grains at large strains.

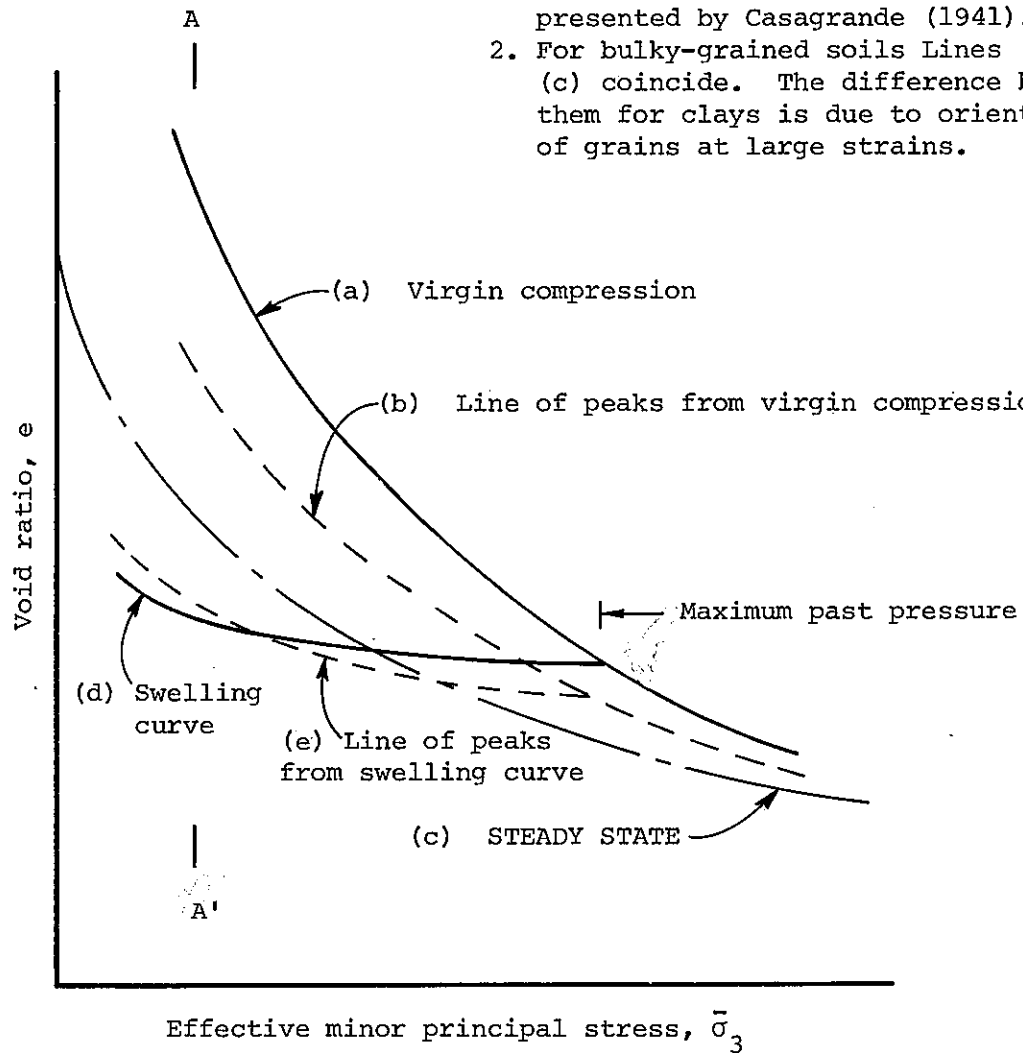
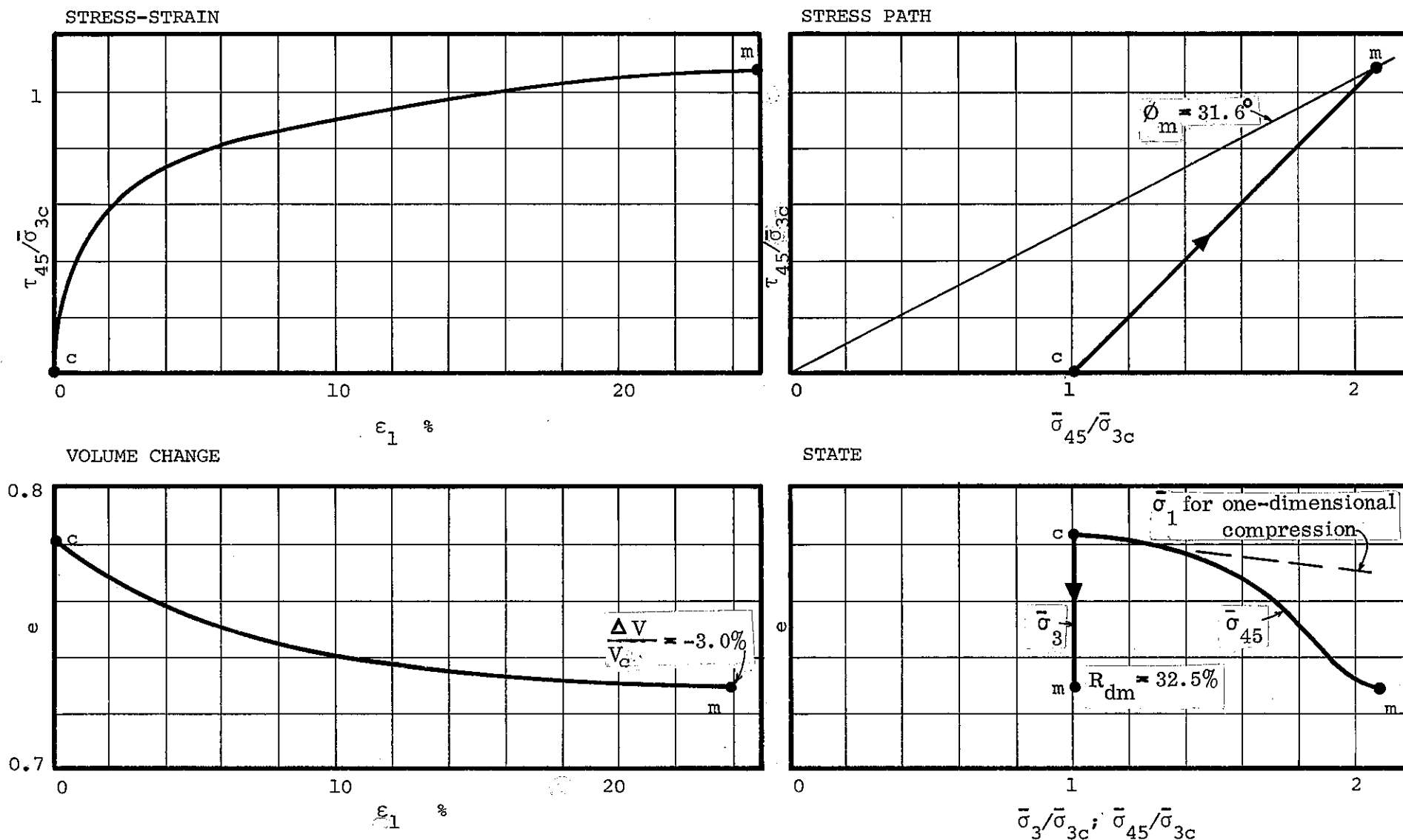


Fig. 8 Postulated Location of Steady State Line Relative to Compression and Swelling Curves for Clays

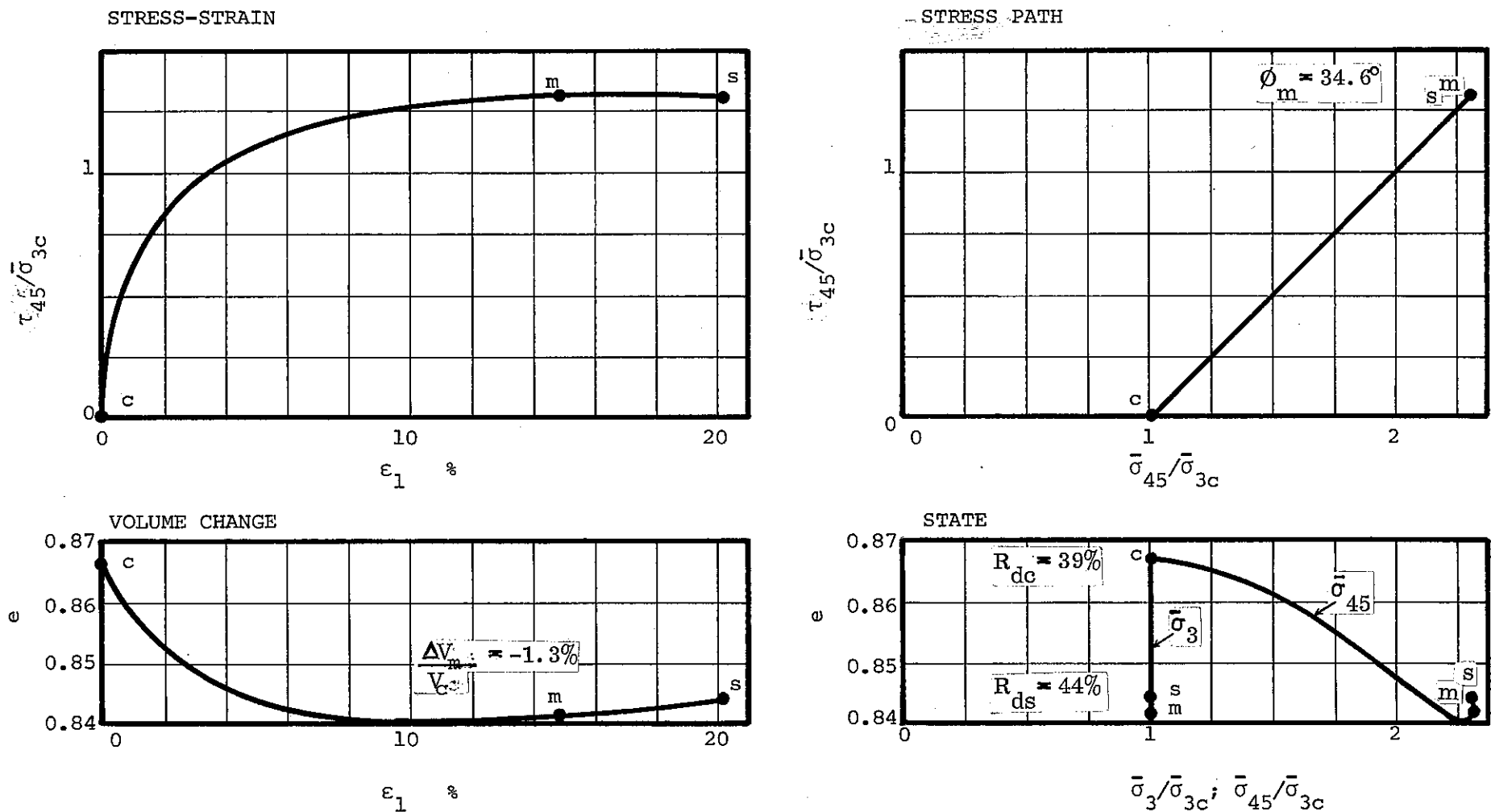


Soil Tested: Fine quartz sand; bulky, subrounded to subangular grains; $D_{10} = 0.097$ mm; $C_u = 1.8$; $s_s = 2.65$; $e_{max} = 0.84$; $e_{min} = 0.50$.

Test Conditions: $\bar{\sigma}_{3c} = 1.0$ kg/cm²; $e_o = 0.783$; $R_{dc} = 17\%$; $u_c = 4.0$ kg/cm²; strain rate 1%/min; lubricated ends; 1.4 in. dia. by 3.5 in. high; compacted in bulked state (w~5%); fully saturated.

Source: Replotted from Castro (1969), Fig. 66, p. 79.

Fig. 9 Highly Contractive Sand Consolidated-Drained Triaxial Compression

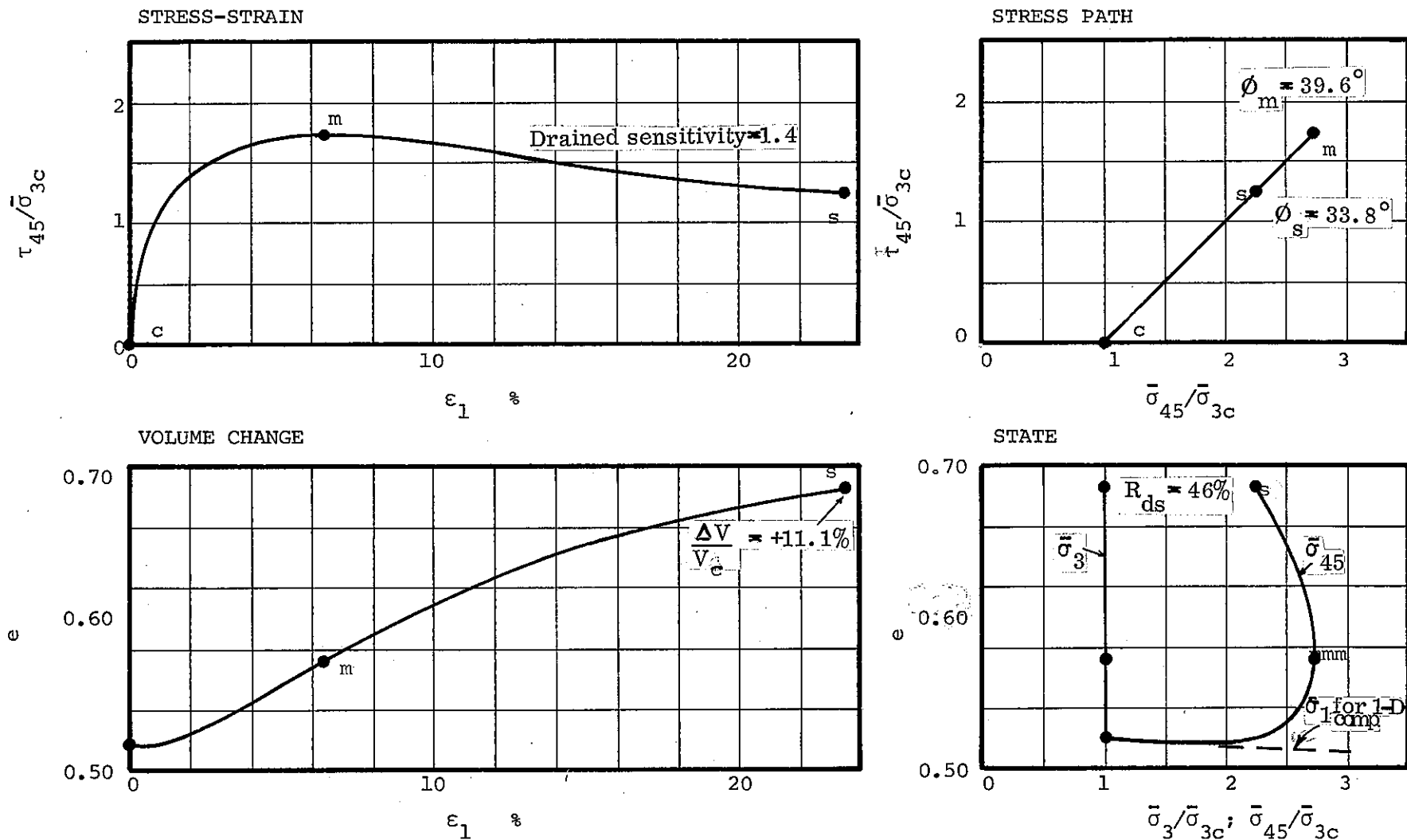


Soil Tested: Fine, uniform Sacramento River sand; bulky, angular to subrounded grains; quartz and feldspar; $D_{10} = 0.17$ mm; $C_u = 1.3$; $e_{max} = 1.03$; $e_{min} = 0.61$; $s = 2.68$.

Test Conditions: $\bar{\sigma}_{3c} = 4.5$ kg/sq cm; $e_c^u = 0.867$; $R_{dc} = 39\%$; 1.4 in. dia. by 3.4 in. high; strain rate equals 0.18%/min; no back pressure or end lubrication.

Source: Replotted from Lee and Seed (1967), Fig. 4. Original data furnished by Lee (1970).

Fig. 10 Slightly Dilative Sand Consolidated-Drained Triaxial Compression

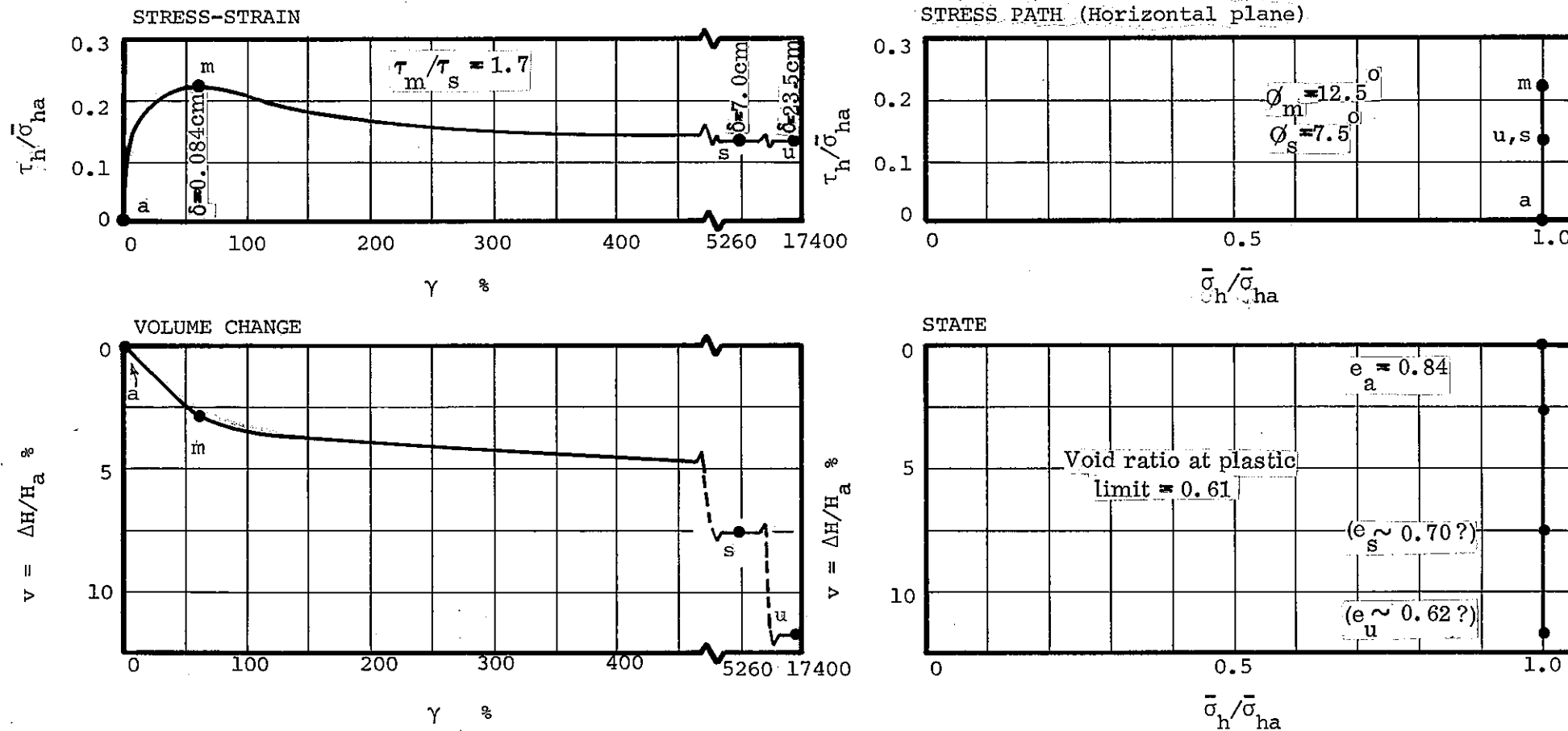


Soil Tested: Fine quartz sand; bulky, subrounded to subangular grains; $D_{10} = 0.097$ mm; $C_u = 1.8$; $s = 2.65$; $e_{min} = 0.50$; $e_{max} = 0.84$.

Test Conditions: $\bar{\sigma}_c^s = 1.0$ kg/sq cm; $e_c = 0.518$; $R_{dc} = 95\%$; $u_c = 4.0$ kg/sq cm; strain rate 1%/min; 1.4 in. dia. by 3.5 in. high; lubricated ends; compacted in bulked state ($w \sim 5\%$).

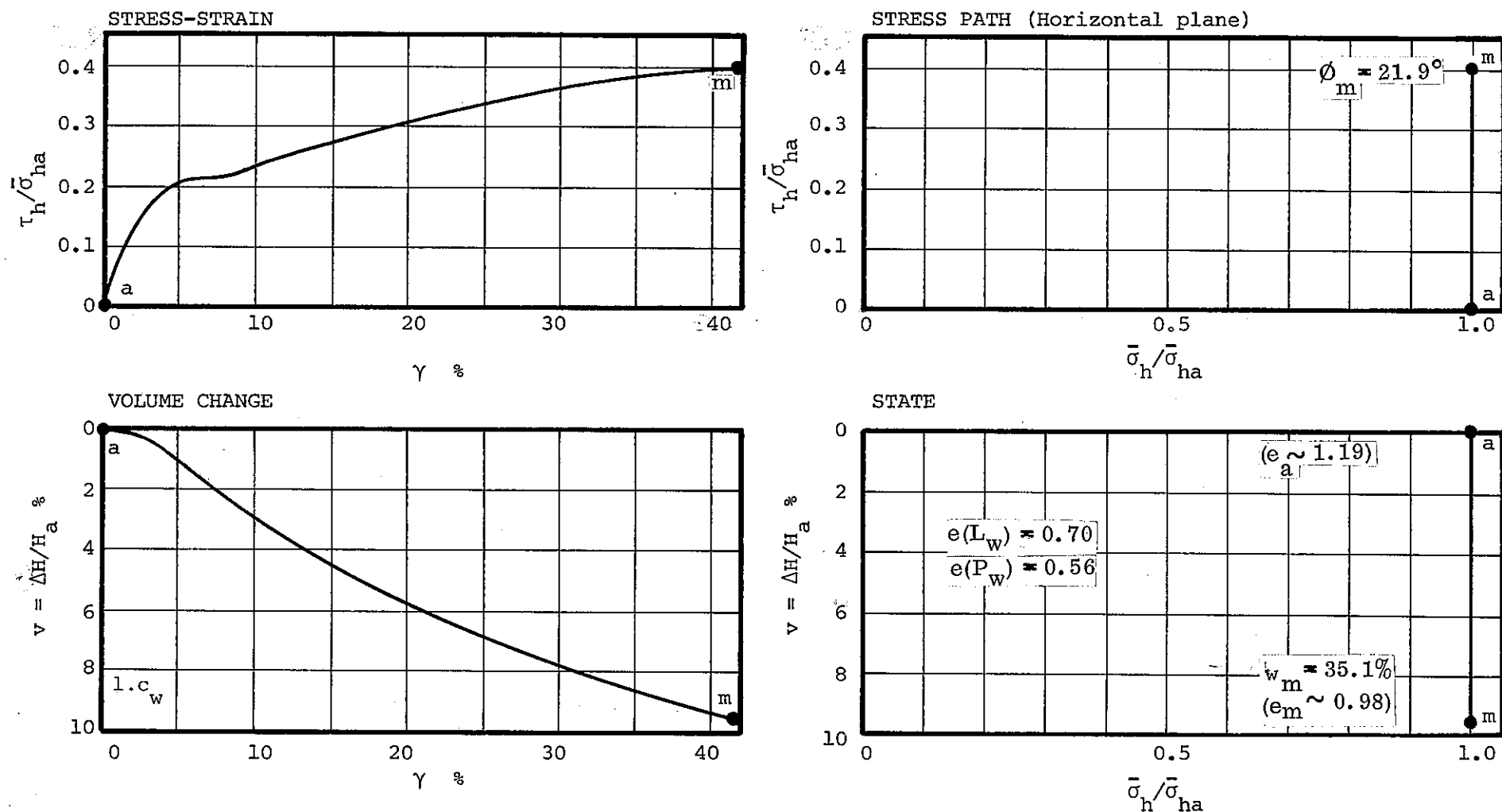
Source: Replotted from Castro (1969); Fig. 66, p. 79.

Fig. 11 Highly Dilative Sand Consolidated-Drained Triaxial Compression



Soil Tested: Pepper Shale; air dried and remolded at $w_i = 61\%$; $L_w = 71$, $P_i = 49$; 73% minus 2μ ; $s_s = 2.76$.
 Test Conditions: $\bar{\sigma}_{ha} = 4.0 \text{ kg/cm}^2$; $w_a = 30.5\%$ ($e_a = 0.84$); displacement rate 0.0056 cm/min on periphery (one rotation in 2.8 days); annular disc, ID = 5.11 cm, OD = 7.11 cm; $H_a = 0.135 \text{ cm}$; $G_w = 100\%$; essentially normally consolidated
 Source: Replotted from LaGatta (1970), Fig. 7-4.

Fig. 12 Highly Contractive Clay Consolidated-Drained Rotation Shear

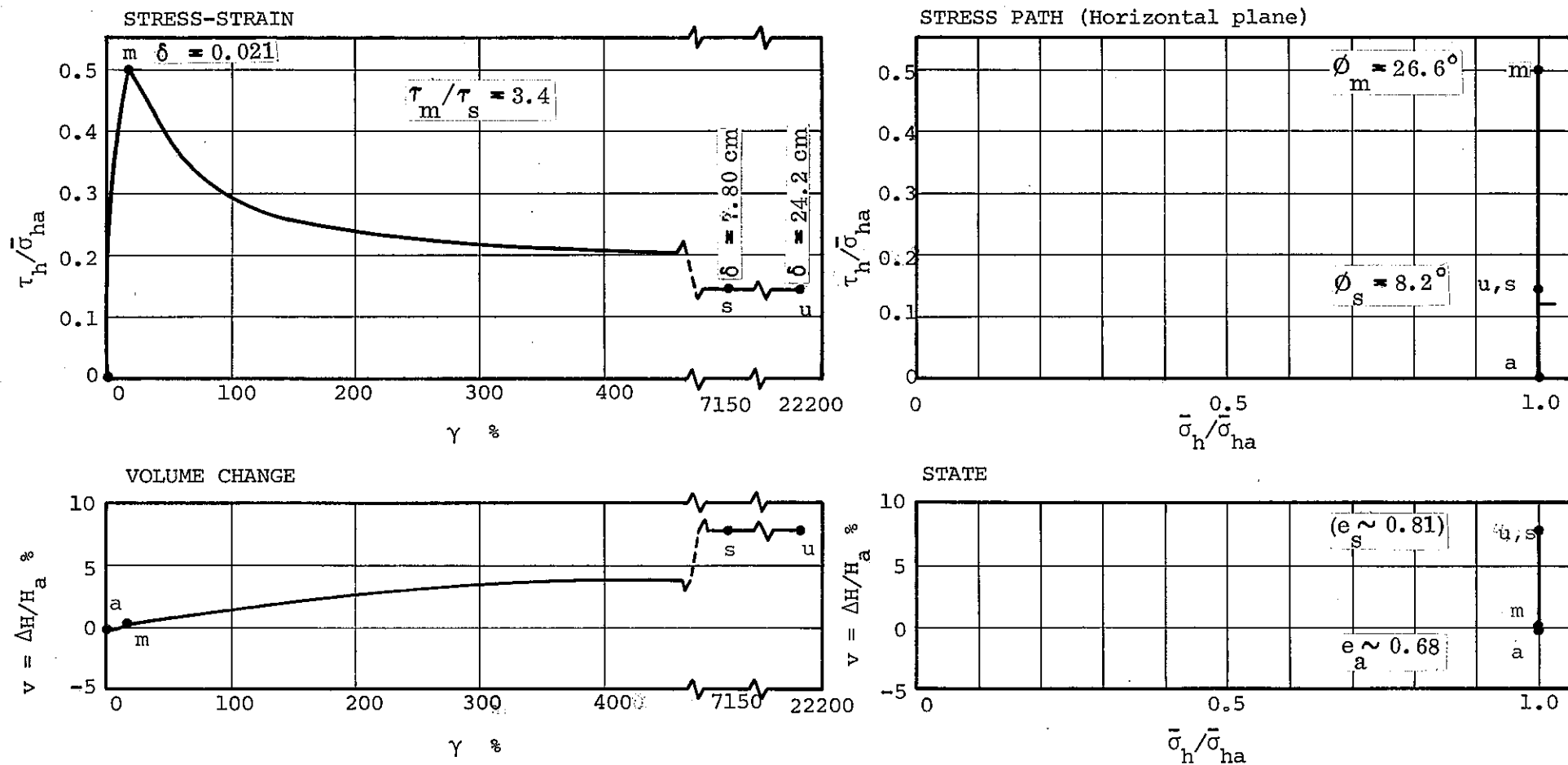


Soil Tested: Manglerud quick silty clay; $w \sim 46\%$, $L \sim 25$; $P_i \sim 5$; undrained sensitivity 40-150; depth 6.30 m (in-situ vertical $\bar{\sigma} = 0.60 \text{ kg/cm}^2$); $\sim 48\% w < 2\mu$; $s_i \sim 2.78$.

Test Conditions: $\bar{\sigma}_{ha} = 0.58 \text{ kg/cm}^2$; $w \sim 43\%$ ($e_a \sim 1.19$); $H_a = 1.01 \text{ cm}$; 8 cm diameter; average rate of shear strain to 'm' 0.024 %/min; undisturbed.

Source: Replotted from Bjerrum and Landva (1966), Fig. 12, Test 12, p. 15. Additional details from Landva (1962), Table 2, Test K-12.

Fig. 13 Very Highly Contractive Clay Consolidated-Drained Direct Shear



Soil Tested: Pepper shale; air dried and remolded at $w_i = 62\%$; $L_i = 71$, $P_i = 49$; 73% minus 2 μ ; $s_u = 2.76$.
 Test Conditions: $\bar{\sigma}_{ha} = 1.0$ kg/cm²; maximum past pressure = 100 kg/cm²; $w_a = 24.7\%$ ($e \sim 0.68$); displacement rate of periphery = 0.0056 cm/min (one rotation in 2.8 days); annular disc, ID = 5.11 cm, OD = 7.11 cm, $H_a = 0.109$ cm.
 Source: Replotted from LaGatta (1970), Fig. 7-16.

Fig. 14 Highly Dilative Clay Consolidated-Drained Rotation Shear

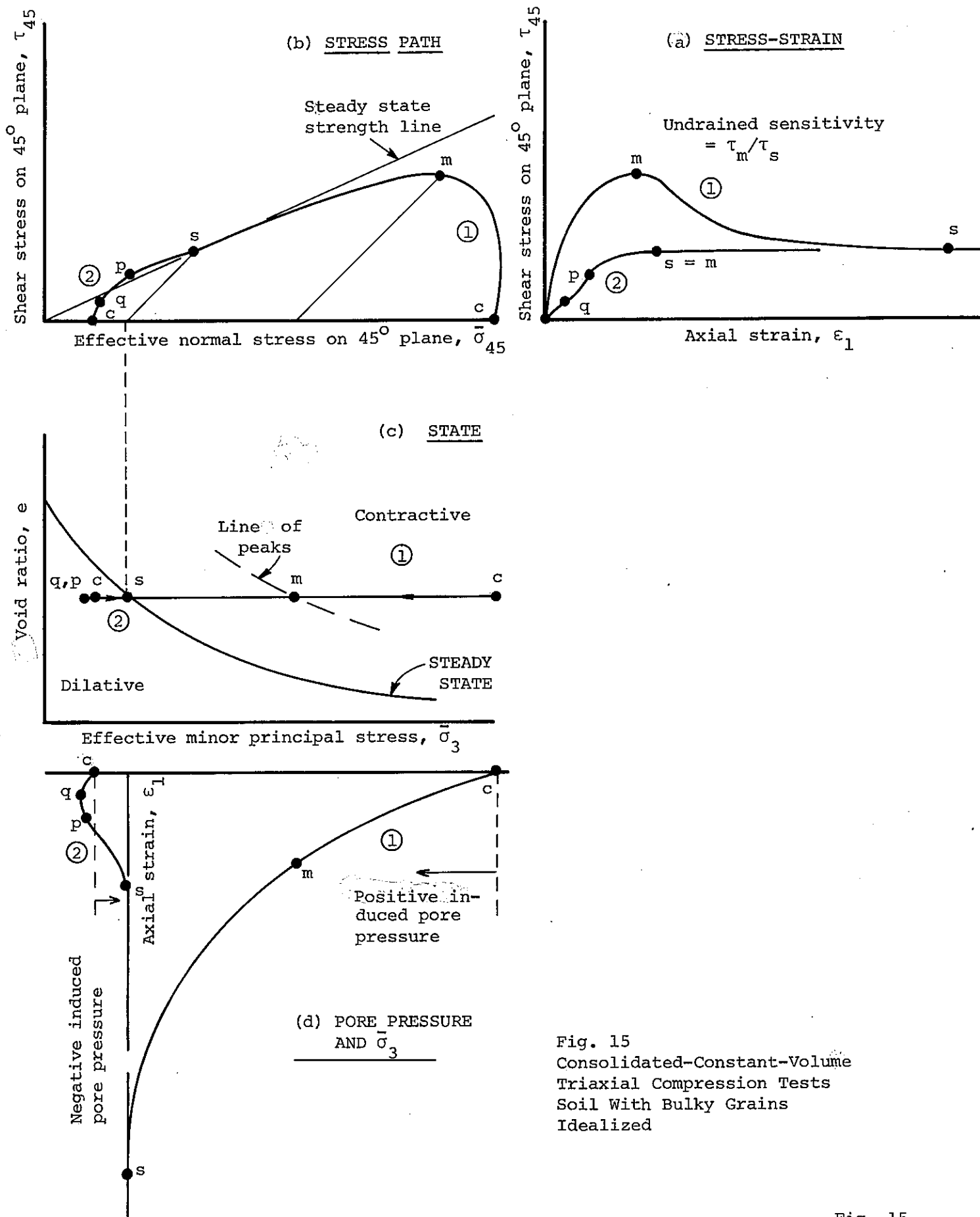
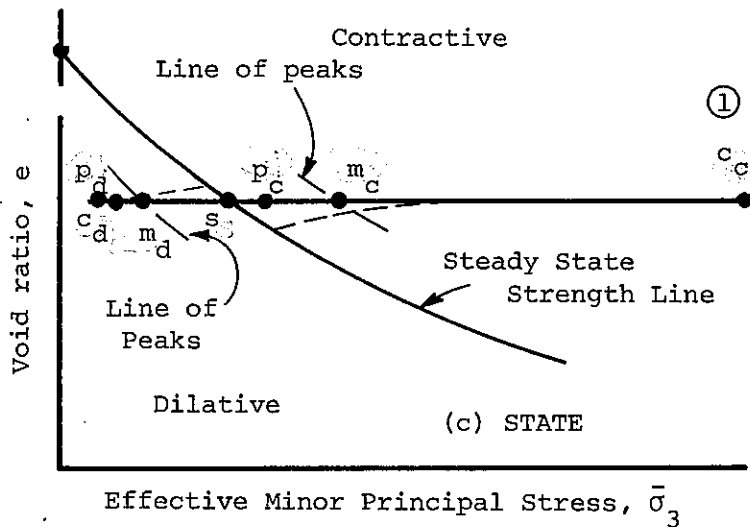
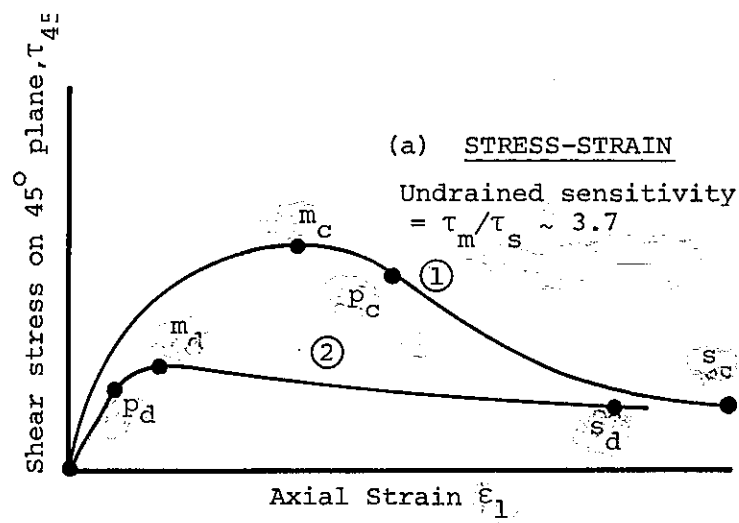
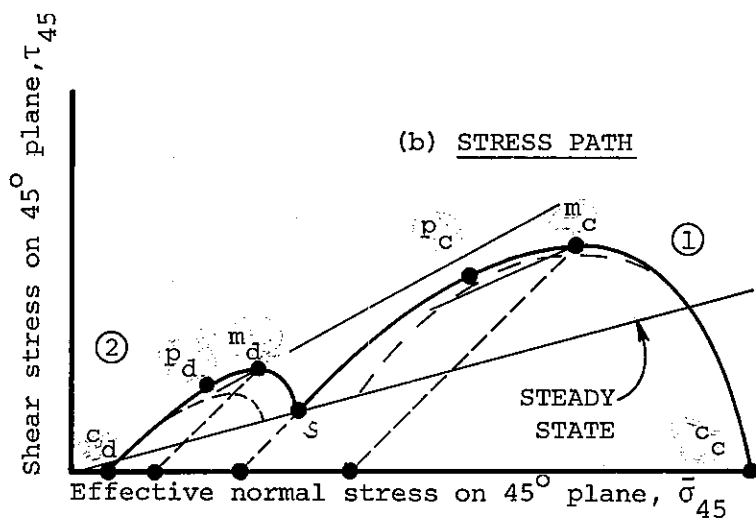


Fig. 15
Consolidated-Constant-Volume
Triaxial Compression Tests
Soil With Bulky Grains
Idealized



State	A-Values	
	Peak	Steady State
Contractive	0.9	4.2
Dilative	-0.2	-1.1

Dashed stress paths show effect of non-uniformities that develop during actual tests. Corresponding changes on state diagram are also shown dashed.

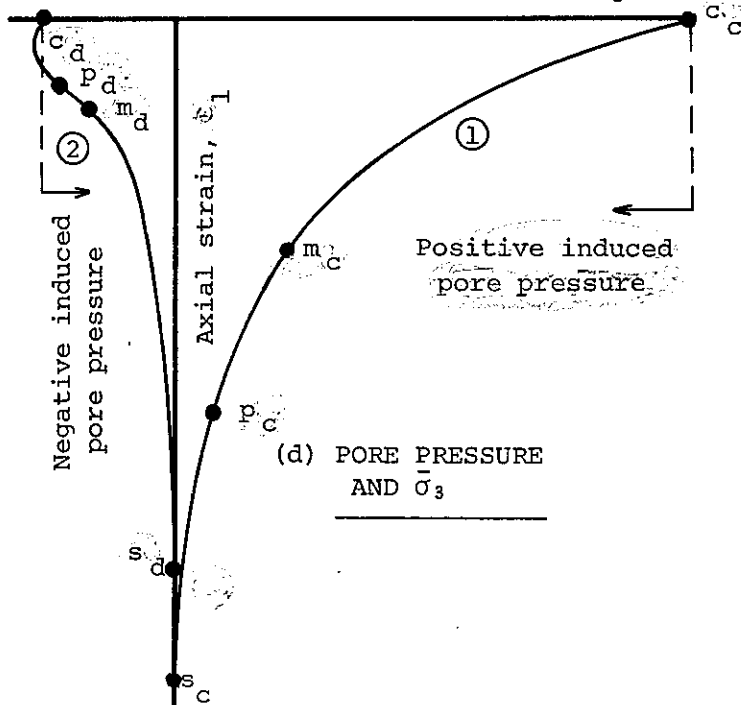
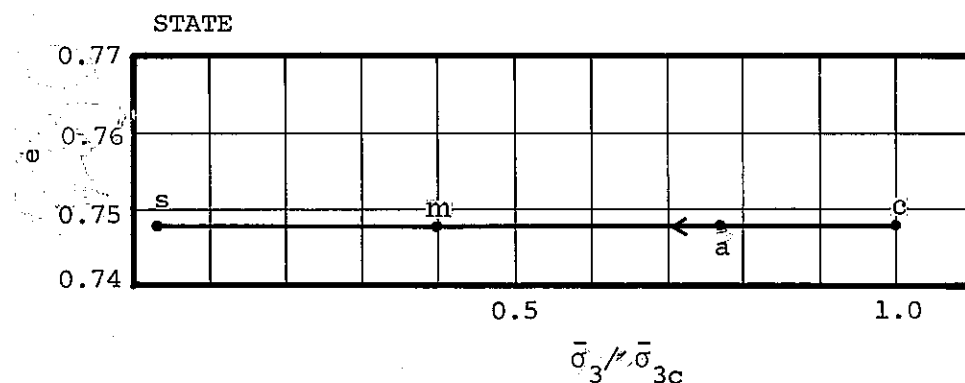
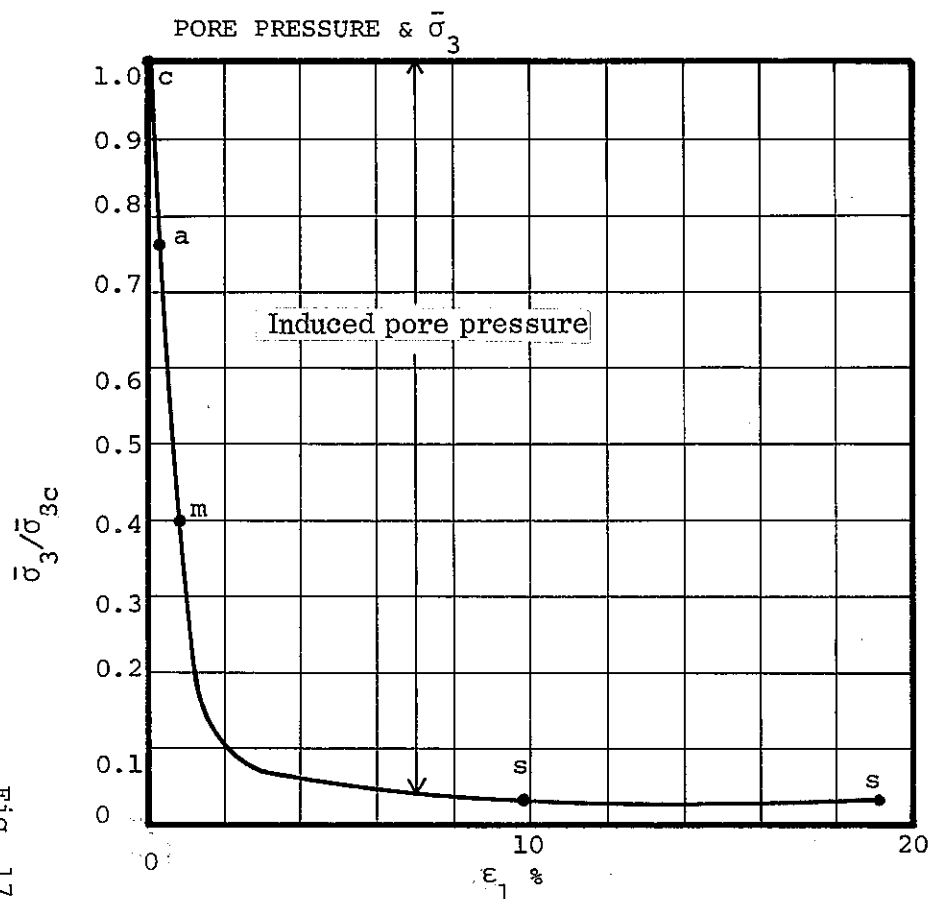
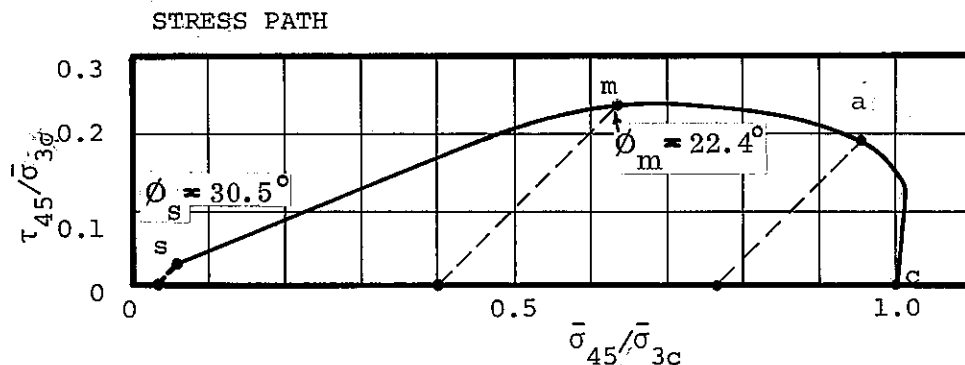
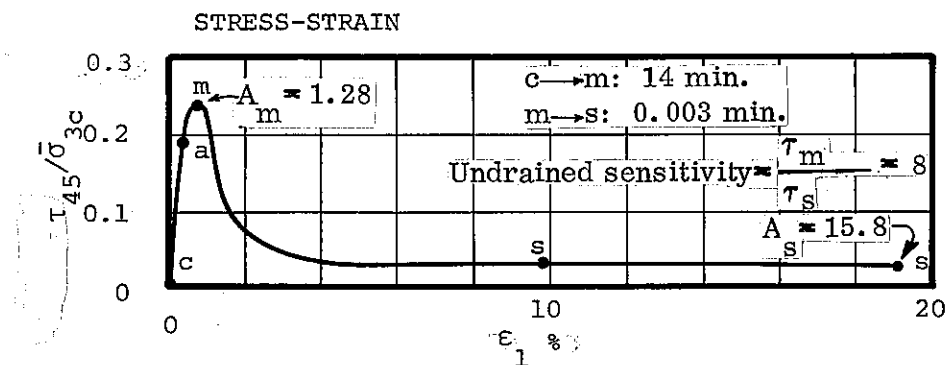


Fig. 16

Consolidated-constant-volume triaxial compression tests on soil containing substantial proportion of platy-grains idealized



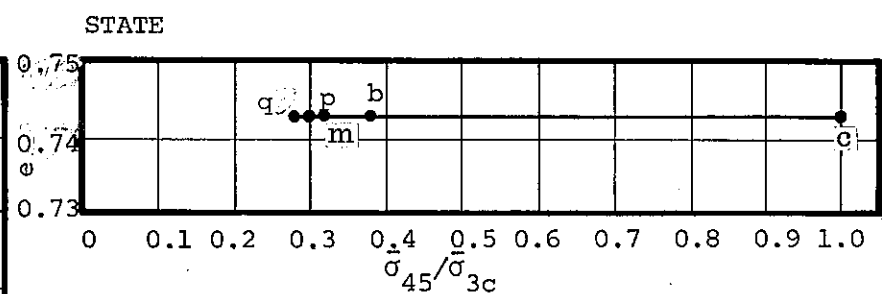
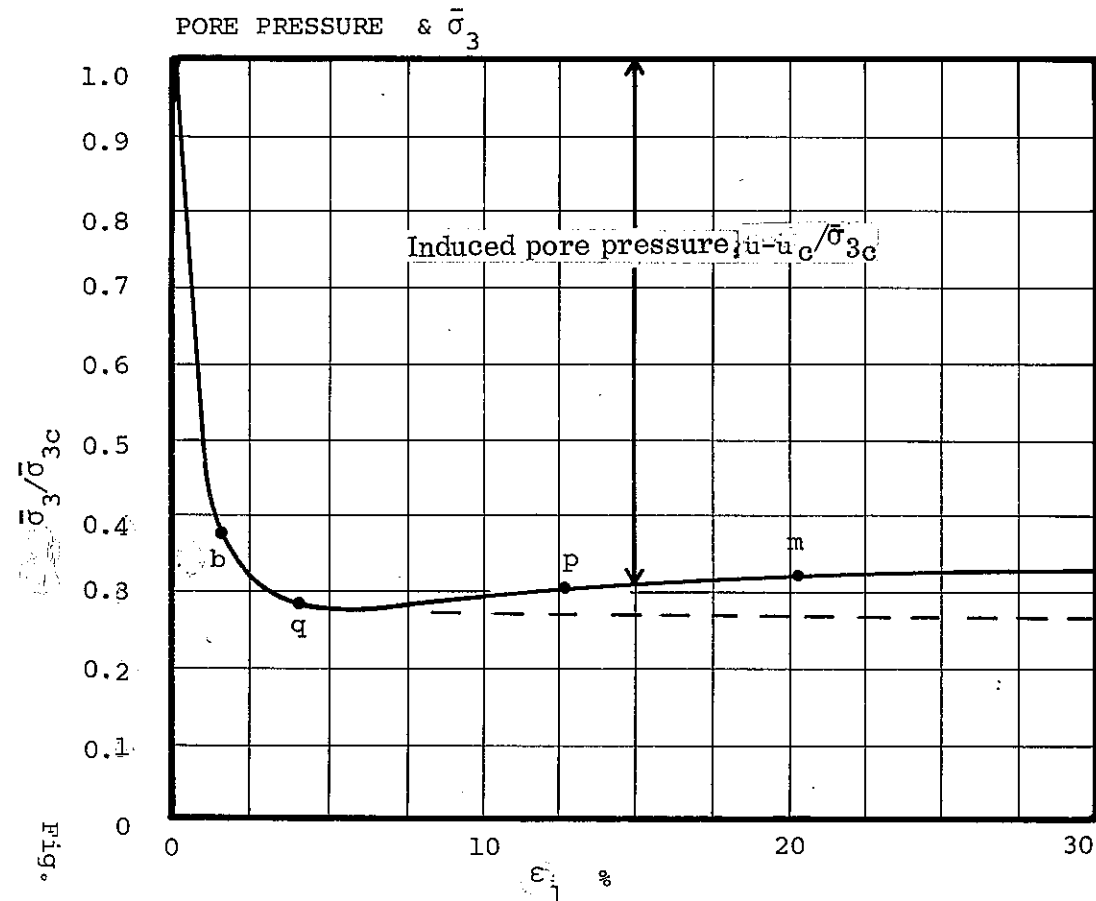
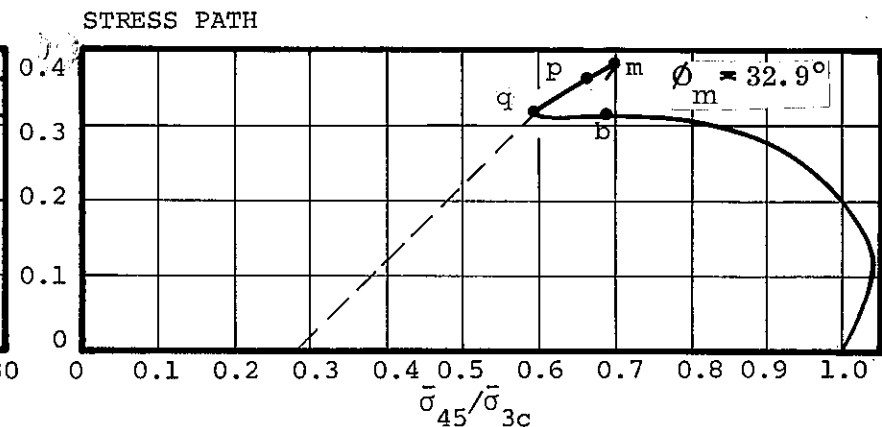
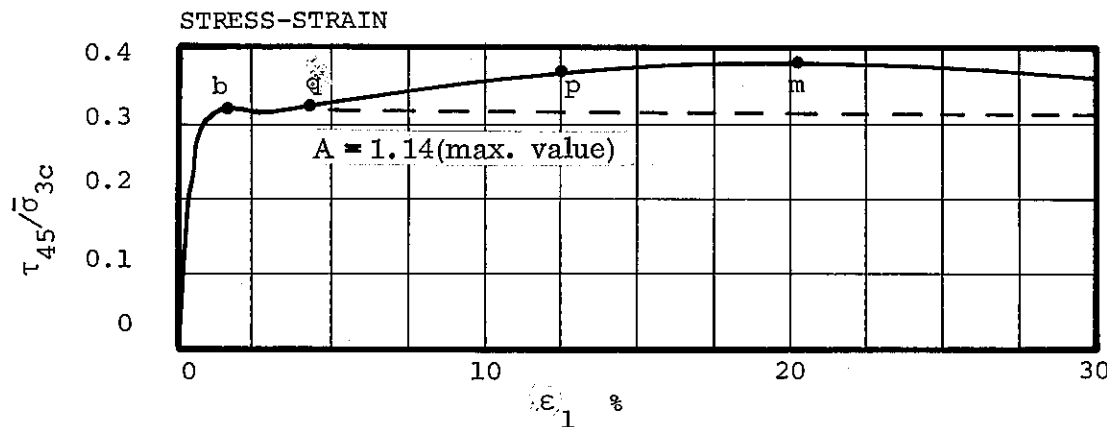
Soil Tested: Fine quartz sand; bulky, subrounded to subangular grains; $D_{10} = 0.097$ mm; $C_u = 1.8$; $\sigma_s = 2.65$; $e_{max} = 0.84$, $e_{min} = 0.50$.

Test Conditions: $\bar{\sigma}_{3c} = 4.0$ kg/cm²; $e_c = 0.75$; $R_{dc} = 27\%$; $\bar{\sigma}_c = 4.0$ kg/cm²; load control (post-peak acceleration); compacted bulked ($W \sim 5\%$); 1.4 in. by 3.5 in. specimen.

Source: Replotted from Castro (1969), Fig. 33, P. 61.

Fig. 17

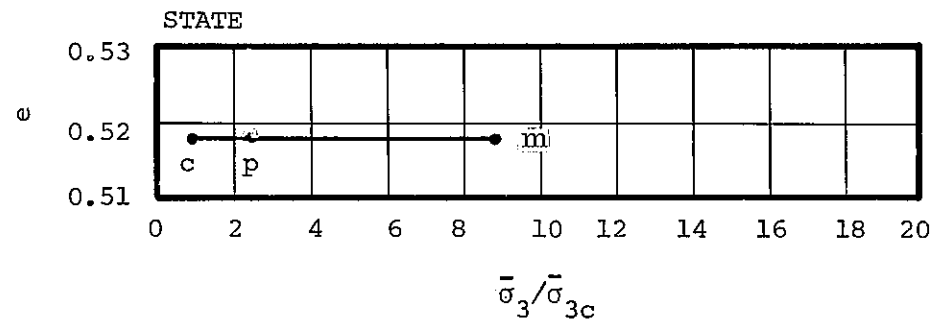
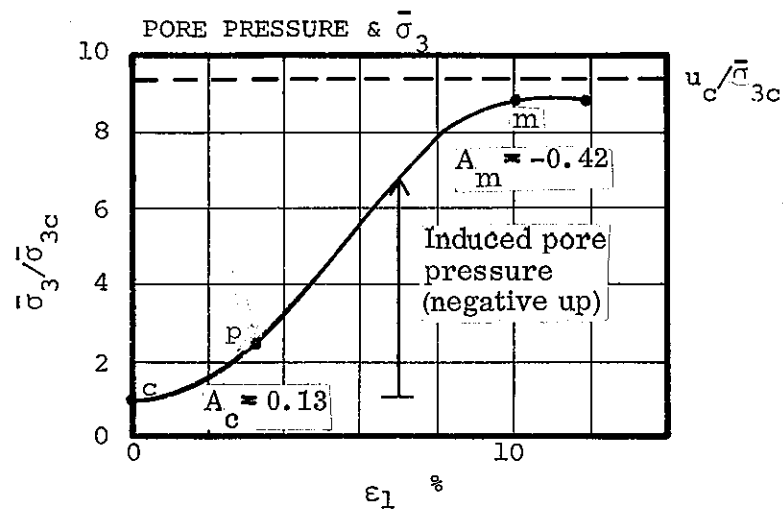
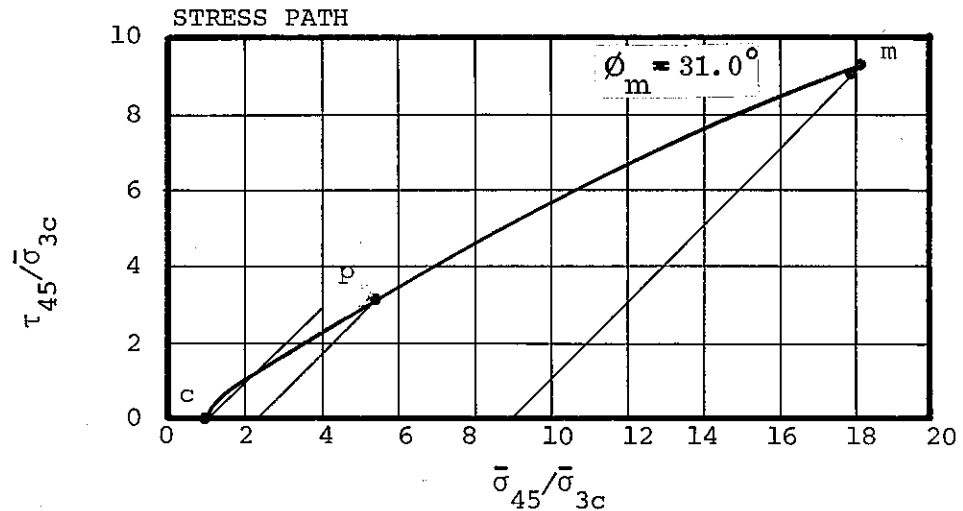
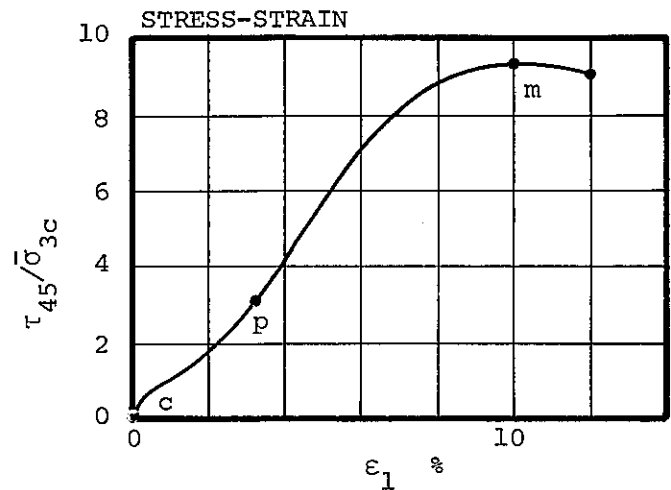
Highly Contractive Sand
Consolidated-Constant-Volume
Triaxial Compression



Soil Tested: Ham river-sand, uniform med-fine sand, 96% quartz, Bulky, subrounded to subangular grains
 $D_{10} = 0.15 \text{ mm}$, $C_u = 2$, $s_g = 2.70$, $e_{\text{max}} = 0.877$
 $e_{\text{min}} = 0.594$.
 Test Conditions: $\bar{\sigma}_{3c} = 35.1 \text{ kg/cm}^2$; $n = 42.7\%$ ($e = 0.74$)
 $R_{dc} = 48.5\%$; $u_c = 0.70 \text{ kg/cm}^2$; strain rate $0.25\%/min$;
 1.49 in. x 3.04 in. specimen; no lubrication; degree of saturation not given.

Source: Replotted from Bishop, Webb, & Skinner (1965),
 Figs. 7 & 8, Skinner (1970)

Fig. 18 Sand Near Steady State Void Ratio Consolidated-Constant-Volume Triaxial Compression

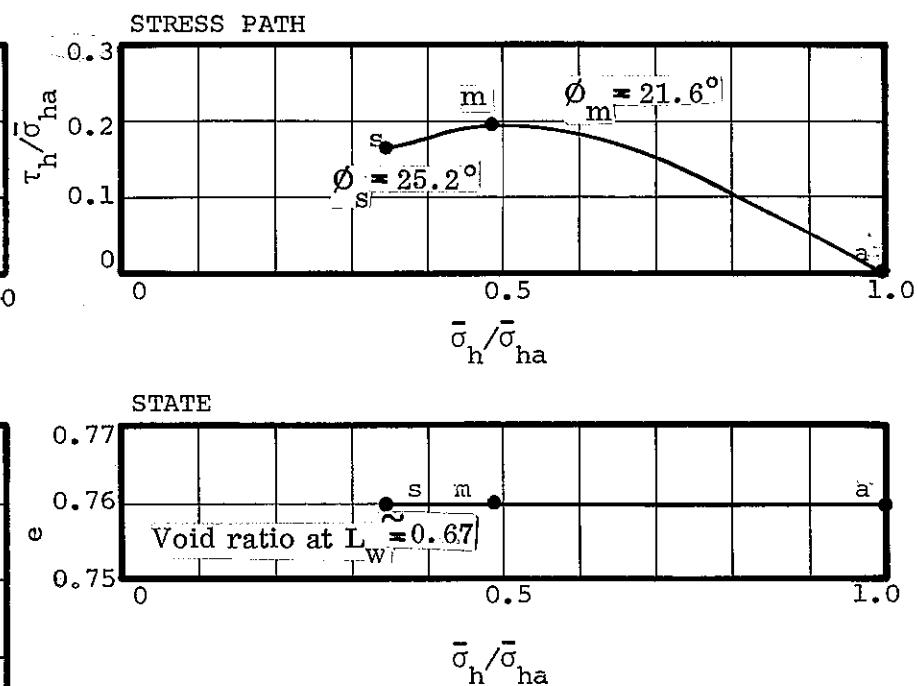
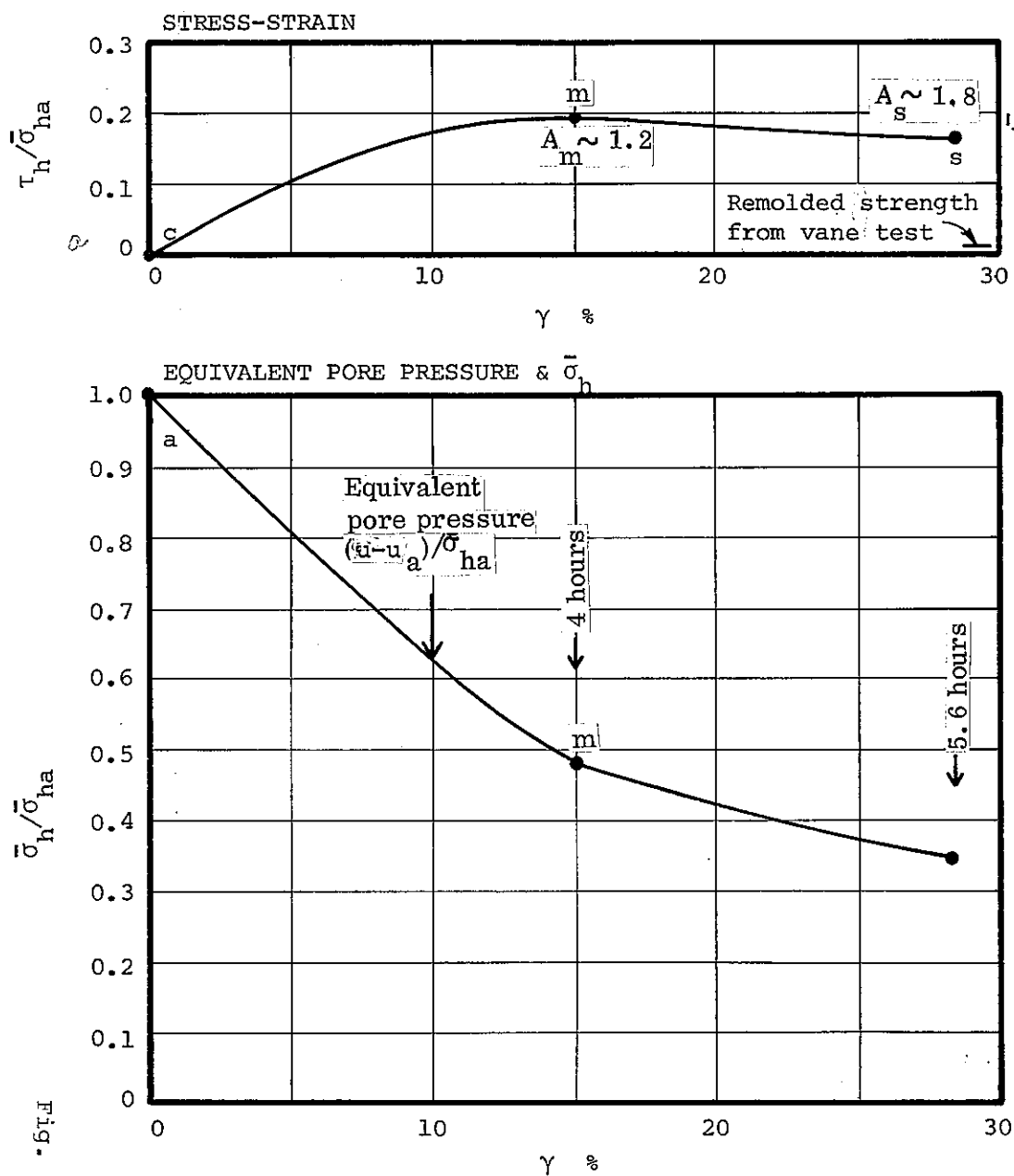


Soil Tested: Coarse Ottawa sand; pure quartz; bulky, rounded grains; $D_{10} = 0.65$ mm; $C_u = 1.2$; $s_s = 2.67$; $e_{max} = 0.72$; $e_{min} = 0.48$.

Test Conditions: $\bar{\sigma}_{3c} = 6.59$ kg/cm²; $e = 0.518$; $R_d = 86\%$; $u_c = 63.5$ kg/cm²; strain rate $\sim 0.033\%$ /min; no lubrication of ends; $G_{wc} = 100\%$.

Source: Replotted from Wissa and Ladd (1965), Fig. 7-7, p. 167.

Fig. 19 Highly Dilative Sand Consolidated Constant-Volume Triaxial Compression
Revised November 25, 1981

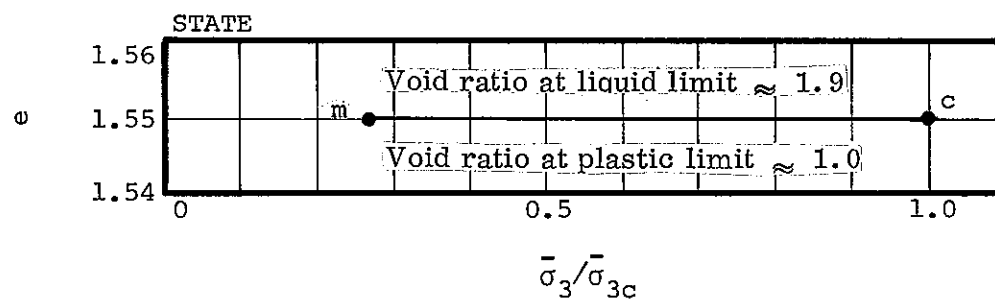
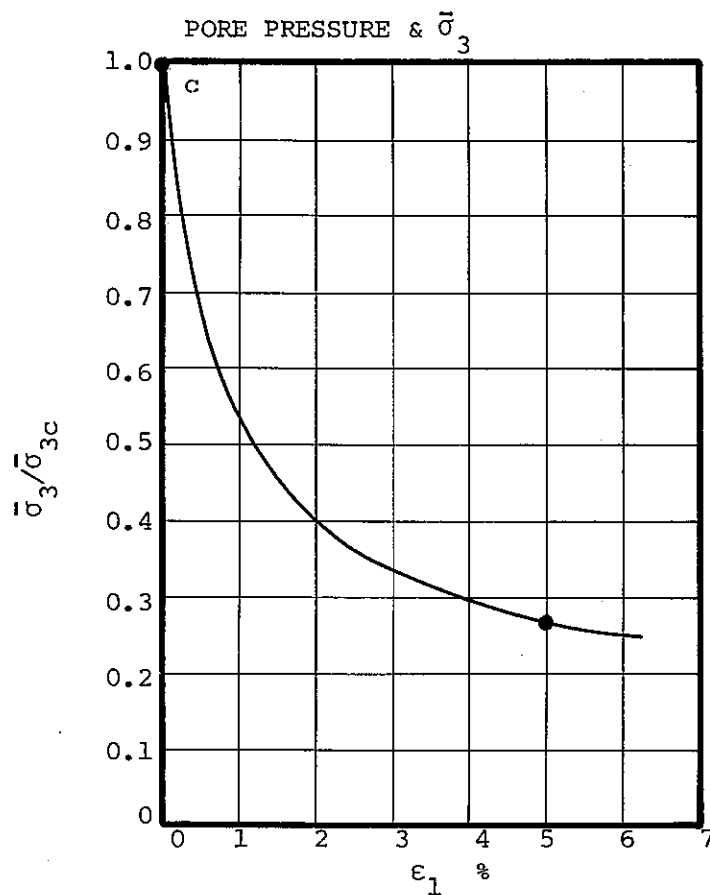
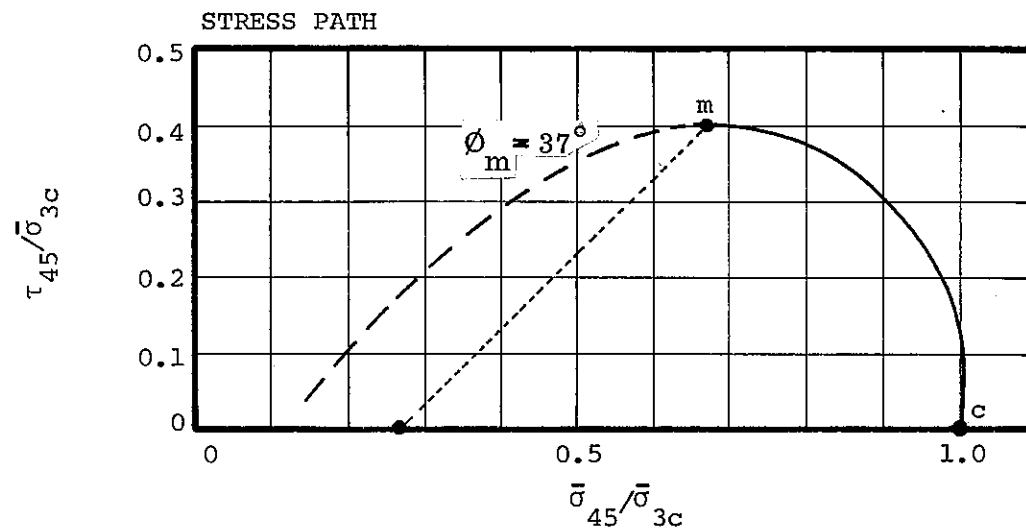
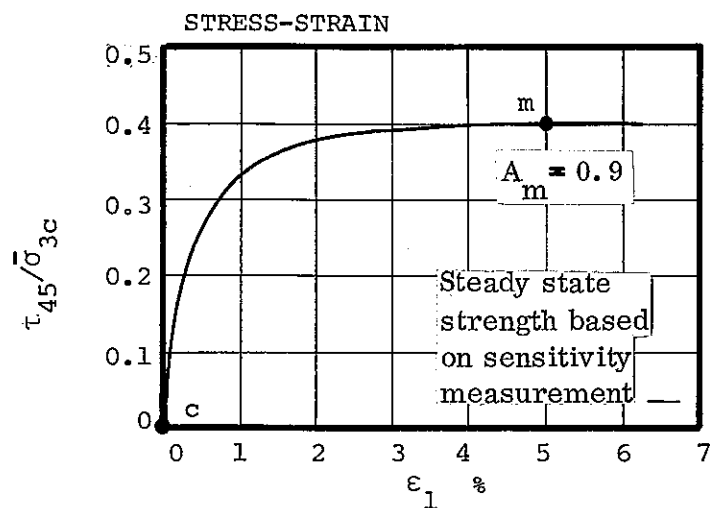


Soil Tested: Manglerud quick silty clay; $w_{nat} \sim 36.4\%$; $L_w \sim 24$; $P_i \sim 5$; undrained sensitivity 40-150; depth 8.33 m (overburden = 0.77 kg/cm²); $\sim 48\% < 2\mu$; $s \sim 2.78$; undisturbed $\bar{\sigma}_{ha} = 2.0$ kg/cm²; $w_s = 28.3\%$ ($e_a \sim 0.76$); 0.89 cm thick (after consolidation); 8 cm dia.; average rate of shear strain 0.084% min. to point 's'; thickness maintained constant ($u = 0$ throughout test).

Test Conditions: $\bar{\sigma}_{ha} = 2.0$ kg/cm²; $w_s = 28.3\%$ ($e_a \sim 0.76$); 0.89 cm thick (after consolidation); 8 cm dia.; average rate of shear strain 0.084% min. to point 's'; thickness maintained constant ($u = 0$ throughout test).

Source: Replotted from Bjerrum & Landva (1966), Fig. 9, p. 12. Additional details from Landva (1962), Table 1, Test K39.

Fig. 20 Very Highly Contractive Clay Consolidated Constant Volume Simple Shear

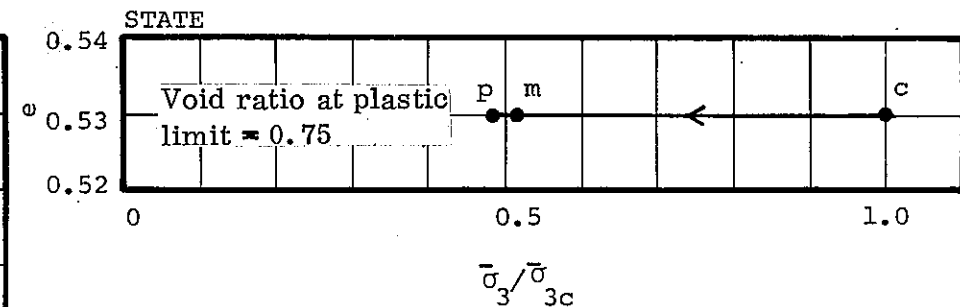
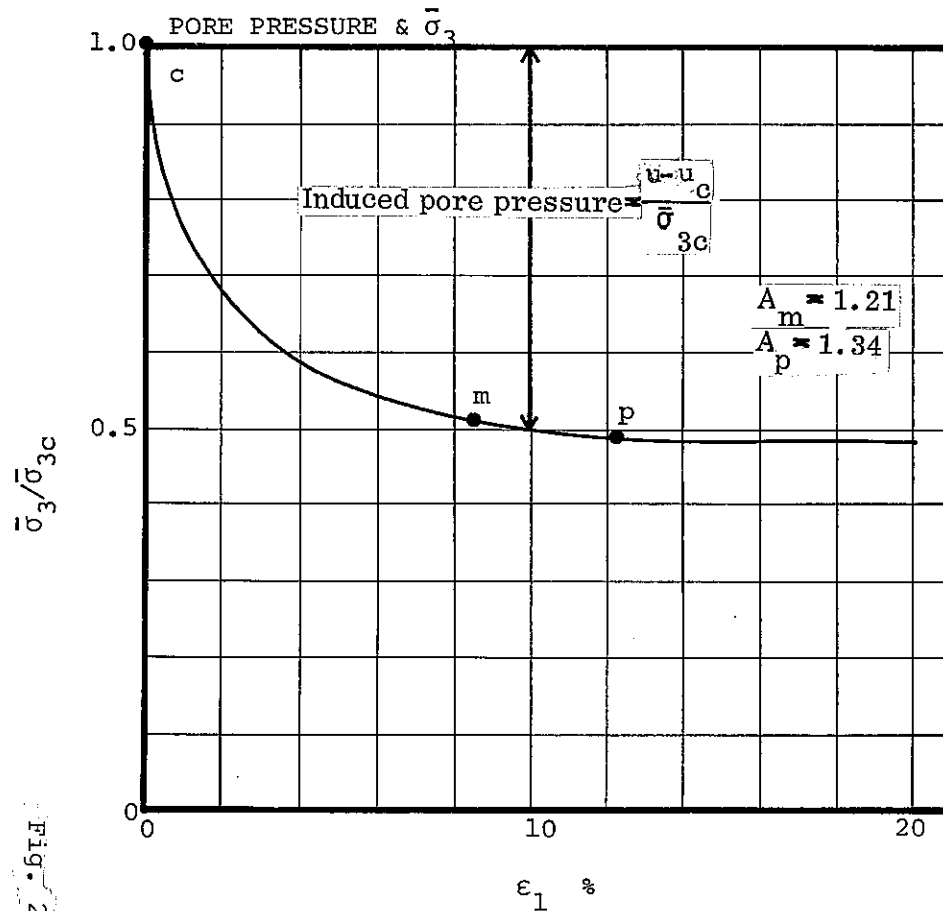
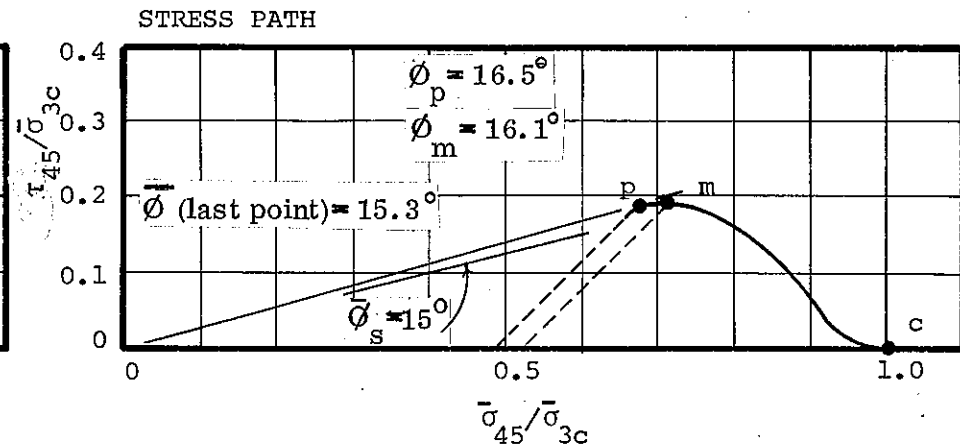
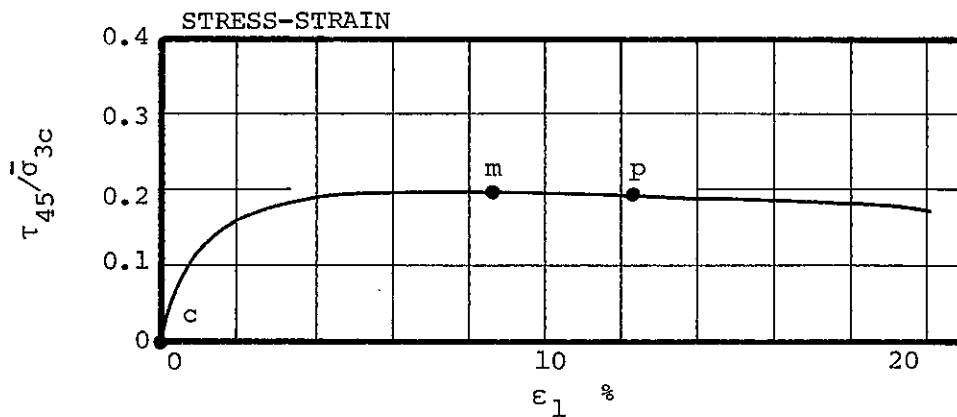


Soil Tested: Kawasaki clay; $L_w = 71$, $P_i \sim 33$, $w_{nat} \sim 72.6\%$; $\sim 38\% < 2\mu$; $s_g = 2.68$; undrained sensitivity ~ 10 ; vertical effective overburden stress $= 1.85 \text{ kg/cm}^2$.

Test Conditions: Undisturbed specimen; $\bar{\sigma}_{3c} = 3.00 \text{ kg/cm}^2$; pore pressure held constant at 2.00 kg/cm^2 ; $B_c = 1.00$; $w_{final} = 57.9\%$ ($e_c \approx 1.55$); strain rate $0.016\%/min.$; $1.4'' \phi \times 3.15''$.

Source: Replotted from Ladd (1965), Figs. 2 & 3, p. 284; additional data from Ladd (1970).

Fig. 21
Highly Contractive Clay
Consolidated-Constant-Volume
Triaxial Compression



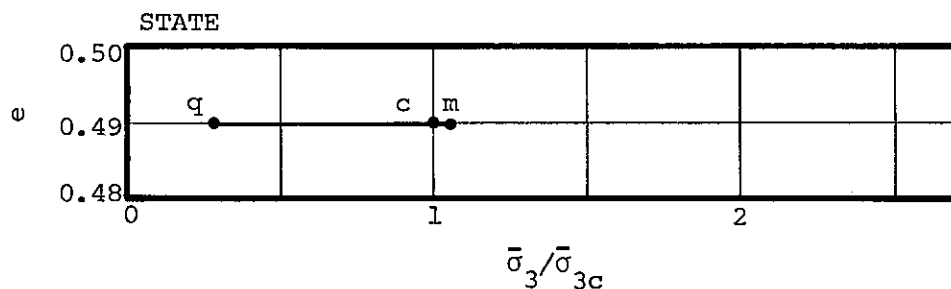
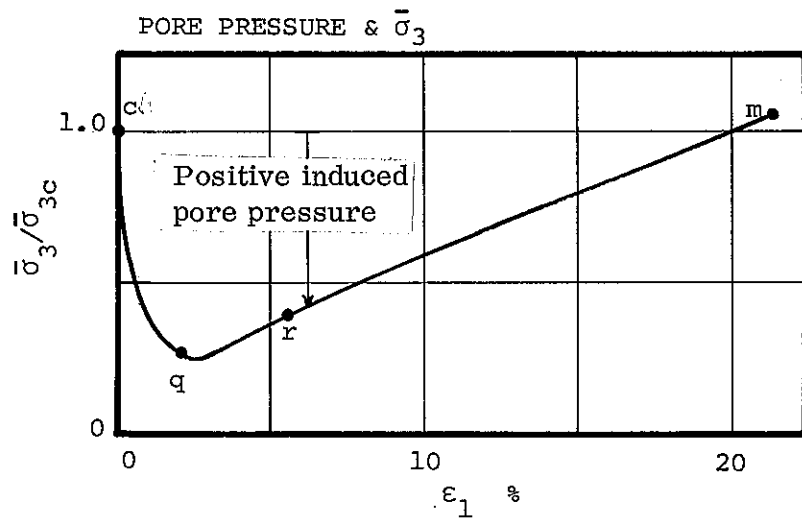
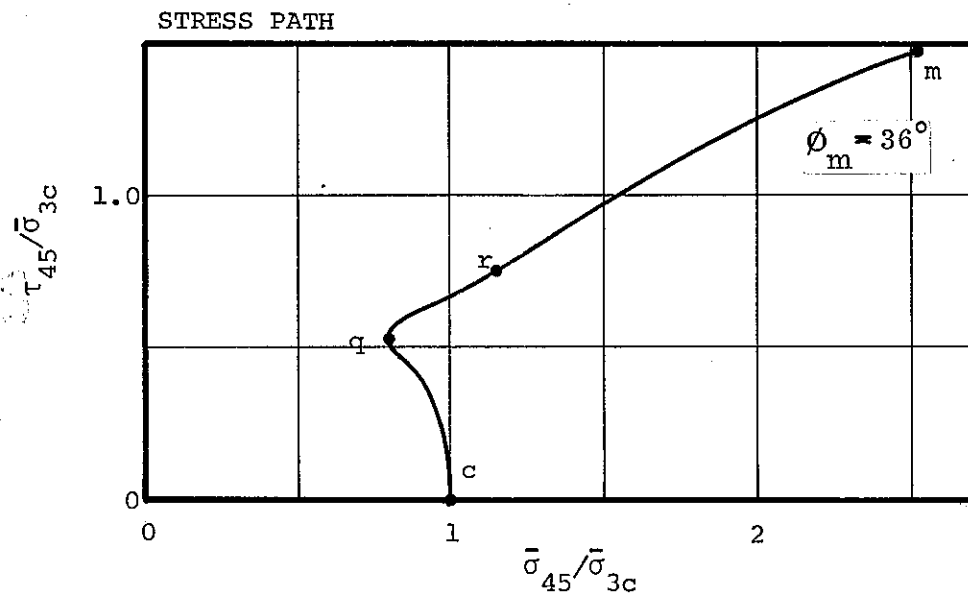
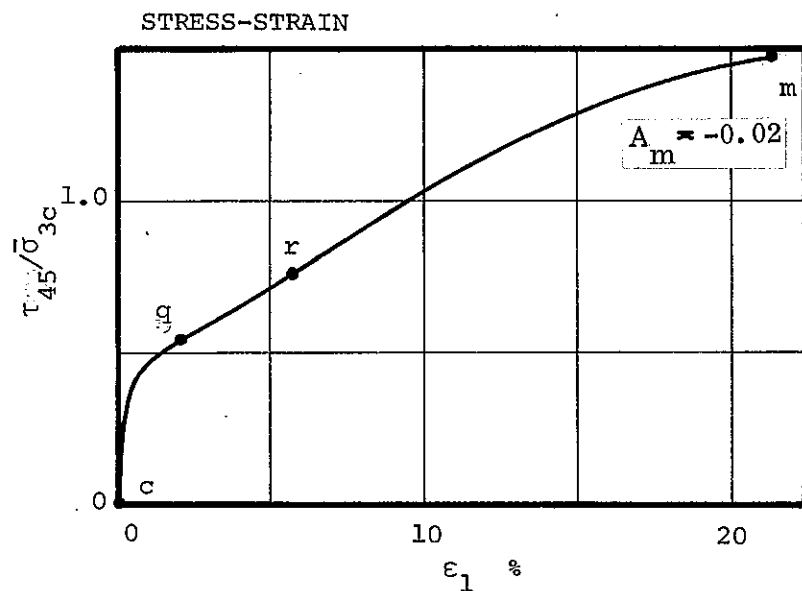
Soil Tested: London clay; $w_{nat} = 23.8\%$; $L_w = 68$, $P_i = 41$; depth 114 ft; $59\% < 2\mu$; $s_s = 2.77$; $p_p \sim 40$ kg/cm²

Test Conditions: Consolidated from slurry at $w = 163\%$; $\bar{\sigma}_{3c} = 60.2$ kg/cm²; $u_c = 2.81$ kg/cm²; $w_c = 19.0\%$; ($e_c \approx 0.53$); $H_o = 7.6$ cm, $D_o = 3.8$ cm; strain rate $\approx 0.0035\%/min.$; $G_{wo} = 99.7\%$.

Source: Replotted from Webb (1966); Vol. II; Fig. G27. See also Bishop, Webb & Lewin (1965), Test E132.

Fig. 22

Highly Contractive Clay
Consolidated-Constant-Volume
Triaxial Compression

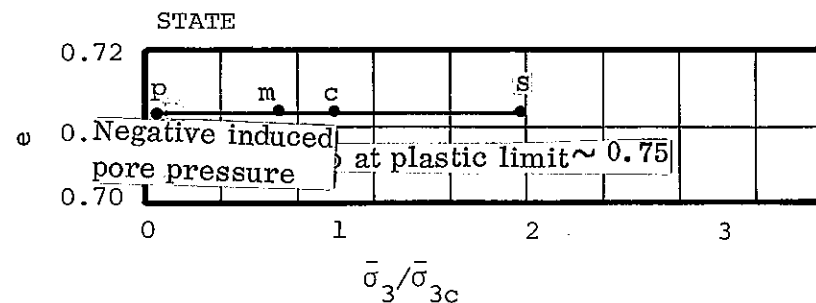
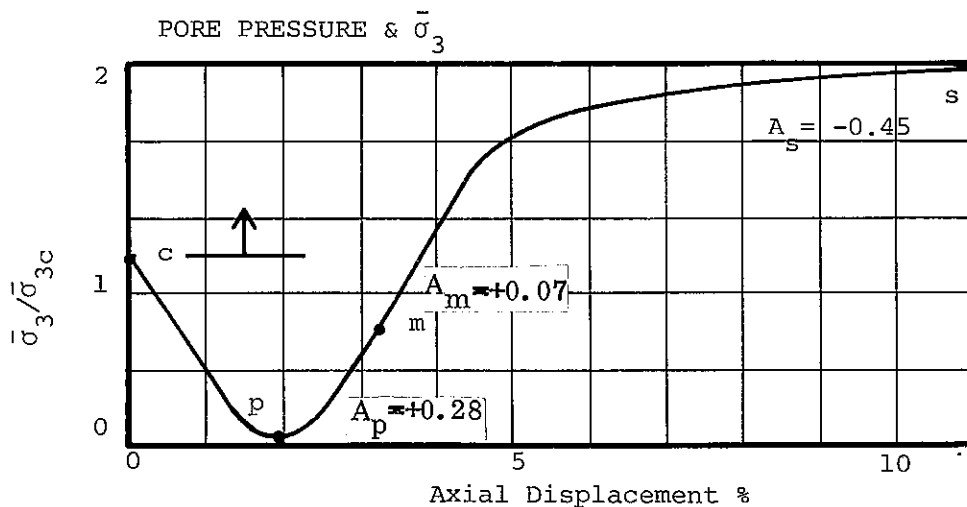
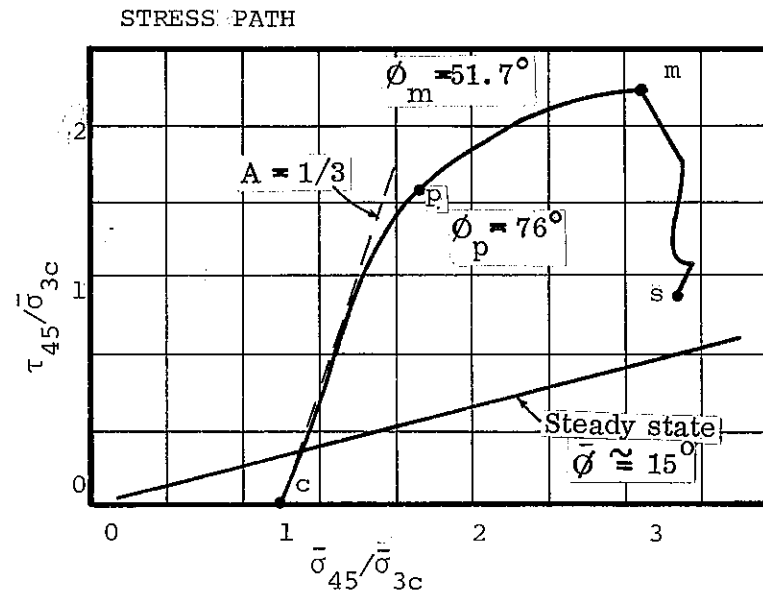
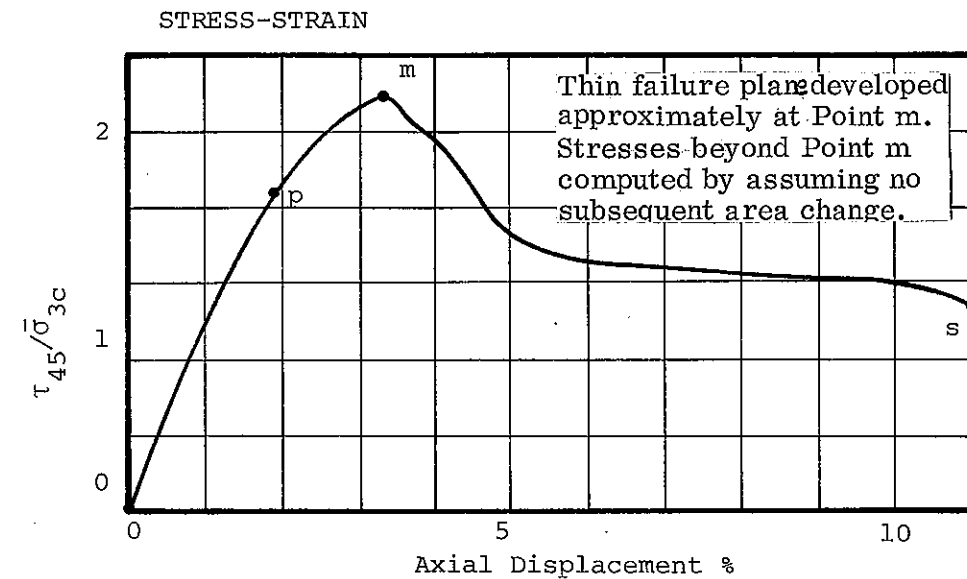


Soil Tested: Canyon Dam silty clay; $L_w = 34$, $P_i = 19$; 20% $< 2\mu$; $s_s = 2.71$; air dried, remolded; calcareous, (shells in +40 mesh); ~75% < 0.074 mm; inorganic.

Test Conditions: $\bar{\sigma}_{3c} = 2.06$ kg/cm²; $e_c = 0.49$; Harvard miniature compacted in 10 layers at $w_o = 15.8\%$, $e_o \approx 0.50$; $w_{opt} = 16.2\%$; load control; time to last point = 440 min. (ave. 0.048%/min); $H_o = 7.14$ cm, $D_o = 3.33$ cm; $u_c = 5.89$ kg/cm².

Source: Replotted from Casagrande & Hirschfeld (1962), Fig. 199.

Fig. 23 Dilative Clay Consolidated-Constant-Volume Triaxial Compression



Soil tested: London Clay; depth 114 ft, $p' \sim 40 \text{ kg/cm}^2$;
 $w_{nat} = 23.8\%$, $L_w = 68$, $P_i = P_{41}$, $59\% < 2\mu$;
 $w_{nat} = 2.77$.

Test Conditions: Undisturbed, $\bar{\sigma}_{3c} = 1.05 \text{ kg/cm}^2$, $u_c = 2.11 \text{ kg/cm}^2$, $w_c = 25.6\%$ ($e_c = 0.712$), c

$G_{wo} = 99\%$, $H_o = 7.6 \text{ cm}$, $D = 3.8 \text{ cm}$.

Replotted from Webb (1966), Vol. 2, Fig. G.14, Test E70. See also Bishop, Webb & Skinner (1965)

Source:

Fig. 24

Highly sensitive Clay
 Consolidated-Constant-Volume
 Triaxial Compression

FIGURE CAPTIONS

- Fig. 1 The State Diagram for Soils
- Fig. 2 Scanning- Electron Microphotographs Viewed Normal to Surface of Natural Slickenside in Bearpaw Clay-Shale
- Fig. 3 The Stress Path
- Fig. 4 Development of a Stress-Strain Curve
- Fig. 5 Consolidated-Drained triaxial Compression Tests: Idealized for Uncemented Soils with Bulky Grains
- Fig. 6 Strength Envelopes for Specimens Prepared at Constant Void Ratio, e_c . Consolidated-Drained Triaxial Compression Tests
- Fig. 7 Consolidated-Drained Triaxial Compression Tests on Soil Containing Substantial Proportion of Flat Grains. Low Stress Levels. Idealized.
- Fig. 8 Postulated Location of Steady State line Relative to Compression and Swelling Curves for Clays.
- Fig. 9 Highly Contractive Sand. Consolidated-Drained. Triaxial Compression
- Fig. 10 Slightly Dilative Sand. Consolidated-Drained. Triaxial Compression
- Fig. 11 Highly Dilative Sand. Consolidated-Drained. Rotation Shear.
- Fig. 12 Highly Contractive Clay. Consolidated-Drained. Rotation Shear.
- Fig. 13 Very Highly Contractive Clay. Consolidated-Drained. Rotation Shear
- Fig. 14 Highly Dilative Clay. Consolidated-Drained. Rotation Shear.
- Fig. 15 Consolidated-Constant-Volume Triaxial Compression Tests. Soil with Bulky-Grains.
- Fig. 16 Consolidated-Constant-Volume Triaxial Compression Tests on Soil Containing Substantial Proportion of Platey Grains. Idealized.
- Fig. 17 Highly Contractive Sand. Consolidated-Constant-Volume. Triaxial Compression.
- Fig. 18 Sand Near Steady State Void Ratio. Consolidated-Constant-Volume. Triaxial Compression.

FIGURE CAPTIONS (continued)

- Fig. 19 Highly Dilative Sand. Consolidated Constant-Volume.
Triaxial Compression.
- Fig. 20 Very Highly Contractive Clay. Consolidated-Constant-
Volume. Simple Shear.
- Fig. 21 Highly Contractive Clay. Consolidated-Constant-Volume.
Triaxial Compression.
- Fig. 22 Highly Contractive Clay. Consolidated-Constant-Volume.
Triaxial Compression.
- Fig. 23 Dilative Clay. Consolidated-Constant-Volume. Triaxial
Compression.
- Fig. 24 Highly Dilative Clay. Consolidated-Constant-Volume.
Triaxial Compression.

STRESS-STRAIN CURVES OF SOILS

KEY WORDS FOR INDEXING

stress	pore pressure
strain	loose
stress-strain	dense
critical state	overconsolidated
steady state	quick
state	normally consolidated
contractive soils	uncemented soils
dilative soils	method of loading
shear strength	drained tests
stress path	undrained tests
volume change	apparatus selection
clays	constant-volume tests
sands	soils
strength tests	